

*The title of
This book*****
ALM ?, pp. 1-?*

© Higher Education Press
and International Press
Beijing-Boston

Minimal surfaces and mean curvature flow

Tobias H. Colding* and William P. Minicozzi II†

Abstract

We discuss recent results on minimal surfaces and mean curvature flow, focusing on the classification and structure of embedded minimal surfaces and the stable singularities of mean curvature flow. This article is dedicated to Rick Schoen.

2000 Mathematics Subject Classification:

Keywords and Phrases:

1 Introduction

The main focus of this survey is on minimal surfaces and mean curvature flow, but to put these topics in perspective we begin with more elementary analysis of the energy of curves and functions. This leads us to first variation formulas for energy and critical points for those. The critical points are of course geodesics and harmonic functions, respectively. We continue by considering the gradient, or rather the negative gradient, flow for energy which leads us to the curve shortening flow and the heat equation. Having touched upon these more elementary topics, we move on to one of our main topics which is minimal surfaces. We discuss first and second variations for area and volume and the gradient (or rather negative) gradient flow for area and volume which is the mean curvature flow. Beginning as elementary as we do allows us later in the survey to draw parallels from the more advanced topics to the simpler ones.

The other topics that we cover are the Birkhoff min-max argument that produces closed geodesics and its higher dimensional analog that gives existence of closed immersed minimal surfaces. We discuss stable and unstable critical points and index of critical points and eventually discuss the very recent classification of all stable self-similar shrinkers for the mean curvature flow. For minimal surfaces,

*MIT, Dept. of Math. 77 Massachusetts Avenue, Cambridge, MA 02139-4307.

†Johns Hopkins University, Dept. of Math. 3400 N. Charles St. Baltimore, MD 21218

stability and Liouville type theorems have played a major role in later developments and we touch upon the Bernstein theorem that is the minimal surface analog of the Liouville theorem for harmonic functions and the curvature estimate that is the analog of the gradient estimate. We discuss various monotone quantities under curve shortening and mean curvature flow like Huisken's volume, the width, and isoperimetric ratios of Gage and Hamilton. We explain why Huisken's monotonicity leads to that blow ups of the flow at singular points in space time can be modeled by self-similar flows and explain why the classification of stable self-similar flows is expected to play a key role in understanding of generic mean curvature flow where the flow begins at a hypersurface in generic position. One of the other main topics of this survey is that of embedded minimal surfaces where we discuss some of the classical examples going back to Euler and Monge's student Meusnier in the 18th century and the recent examples of Hoffman-Weber-Wolf and various examples that date in between. The final main results that we discuss are the recent classification of embedded minimal surfaces and some of the uniqueness results that are now known.

It is a great pleasure for us to dedicate this article to Rick Schoen.

2 Harmonic functions and the heat equation

We begin with a quick review of the energy functional on functions, where the critical points are called harmonic functions and the gradient flow is the heat equation. This will give some context for the main topics of this survey, minimal surfaces and mean curvature flow, that are critical points and gradient flows, respectively, for the area functional.

2.1 Harmonic functions

Given a differentiable function $u : \mathbf{R}^n \rightarrow \mathbf{R}$, the energy is defined to be

$$E(u) = \frac{1}{2} \int |\nabla u|^2 = \frac{1}{2} \int \left(\left| \frac{\partial u}{\partial x_1} \right|^2 + \cdots + \left| \frac{\partial u}{\partial x_n} \right|^2 \right). \quad (1)$$

This gives a functional defined on the space of functions. We can construct a curve in the space of functions by taking a smooth function ϕ with compact support and considering the one-parameter family of functions $u + t\phi$. Restricting the energy functional to this curve gives

$$E(u + t\phi) = \frac{1}{2} \int |\nabla(u + t\phi)|^2 = \frac{1}{2} \int |\nabla u|^2 + t \int \langle u, \nabla \phi \rangle + \frac{t^2}{2} \int |\nabla \phi|^2. \quad (2)$$

Differentiating at $t = 0$, we get that the directional derivative of the energy functional (in the direction ϕ) is

$$\frac{d}{dt}_{t=0} E(u + t\phi) = \int \langle \nabla u, \nabla \phi \rangle = - \int \phi \Delta u, \quad (3)$$

where the last equality used the divergence theorem and the fact that ϕ has compact support. We conclude that:

Lemma 1. *The directional derivative $\frac{d}{dt}_{t=0}E = 0$ for all ϕ if and only if*

$$\Delta u = \frac{\partial^2 u}{\partial x_1^2} + \cdots + \frac{\partial^2 u}{\partial x_n^2} = 0. \quad (4)$$

Thus, we see that the critical points for energy are the functions u with $\Delta u = 0$; these are called harmonic functions. In fact, something stronger is true. Namely, harmonic functions are not just critical points for the energy functional, but are actually minimizers.

Lemma 2. *If $\Delta u = 0$ on a bounded domain Ω and ϕ vanishes on $\partial\Omega$, then*

$$\int_{\Omega} |\nabla(u + \phi)|^2 = \int_{\Omega} |\nabla u|^2 + \int_{\Omega} |\nabla \phi|^2.$$

Proof. Since $\Delta u = 0$ and ϕ vanishes on $\partial\Omega$, the divergence theorem gives

$$0 = \int_{\Omega} \operatorname{div}(\phi \nabla u) = \int_{\Omega} \langle \nabla \phi, \nabla u \rangle. \quad (5)$$

So we conclude that

$$\begin{aligned} \int_{\Omega} |\nabla(u + \phi)|^2 &= \int_{\Omega} |\nabla u|^2 + 2 \langle \nabla \phi, \nabla u \rangle + \int_{\Omega} |\nabla \phi|^2 \\ &= \int_{\Omega} |\nabla u|^2 + \int_{\Omega} |\nabla \phi|^2. \end{aligned}$$

□

2.2 The heat equation

The heat equation is the (negative) gradient flow (or steepest descent) for the energy functional. This means that we evolve a function $u(x, t)$ over time in the direction of its Laplacian Δu , giving the linear parabolic heat equation

$$\frac{\partial u}{\partial t} = \Delta u. \quad (6)$$

Given any finite energy solution u of the heat equation that decays fast enough to justify integrating by parts, the energy is non-increasing along the flow. In fact, we have

$$\frac{d}{dt}E(u) = - \int \frac{\partial u}{\partial t} \Delta u = - \int (\Delta u)^2.$$

Obviously, harmonic functions are fixed points, or *static solutions*, of the flow.

2.3 Negative gradient flows near a critical point

We are interested in the dynamical properties of the heat equation near a harmonic function. Before getting to this, it is useful to recall the simple finite dimensional case. Suppose therefore that $f : \mathbf{R}^2 \rightarrow \mathbf{R}$ is a smooth function with a non-degenerate critical point at 0 (so $\nabla f(0) = 0$ but the Hessian of f at 0 has rank 2). The behavior of the negative gradient flow

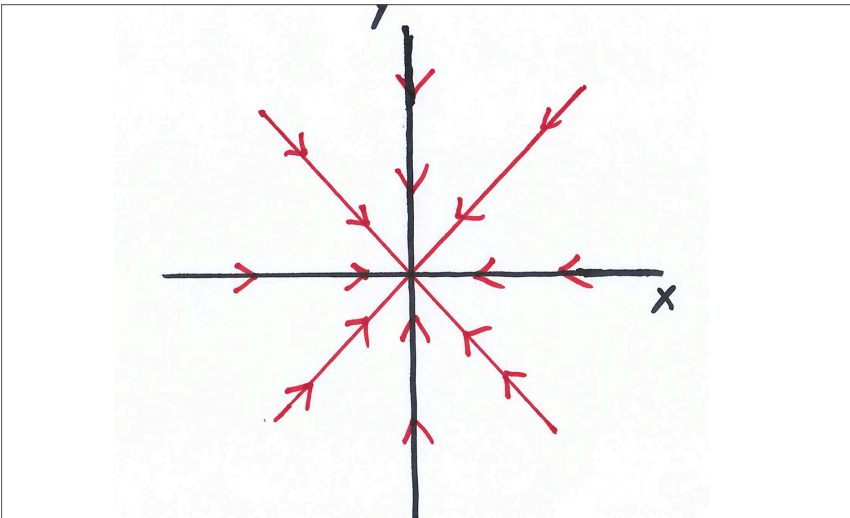
$$(x', y') = -\nabla f(x, y)$$

is determined by the Hessian of f at 0.

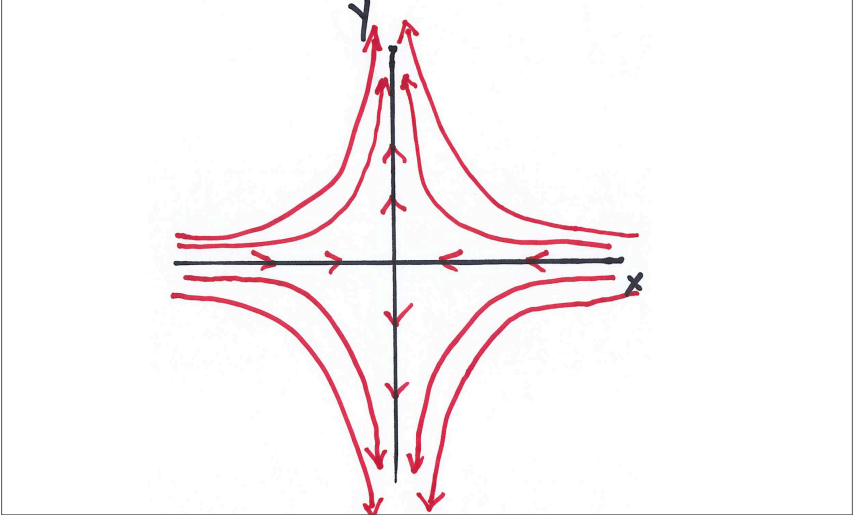
The behavior depends on the index of the critical point, as is illustrated by the following examples:

- (Index 0): The function $f(x, y) = x^2 + y^2$ has a minimum at 0. The vector field is $(-2x, -2y)$ and the flow lines are rays into the origin. Thus every flow line limits to 0.
- (Index 1): The function $f(x, y) = x^2 - y^2$ has an index one critical point at 0. The vector field is $(-2x, 2y)$ and the flow lines are level sets of the function $h(x, y) = xy$. Only points where $y = 0$ are on flow lines that limit to the origin.
- (Index 2): The function $f(x, y) = -x^2 - y^2$ has a maximum at 0. The vector field is $(2x, 2y)$ and the flow lines are rays out of the origin. Thus every flow line limits to ∞ and it is impossible to reach 0.

Thus, we see that the critical point 0 is “generic”, or dynamically stable, if and only if it has index 0. When the index is positive, the critical point is not generic and a “random” flow line will miss the critical point.



$f(x, y) = x^2 + y^2$ has a minimum at 0. Flow lines: Rays through the origin.



$f(x, y) = x^2 - y^2$ has an index one critical point at 0. Flow lines: Level sets of xy . Only points where $y = 0$ limit to the origin.

2.4 Heat flow near a harmonic function

To analyze the dynamical properties of the heat flow, suppose first that u satisfies the heat equation on a bounded domain Ω with $u = 0$ on $\partial\Omega$. By the maximum principle, a harmonic function that vanishes on $\partial\Omega$ is identically zero. Thus, we expect that u limits towards 0. We show this next.

Since $u = 0$ on $\partial\Omega$, applying the divergence theorem to $u\nabla u$ gives

$$\int_{\Omega} |\nabla u|^2 = - \int_{\Omega} u \Delta u.$$

Applying Cauchy-Schwarz and then the Dirichlet Poincaré inequality gives

$$\left(\int_{\Omega} |\nabla u|^2 \right)^2 \leq \int_{\Omega} u^2 \int_{\Omega} (\Delta u)^2 \leq C \int_{\Omega} |\nabla u|^2 \int_{\Omega} (\Delta u)^2.$$

Finally, dividing both sides by $\int_{\Omega} |\nabla u|^2$ gives

$$2E(t) \equiv 2E(u(\cdot, t)) = \int_{\Omega} |\nabla u|^2 \leq C \int_{\Omega} (\Delta u)^2 = -C E'(t),$$

where $C = C(\Omega)$ is the constant from the Dirichlet Poincaré inequality. Integrating this gives that $E(t)$ decays exponentially with

$$E(t) \leq E(0) e^{-\frac{2}{C} t}.$$

Finally, another application of the Poincaré inequality shows that $\int u^2(x, t)$ also decays exponentially in t , as we expected.

If u does not vanish on $\partial\Omega$, there is a unique harmonic function w with

$$u|_{\partial\Omega} = w|_{\partial\Omega}.$$

It follows that $(u - w)$ also solves the heat equation and is zero on $\partial\Omega$. By the previous argument, $(u - w)$ decays exponentially and we conclude that all harmonic functions are attracting critical points of the flow. Since we have already shown that harmonic functions are minimizers for the energy functional, and thus index zero critical points, this is exactly what the finite dimensional toy model suggests.

3 Energy of a curve

Geodesics in a Riemannian manifold M^n arise variationally in two ways. They are critical points of the energy functional restricted to maps into M (generalizing harmonic functions) and they are also critical points of the length functional. We will first analyze the energy functional on curves.

3.1 Critical points for energy are geodesics

Suppose γ is a closed curve in a Riemannian manifold M^n , i.e.,

$$\gamma : \mathbf{S}^1 \rightarrow M,$$

where the circle \mathbf{S}^1 is identified with $\mathbf{R}/2\pi\mathbf{Z}$. The energy of γ is

$$E(\gamma) = \frac{1}{2} \int_{\mathbf{S}^1} |\gamma'|^2.$$

A variation of γ is a curve in the space of curves that goes through γ . We can specify this by a map

$$F : \mathbf{S}^1 \times [-\epsilon, \epsilon] \rightarrow M^n$$

with $F(\cdot, 0) = \gamma$. The variation vector field V is the tangent vector to this path given by $V = \frac{\partial F}{\partial t}$. An easy calculation shows that

$$\left. \frac{d}{dt} \right|_{t=0} E(\gamma(\cdot, t)) = \int \langle \gamma', F_{s,t} \rangle = - \int \langle \gamma'', V \rangle,$$

where $\gamma'' = \nabla_{\gamma'} \gamma'$. We conclude that

$$\left. \frac{d}{dt} \right|_{t=0} E = 0 \text{ for all } V$$

if and only if $\gamma'' = 0$. Such a curve is called a geodesic.

3.2 Second variation of energy of a curve in a surface

We have seen that a closed geodesic $\gamma : \mathbf{S}^1 \rightarrow M^2$ in a surface M is a critical point for energy. The hessian of the energy functional is given by the second variation formula. For simplicity, we assume that $|\gamma'| = 1$ and $V = \phi \mathbf{n}$ is a normal variation where \mathbf{n} is the unit normal to γ , so $V' = \phi' \mathbf{n}$. We compute

$$\begin{aligned} \frac{d^2}{dt^2} \Big|_{t=0} E(t) &= \int (|F_{s,t}|^2 - \langle \gamma', F_{s,tt} \rangle) = \int (|F_{t,s}|^2 - \langle \gamma', F_{s,tt} \rangle) \\ &= \int (|V'|^2 - \langle \gamma', F_{s,tt} \rangle) = \int (|\phi'|^2 - K \phi^2) \\ &= - \int (\phi'' \phi + K \phi^2), \end{aligned}$$

where K is the curvature of M .

In this calculation, we used that $F_{ss} = 0$ since γ is a geodesic and that the curvature K comes in when one changes the order of derivatives, i.e.,

$$\langle F_s, F_{s,tt} \rangle = \langle F_s, F_{tt,s} \rangle + K [|F_s|^2 |F_t|^2 - \langle F_s, F_t \rangle^2].$$

Using that $F_s = V = \phi \mathbf{n}$ is perpendicular to $F_t = \gamma'$ and $|\gamma'| = 1$ gives

$$\langle F_s, F_{s,tt} \rangle = \langle F_s, F_{tt,s} \rangle + K \phi^2.$$

A geodesic γ_0 is stable if the Hessian of the energy functional at γ_0 has index zero, i.e., if

$$\frac{d^2}{dt^2} \Big|_{t=0} E(t) \geq 0,$$

for all variations of γ_0 . Roughly speaking, stable geodesics minimize energy compared to nearby curves.

3.3 Geodesics in a free homotopy class

The simplest way to produce geodesics is to look for minima of the energy functional. To get a closed geodesic, the minimization is done in a free homotopy class. A free homotopy class of a closed curve $c : \mathbf{S}^1 \rightarrow M$ on a manifold M consists of all the curves that are homotopic to c . Namely, a curve γ is freely homotopic to c if there exists a one parameter family

$$F : \mathbf{S}^1 \times [0, 1] \rightarrow M$$

so $F(\cdot, 0) = c$ and $F(\cdot, 1) = \gamma$. The difference between a homotopy class and a free homotopy class is that there is no fixed base point for a free homotopy class.

Standard arguments in Riemannian geometry then give:

Lemma 3. *In each free homotopy class on a closed manifold, there is at least one curve that realizes the smallest energy. This minimizing curve is a geodesic and is non-trivial if the homotopy class is non-trivial.*

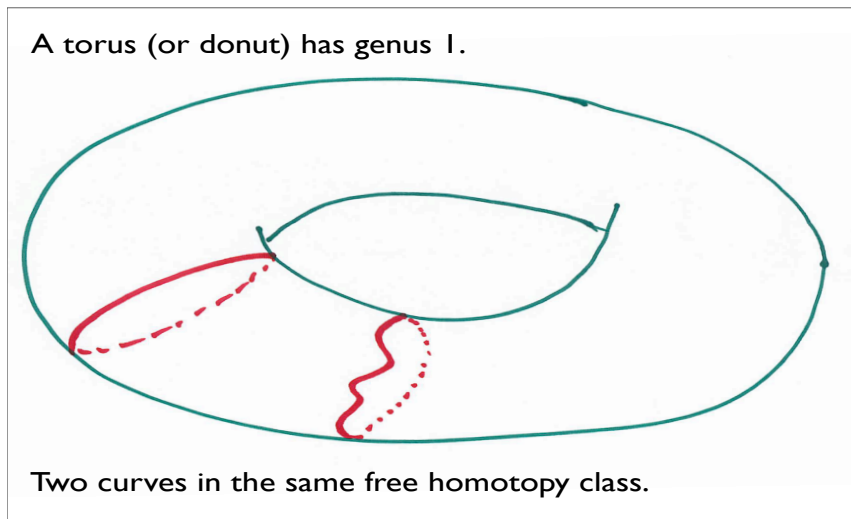


Figure 1: Freely homotopic curves.

4 Birkhoff: A closed geodesic on a two sphere

In the 1910s, Birkhoff came up with an ingenious method of constructing non-trivial closed geodesics on a topological 2-sphere. Since \mathbf{S}^2 is simply-connected, this cannot be done by minimizing in a free homotopy class. Birkhoff's instead used a min-max argument to find higher index critical points. We will describe Birkhoff's idea and some related results in this section; see [B1], [B2] and section 2 in [Cr] for more about Birkhoff's ideas.

4.1 Sweepouts and the width

The starting point is a min-max construction that uses a non-trivial homotopy class of maps from \mathbf{S}^2 to construct a geometric metric called the width. Later, we will see that this invariant is realized as the length of a closed geodesic. Of course, one has to assume that such a non-trivial homotopy class exists (it does on \mathbf{S}^2 , but not on higher genus surfaces; fortunately, it is easy to construct minimizers on higher genus surfaces).

Let Ω be the set of continuous maps

$$\sigma : \mathbf{S}^1 \times [0, 1] \rightarrow M$$

with the following three properties:

- For each t the map $\sigma(\cdot, t)$ is in $W^{1,2}$.
- The map $t \rightarrow \sigma(\cdot, t)$ is continuous from $[0, 1]$ to $W^{1,2}$.
- σ maps $\mathbf{S}^1 \times \{0\}$ and $\mathbf{S}^1 \times \{1\}$ to points.

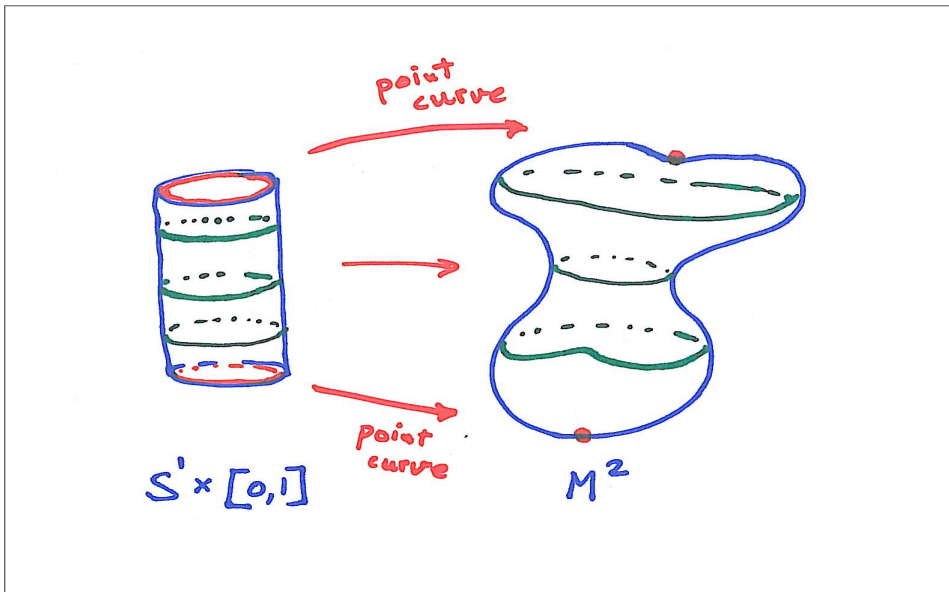


Figure 2: A sweepout.

Given a map $\hat{\sigma} \in \Omega$, the homotopy class $\Omega_{\hat{\sigma}}$ is defined to be the set of maps $\sigma \in \Omega$ that are homotopic to $\hat{\sigma}$ through maps in Ω . The width $W = W(\hat{\sigma})$ associated to the homotopy class $\Omega_{\hat{\sigma}}$ is defined by taking inf of max of the energy of each slice. That is, set

$$W = \inf_{\sigma \in \Omega_{\hat{\sigma}}} \max_{t \in [0,1]} E(\sigma(\cdot, t)), \quad (7)$$

where the energy is given by

$$E(\sigma(\cdot, t)) = \int_{\mathbf{S}^1} |\partial_x \sigma(x, t)|^2 dx.$$

The width is always non-negative and is positive if $\hat{\sigma}$ is in a non-trivial homotopy class.

A particularly interesting example is when M is a topological 2-sphere and the induced map from \mathbf{S}^2 to M has degree one. In this case, the width is positive and realized by a non-trivial closed geodesic. To see that the width is positive on non-trivial homotopy classes, observe that if the maximal energy of a slice is sufficiently small, then each curve $\sigma(\cdot, t)$ is contained in a convex geodesic ball in M . Hence, a geodesic homotopy connects σ to a path of point curves, so σ is homotopically trivial.

4.2 Pulling the sweepout tight to obtain a closed geodesic

The key to finding the closed geodesic is to “pull the sweepout tight” using the Birkhoff curve shortening process (or BCSP). The BCSP is a kind of discrete

gradient flow on the space of curves. It is given by subdividing a curve and then replacing first the even segments by minimizing geodesics, then replacing the odd segments by minimizing geodesics, and finally reparameterizing the curve so it has constant speed.

It is not hard to see that the BCSP has the following properties:

- It is continuous on the space of curves.
- Closed geodesics are fixed under the BCSP.
- If a curve is fixed under BCSP, then it is a geodesic.

It is possible to make each of these three properties quantitative.

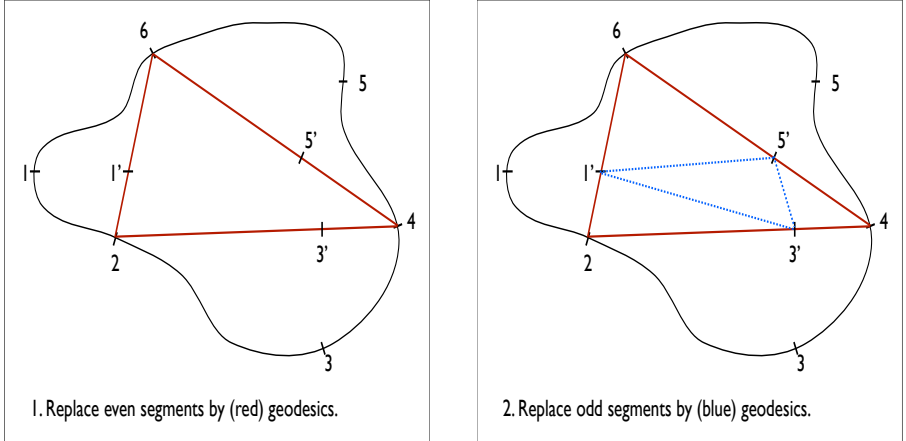


Figure 3: Birkhoff's curve shortening process.

Using this map and more refined versions of these properties, we showed the existence of a sequence of tightened sweepouts:

Theorem 4. (Colding-Minicozzi, [CM2]) *There exists a sequence of sweepouts γ^j with the property that: Given $\epsilon > 0$, there is $\delta > 0$ so that if $j > 1/\delta$ and*

$$2\pi E(\gamma^j(\cdot, t_0)) = \text{Length}^2(\gamma^j(\cdot, t_0)) > 2\pi(W - \delta), \quad (8)$$

then for this j we have $\text{dist}(\gamma^j(\cdot, t_0), G) < \epsilon$ where G is the set of closed geodesics.

As an immediate consequence, we get the existence of non-trivial closed geodesics for any metric on \mathbf{S}^2 ; this is due to Birkhoff. See [LzW1] for an alternative proof using the harmonic map heat flow.

4.3 Sweepouts by spheres

We will now define a two-dimensional version of the width, where we sweepout by spheres instead of curves. Let Ω be the set of continuous maps

$$\sigma : \mathbf{S}^2 \times [0, 1] \rightarrow M$$

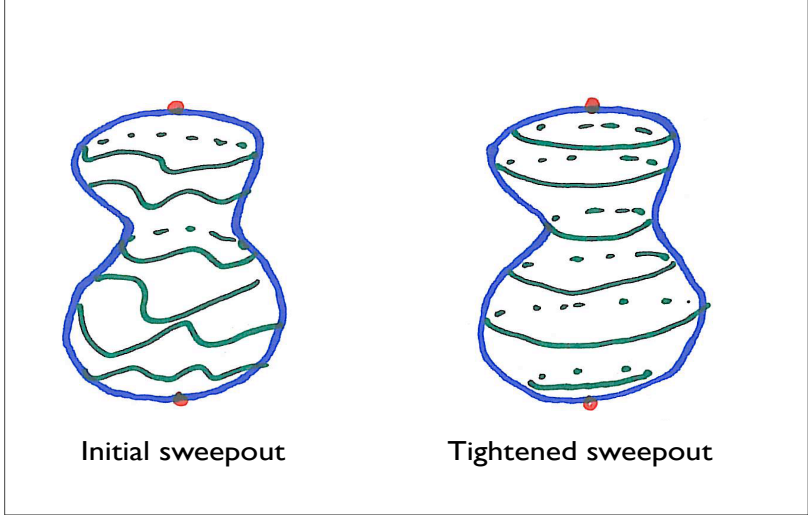


Figure 4: Tightening the sweepout.

so that:

- For each $t \in [0, 1]$ the map $\sigma(\cdot, t)$ is in $C^0 \cap W^{1,2}$.
- The map $t \rightarrow \sigma(\cdot, t)$ is continuous from $[0, 1]$ to $C^0 \cap W^{1,2}$.
- σ maps $\mathbf{S}^2 \times \{0\}$ and $\mathbf{S}^2 \times \{1\}$ to points.

Given a map $\beta \in \Omega$, the homotopy class Ω_β is defined to be the set of maps $\sigma \in \Omega$ that are homotopic to β through maps in Ω . We will call any such β a *sweepout*.

The (energy) width $W_E = W_E(\beta, M)$ associated to the homotopy class Ω_β is defined by taking the infimum of the maximum of the energy of each slice. That is, set

$$W_E = \inf_{\sigma \in \Omega_\beta} \max_{t \in [0,1]} E(\sigma(\cdot, t)), \quad (9)$$

where the energy is given by

$$E(\sigma(\cdot, t)) = \frac{1}{2} \int_{\mathbf{S}^2} |\nabla_x \sigma(x, t)|^2 dx. \quad (10)$$

The next result gives the existence of a sequence of good sweepouts.

Theorem 5. (Colding-Minicozzi, [CM19]) *Given a metric g on M and a map $\beta \in \Omega$ representing a non-trivial class in $\pi_3(M)$, there exists a sequence of sweepouts $\gamma^j \in \Omega_\beta$ with $\max_{s \in [0,1]} E(\gamma_s^j) \rightarrow W(g)$, and so that given $\epsilon > 0$, there exist \bar{j} and $\delta > 0$ so that if $j > \bar{j}$ and*

$$\text{Area}(\gamma^j(\cdot, s)) > W(g) - \delta, \quad (11)$$

then there are finitely many harmonic maps $u_i : \mathbf{S}^2 \rightarrow M$ with

$$d_V(\gamma^j(\cdot, s), \cup_i \{u_i\}) < \epsilon. \quad (12)$$

In (12), we have identified each map u_i with the varifold associated to the pair (u_i, \mathbf{S}^2) and then taken the disjoint union of these \mathbf{S}^2 's to get $\cup_i \{u_i\}$. The distance d_V in (12) is a weak measure-theoretic distance called “varifold distance”; see [CM19] or Chapter 3 of [CM14] for the definition.

One immediate consequence of Theorem 5 is that if s_j is any sequence with $\text{Area}(\gamma^j(\cdot, s_j))$ converging to the width $W(g)$ as $j \rightarrow \infty$, then a subsequence of $\gamma^j(\cdot, s_j)$ converges to a collection of harmonic maps from \mathbf{S}^2 to M . In particular, the sum of the areas of these maps is exactly $W(g)$ and, since the maps are automatically conformal, the sum of the energies is also $W(g)$. The existence of at least one non-trivial harmonic map from \mathbf{S}^2 to M was first proven in [SaUh], but they allowed for loss of energy in the limit; cf. also [St]. Ruling out this possible energy loss in various settings is known as the “energy identity” and it can be rather delicate. This energy loss was ruled out by Siu and Yau, using also arguments of Meeks and Yau (see Chapter VIII in [ScYa2]). This was also proven later by Jost, [Jo].

5 Curve shortening flow

The Birkhoff curve shortening process was a kind of discrete gradient flow on the space of curves. We turn next to a continuous gradient flow that is called the curve shortening flow.

Suppose that γ_0 again is a curve but this time we will think of it as an embedded submanifold in \mathbf{R}^2 or, more generally, a surface M^2 . We can again look at variations γ_t of the one-dimensional submanifold γ_0 and get for lengths:

$$\left. \frac{d}{dt} \right|_{t=0} \text{Length}(\gamma_t) = \int_{\gamma_0} h \langle \mathbf{n}, V \rangle,$$

where h is the (geodesic) curvature of the one-dimensional submanifold given by

$$h = \langle \nabla_{e_1} \mathbf{n}, e_1 \rangle,$$

where e_1 is a unit vector tangent to the curve γ_0 and \mathbf{n} is the unit normal to γ_0 . It follows that

1. γ_0 is a critical point for length if and only if it is a geodesic (after being reparameterized to have constant speed).
2. The negative gradient flow for the length functional in \mathbf{R}^2 is the *curve shortening flow*

$$\partial_t x = h \mathbf{n}.$$

The simplest (non-trivial) solution of the curve shortening flow is given by a one-parameter family of concentric circles with radius

$$r(t) = \sqrt{-2t}$$

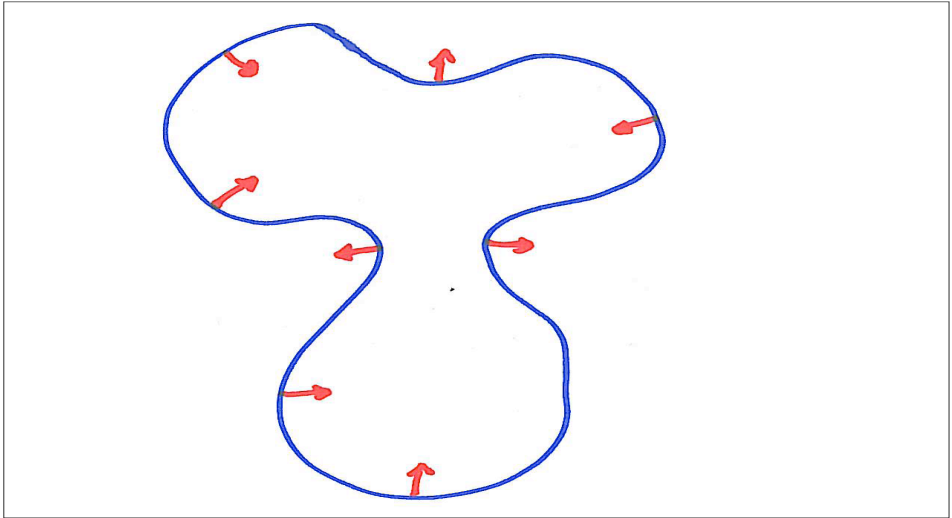


Figure 5: Curve shortening flow: the curve evolves by its geodesic curvature. The red arrows indicate direction of flow.

for t in $(-\infty, 0)$. This is an *ancient* solution since it is defined for all $t < 0$, it is *self-similar* since the shape is preserved (i.e., we can think of it as a fixed circle moving under rigid motions of \mathbf{R}^2), and it becomes *extinct* at the origin in space and time.

5.1 Self-similar solutions

A solution of the curve shortening flow is self-similar if the shape does not change with time. The simplest example is a static solution, like a straight line, that does not change at all. The next simplest is given by concentric shrinking circles, but there are many other interesting possibilities. There are three types of self-similar solutions that are most frequently considered:

- Self-similar shrinkers.
- Self-similar translators.
- Self-similar expanders.

We will explain shrinkers first. Suppose that c_t is a one-parameter family of curves flowing by the curve shortening flow for $t < 0$. We say that c_t is a *self-similar shrinker* if

$$c_t = \sqrt{-t} c_{-1}$$

for all $t < 0$. For example, circles of radius $\sqrt{-2t}$ give such a solution. In 1986, Abresch and Langer, [AbLa], classified such solutions and showed that the shrinking circles give the only embedded one (cf. Andrews, [An]). In 1987, Epstein-Weinstein, [EpW], showed a similar classification and analyzed the dynamics of the curve shortening flow near a shrinker.

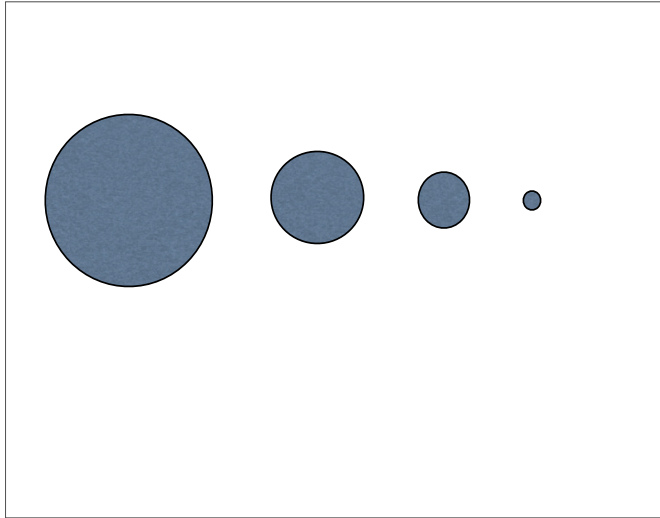


Figure 6: Four snapshots in time of concentric circles shrinking under the curve shortening flow.

We say that c_t is a *self-similar translator* if there is a constant vector $V \in \mathbf{R}^2$ so that

$$c_t = c_0 + tV$$

for all $t \in \mathbf{R}$. These solutions are *eternal* in that they are defined for all time. It is easy to see that any translator must be non-compact. Calabi discovered a self-similar translator in the plane that he named the *grim reaper*. Calabi's Grim Reaper is given as the graph of the function

$$u(x, t) = t - \log \sin x.$$

Self-similar expanders are similar to shrinkers, except that they move by expanding dilations. In particular, the solutions are defined as t goes to $+\infty$. It is not hard to see that expanders must be non-compact.

There are other possible types of self-similar solutions, where the solutions move by one-parameter families of rigid motions over time. See Halldorsson, [Hh], for other self-similar solutions to the curve shortening flow.

5.2 Theorems of Gage-Hamilton and Grayson

In 1986, building on earlier work of Gage, [Ga1] and [Ga2], Gage and Hamilton classified closed convex solutions of the curve shortening flow:

Theorem 6. (*Gage-Hamilton, [GaH]*) *Under the curve shortening flow every simple closed convex curve remains smooth and convex and eventually becomes extinct in a "round point".*

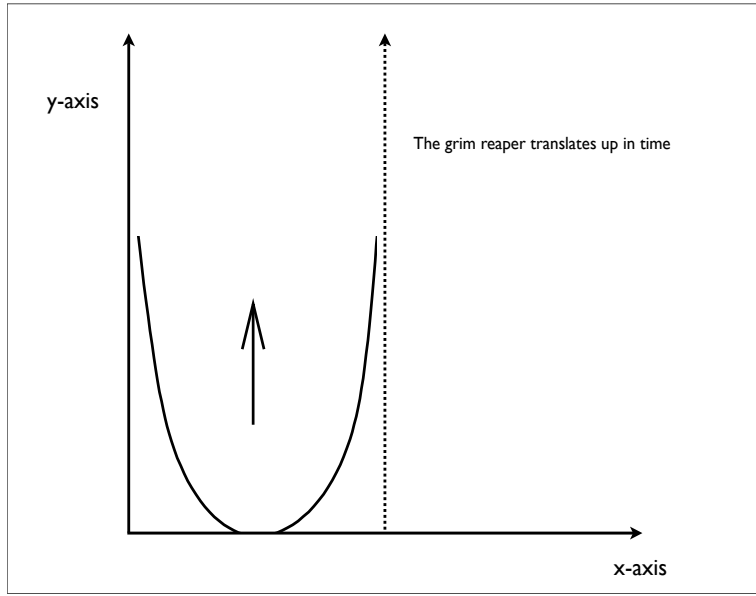


Figure 7: Calabi's grim reaper moves by translations.

More precisely, they showed that the flow becomes extinct in a point and if the flow is rescaled to keep the enclosed area constant, then the resulting curves converge to a round circle. They did this by tracking the isoperimetric ratio and showing that it was approaching the optimal ratio which is achieved by round circles.

In 1987, M. Grayson, [G1], showed that any simple closed curve eventually becomes convex under the flow:

Theorem 7. (Grayson, [G1]) *Any simple closed curve eventually becomes convex under the curve shortening flow. Thus, by the result of Gage-Hamilton, it becomes extinct in a “round point”.*

5.3 Isoperimetric monotonicity under the curve shortening flow

In 1995, Hamilton, [Ha1], and Huisken, [H5], discovered two beautiful new ways to prove Grayson's theorem. Both of these relied on proving monotonicity of various isoperimetric ratios under the curve shortening flow and using these to rule out singularities other than shrinking circles. Recently, Andrews and Bryan, [AnB] discovered another monotone quantity and used it to give a self-contained¹ proof of Grayson's theorem. We will describe two monotone quantities discovered by Hamilton.

¹“Self-contained” means avoiding the use of a blow up analysis.

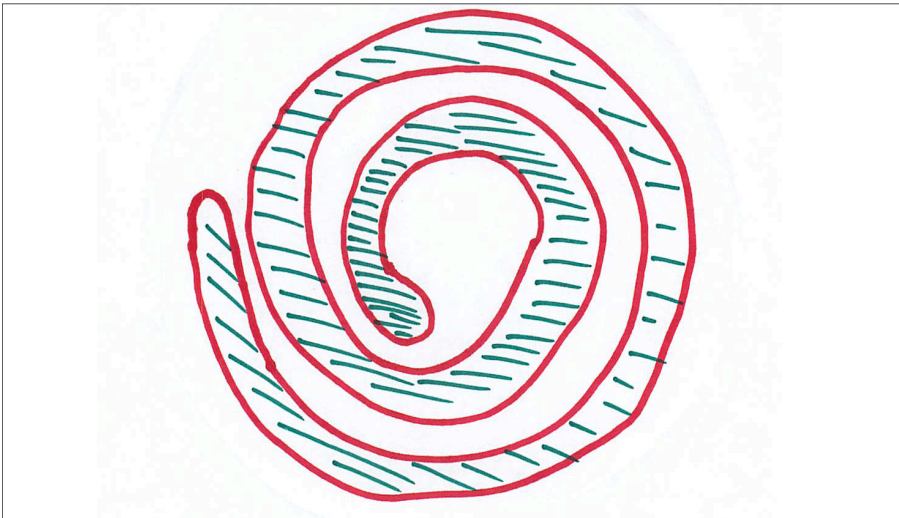


Figure 8: The snake manages to unwind quickly enough to become convex before extinction.

For both of Hamilton's quantities, we start with a simple closed curve

$$c : \mathbf{S}^1 \rightarrow \mathbf{R}^2.$$

The image of c encloses a region in \mathbf{R}^2 . Each simple curve γ inside this region with boundary in the image of c divides the region into two subdomains; let A_1 and A_2 be the areas of these subdomains and let L be the length of the dividing curve γ .

Hamilton's first quantity I is defined to be

$$I = \inf_{\gamma} L^2 \left(\frac{1}{A_1} + \frac{1}{A_2} \right),$$

where the infimum is over all possible dividing curves γ .

Theorem 8. (Hamilton, [Ha1]) *Under the curve shortening flow, I increases if $I \leq \pi$.*

Hamilton's second quantity J is defined to be

$$J = \inf_{\gamma} \frac{L}{L_0},$$

where the infimum is again taken over all possible dividing curves γ and the quantity $L_0 = L_0(A_1, A_2)$ is the length of the shortest curve which divides a circle of area $A_1 + A_2$ into two pieces of area A_1 and A_2 .

Theorem 9. (Hamilton, [Ha1]) *Under the curve shortening flow, J always increases.*

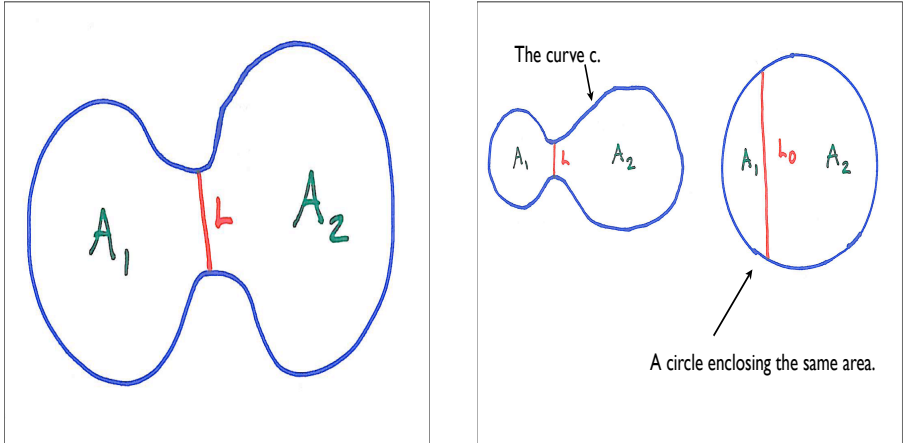


Figure 9: The minimizing curve γ in Hamilton's first isoperimetric quantity. Figure 10: Defining the length L_0 in Hamilton's second isoperimetric quantity.

We will give a rough idea why these theorems are related to Grayson's theorem. Grayson had to rule out a singularity developing before the curve became convex. As you approach a singularity, the geodesic curvature h must be larger and larger. Since the curve is compact, one can magnify the curve just before this singular time to get a new curve where the maximum of $|h|$ is one. There is a blow up analysis that shows that this dilated curve must look like a circle unless it is very long and skinny (like the grim reaper). Finally, a bound on any of these isoperimetric quantities rules out these long skinny curves.

6 Minimal surfaces

We turn next to higher dimensions and the variational properties of the area functional. Critical points of the area functional are called *minimal surfaces*. In this section, we will give a rapid overview of some of the basic properties of minimal surfaces; see the book [CM14] for more details.

6.1 The first variation of area for surfaces

Let Σ_0 be a hypersurface in \mathbf{R}^{n+1} and \mathbf{n} its unit normal. Given a vector field

$$V : \Sigma \rightarrow \mathbf{R}^{n+1}$$

with compact support, we get a one-parameter family of hypersurfaces

$$\Sigma_s = \{x + sV(x) \mid x \in \Sigma_0\}.$$

The first variation of area (or volume) is

$$\left. \frac{d}{ds} \right|_{s=0} \text{Vol}(\Sigma_s) = \int_{\Sigma_0} \text{div}_{\Sigma_0} V,$$

where the divergence div_{Σ_0} is defined by

$$\text{div}_{\Sigma_0} V = \sum_{i=1}^n \langle \nabla_{e_i} V, e_i \rangle,$$

where e_i is an orthonormal frame for Σ . The vector field V can be decomposed into the part V^T tangent to Σ and the normal part V^\perp . The divergence of the normal part $V^\perp = \langle V, \mathbf{n} \rangle \mathbf{n}$ is

$$\text{div}_{\Sigma_0} V^\perp = \langle \nabla_{e_i} (\langle V, \mathbf{n} \rangle \mathbf{n}), e_i \rangle = \langle V, \mathbf{n} \rangle \langle \nabla_{e_i} \mathbf{n}, e_i \rangle = H \langle V, \mathbf{n} \rangle,$$

where the mean curvature scalar H is

$$H = \text{div}_{\Sigma_0}(\mathbf{n}) = \sum_{i=1}^n \langle \nabla_{e_i} \mathbf{n}, e_i \rangle.$$

With this normalization, H is n/R on the n -sphere of radius R .

6.2 Minimal surfaces

By Stokes' theorem, $\text{div}_{\Sigma_0} V^T$ integrates to zero. Hence, since $\text{div}_{\Sigma_0} V^\perp = H \langle V, \mathbf{n} \rangle$, we can rewrite the first variation formula as

$$\left. \frac{d}{ds} \right|_{s=0} \text{Vol}(\Sigma_s) = \int_{\Sigma_0} H \langle V, \mathbf{n} \rangle.$$

A hypersurface Σ_0 is *minimal* when it is a critical point for the area functional, i.e., when the first variation is zero for every compactly supported vector field V . By the first variation formula, this is equivalent to $H = 0$.

6.3 Minimal graphs

If Σ is the graph of a function $u : \mathbf{R}^n \rightarrow \mathbf{R}$, then the upward-pointing unit normal is given by

$$\mathbf{n} = \frac{(-\nabla u, 1)}{\sqrt{1 + |\nabla_{\mathbf{R}^n} u|^2}}, \quad (13)$$

and the mean curvature of Σ is given by

$$H = -\text{div}_{\mathbf{R}^n} \left(\frac{\nabla_{\mathbf{R}^n} u}{\sqrt{1 + |\nabla_{\mathbf{R}^n} u|^2}} \right). \quad (14)$$

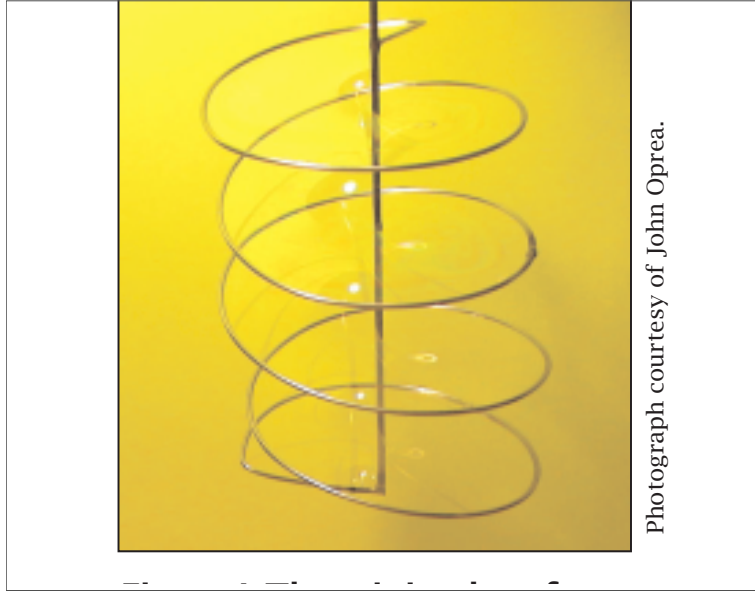


Figure 11: The minimal surface called the helicoid is a double-spiral staircase. This photo shows half of a helicoid as a soap film.

Thus, minimal graphs are solutions of the nonlinear divergence-form PDE

$$\operatorname{div}_{\mathbf{R}^n} \left(\frac{\nabla_{\mathbf{R}^n} u}{\sqrt{1 + |\nabla_{\mathbf{R}^n} u|^2}} \right) = 0. \quad (15)$$

Every smooth hypersurface is locally graphical, so small pieces of a minimal surface satisfy this equation (over some plane).

In 1916, Bernstein proved that planes were the only entire solutions of the minimal surface equation:

Theorem 10. (Bernstein, [Be]) *Any minimal graph over all of \mathbf{R}^2 must be flat (i.e., u is an affine function).*

Remarkably, this theorem holds for $n \leq 7$, but there are non-flat entire minimal graphs in dimensions 8 and up.

The Bernstein theorem should be compared with the classical Liouville theorem for harmonic functions:

Theorem 11. (Liouville) *A positive harmonic function on \mathbf{R}^n must be constant.*

6.4 Consequences of the first variation formula

Suppose that $\Sigma \subset \mathbf{R}^{n+1}$ is a hypersurface with normal \mathbf{n} . Given $f : \mathbf{R}^{n+1} \rightarrow \mathbf{R}$, the Laplacian on Σ applied to f is

$$\Delta_{\Sigma} f \equiv \operatorname{div}_{\Sigma}(\nabla f)^T = \sum_{i=1}^n \operatorname{Hess}_f(e_i, e_i) - \langle \nabla f, \mathbf{n} \rangle H, \quad (16)$$

where e_i is a frame for Σ and Hess_f is the \mathbf{R}^{n+1} Hessian of f . We will use this formula several times with different choices of f .

First, when f is the i -th coordinate function x_i , (16) becomes

$$\Delta_{\Sigma} x_i = -\langle \partial_i, \mathbf{n} \rangle H.$$

We see that:

Lemma 12. Σ is minimal \iff all coordinate functions are harmonic.

Combining this with the maximum principle, we get Osserman's convex hull property, [Os3]:

Proposition 13. If Σ is compact and minimal, then Σ is contained in the convex hull of $\partial\Sigma$.

Proof. If not, then we could choose translate and rotate Σ so that $\partial\Sigma \subset \{x_1 < 0\}$ but Σ contains a point $p \in \{x_1 > 0\}$. However, the function x_1 is harmonic on Σ , so the maximum principle implies that its maximum is on $\partial\Sigma$. This contradiction proved the proposition. \square

Applying (16) with $f = |x|^2$ and noting that the \mathbf{R}^{n+1} Hessian of $|x|^2$ is twice the identity and the gradient is $2x$, we see that

$$\Delta_{\Sigma} |x|^2 = 2n - 2\langle x, \mathbf{n} \rangle H,$$

when $\Sigma \subset \mathbf{R}^{n+1}$ is a hypersurface. When Σ is minimal, this becomes

$$\Delta_{\Sigma} |x|^2 = 2n.$$

This identity is the key for the monotonicity formula:

Theorem 14. If $\Sigma \subset \mathbf{R}^{n+1}$ is a minimal hypersurface, then

$$\frac{d}{dr} \frac{\operatorname{Vol}(B_r \cap \Sigma)}{r^n} = \frac{1}{r^{n+1}} \int_{\partial B_r \cap \Sigma} \frac{|x^{\perp}|^2}{|x^T|} \geq 0.$$

Moreover, the density ratio is constant if and only if $x^{\perp} \equiv 0$; this is equivalent to Σ being a cone with its vertex at the origin (i.e., Σ is invariant with respect to dilations about 0).

6.5 Examples of minimal surfaces

6.5.1 The Catenoid

The catenoid, shown in figure 12, is the only non-flat minimal surface of revolution. It was discovered by Euler in 1744 and shown to be minimal by Meusnier (a student of Monge) in 1776. It is a complete embedded topological annulus (i.e., genus zero and two ends) and is given as the set where $x_1^2 + x_2^2 = \cosh^2(x_3)$ in \mathbf{R}^3 . It is easy to see that the catenoid has finite total curvature.

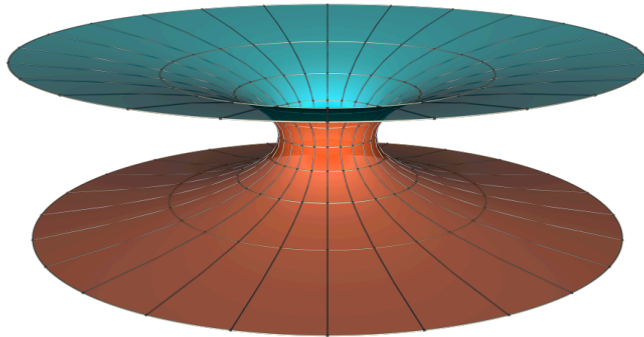


Figure 12: The catenoid given by revolving $x_1 = \cosh x_3$ around the x_3 -axis. Credit: Matthias Weber, www.indiana.edu/~minimal.

6.5.2 The Helicoid

The helicoid (see figure 13) is given as the set $x_3 = \tan^{-1} \left(\frac{x_2}{x_1} \right)$; alternatively, it is given in parametric form by

$$(x_1, x_2, x_3) = (t \cos s, t \sin s, s), \quad (17)$$

where $s, t \in \mathbf{R}$. It was discovered by Meusnier (a student of Monge) in 1776. It is complete, embedded, singly-periodic and simply connected.

The helicoid is a ruled surface since its intersections with horizontal planes $\{x_3 = s\}$ are straight lines. These lines lift and rotate with constant speed to form a double spiral staircase. In 1842, Catalan showed that the helicoid is the only (non-flat) ruled minimal surface. A surface is said to be “ruled” if it can be parameterized by

$$X(s, t) = \beta(t) + s \delta(t) \text{ where } s, t \in \mathbf{R}, \quad (18)$$

and β and δ are curves in \mathbf{R}^3 . The curve $\beta(t)$ is called the “directrix” of the surface, and a line having $\delta(t)$ as direction vector is called a “ruling”. For the standard helicoid, the x_3 -axis is a directrix, and for each fixed t the line $s \rightarrow (s \cos t, s \sin t, t)$ is a ruling.

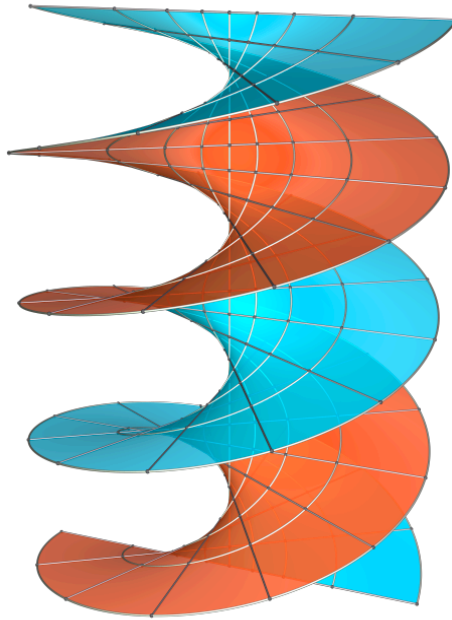


Figure 13: The helicoid, with the ruling pictured. Credit: Matthias Weber, www.indiana.edu/~minimal.

6.5.3 The Riemann Examples

Around 1860, Riemann, [Ri], classified all minimal surfaces in \mathbf{R}^3 that are foliated by circles and straight lines in horizontal planes. He showed that the only such surfaces are the plane, the catenoid, the helicoid, and a two-parameter family that is now known as the Riemann examples. The surfaces that he discovered formed a family of complete embedded minimal surfaces that are singly-periodic and have genus zero. Each of the surfaces has infinitely many parallel planar ends connected by necks (“pairs of pants”).

Modulo rigid motions, this is a 2 parameter family of minimal surfaces. The parameters are:

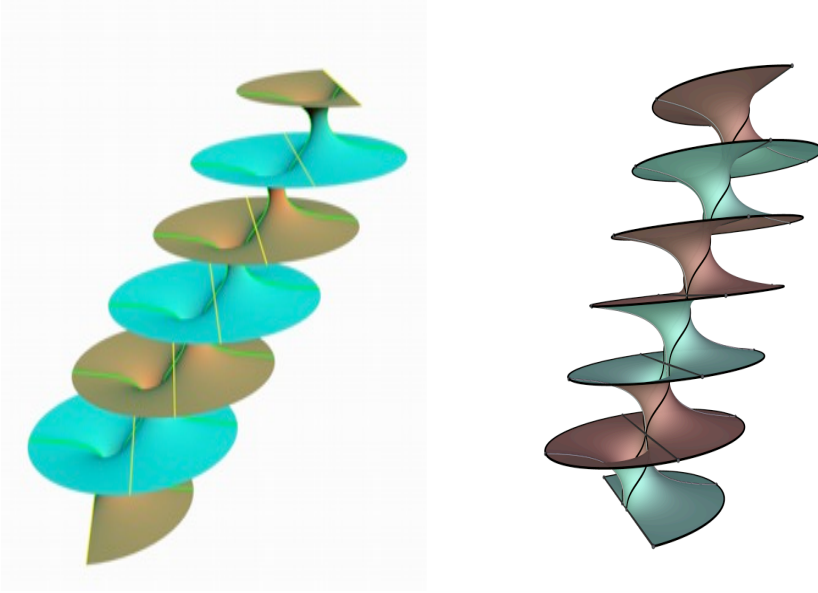


Figure 14: Two of the Riemann examples. The second one is starting to degenerate to helicoids. Credit: Matthias Weber, www.indiana.edu/~minimal.

- Neck size.
- Angle between period vector and the ends.

If we keep the neck size fixed and allow the angle to become vertical (i.e., perpendicular to the planar ends), the family degenerates to a pair of oppositely oriented helicoids. On the other hand, as the angle goes to zero, the family degenerates to a catenoid.

6.5.4 The Genus One Helicoid

In 1993, Hoffman-Karcher-Wei gave numerical evidence for the existence of a complete embedded minimal surface with genus one that is asymptotic to a helicoid; they called it a “genus one helicoid”. In [HoWW], Hoffman, Weber and Wolf constructed such a surface as the limit of “singly-periodic genus one helicoids”, where each singly-periodic genus one helicoid was constructed via the Weierstrass representation. Later, Hoffman and White constructed a genus one helicoid variationally in [HoWh1].

6.6 Second variation

Minimal surfaces are critical points for the area functional, so it is natural to look at the second derivative of the area functional at a minimal surface. This is called

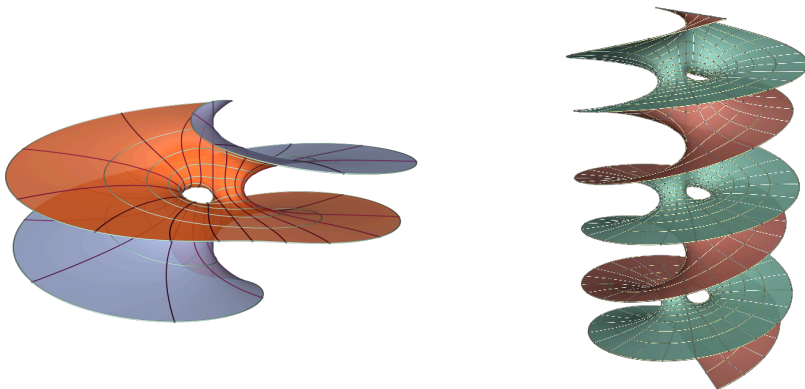


Figure 15: The genus one helicoid.

Figure 16: A periodic minimal surface asymptotic to the helicoid, whose fundamental domain has genus one.

Credit: Matthias Weber, www.indiana.edu/~minimal.

the second variation and it has played an important role in the subject since at least the work of Simons, [Sim], in 1968.

To make this precise, let Σ_0 be a 2-sided minimal hypersurface in \mathbf{R}^{n+1} , \mathbf{n} its unit normal, f a function, and define the normal variation

$$\Sigma_s = \{x + s f(x) \mathbf{n}(x) \mid x \in \Sigma_0\}.$$

A calculation (see, e.g., [CM14]) shows that the second variation of area along this one-parameter family of hypersurfaces is given by

$$\frac{d^2}{ds^2} \Big|_{s=0} \text{Vol}(\Sigma_s) = \int_{\Sigma_0} |\nabla f|^2 - |A|^2 f^2 = - \int_{\Sigma_0} f (\Delta + |A|^2) f, \quad (19)$$

where A is the second fundamental form.

When Σ_0 is minimal in a Riemannian manifold M , the formula becomes

$$\frac{d^2}{ds^2} \Big|_{s=0} \text{Vol}(\Sigma_s) = \int_{\Sigma_0} |\nabla f|^2 - |A|^2 f^2 - \text{Ric}_M(\mathbf{n}, \mathbf{n}) f^2,$$

where Ric_M is the Ricci curvature of M .

A minimal surface Σ_0 is *stable* when it passes the second derivative test, i.e., when

$$0 \leq \frac{d^2}{ds^2} \Big|_{s=0} \text{Vol}(\Sigma_s) = - \int_{\Sigma_0} f (\Delta + |A|^2) f,$$

for *every* compactly supported variation Σ_s . Analytically, stability means that the Jacobi operator $\Delta + |A|^2$ is non-negative.

There is a useful analytic criterion to determine stability:

Proposition 15. (*Fischer-Colbrie and Schoen, [FiSc]*) *A 2-sided minimal hypersurface $\Sigma \subset \mathbf{R}^3$ is stable if and only if there is a positive function u with $\Delta u = -|A|^2 u$.*

Since the normal part of a constant vector field automatically satisfies the Jacobi equation, we conclude that minimal graphs are stable. The same argument implies that minimal multi-valued graphs are stable.²

Stability is a natural condition given the variational nature of minimal surfaces, but one of the reasons that stability is useful is the following curvature estimate of R. Schoen, [Sc1]:

Theorem 16. (*Schoen, [Sc1]*) *If $\Sigma_0 \subset \mathbf{R}^3$ is stable and 2-sided and \mathcal{B}_R is a geodesic ball in Σ_0 , then*

$$\sup_{\mathcal{B}_{\frac{R}{2}}} |A| \leq \frac{C}{R},$$

where C is a fixed constant.

When Σ_0 is complete, we can let R go to infinity and conclude that Σ_0 is a plane. This Bernstein theorem was proven independently by do Carmo-Peng, [dCP], and Fischer-Colbrie-Schoen, [FiSc].

See [CM15] for a different proof of Theorem 16 and a generalization to surfaces that are stable for a parametric elliptic integrand. The key point for getting the curvature estimate is to establish uniform area bounds just using stability:

Theorem 17. (*Colding-Minicozzi, [CM15]*) *If $\Sigma^2 \subset \mathbf{R}^3$ is stable and 2-sided and \mathcal{B}_{r_0} is simply-connected, then*

$$\text{Area}(\mathcal{B}_{r_0}) \leq \frac{4\pi}{3} r_0^2. \quad (20)$$

The corresponding result is not known in higher dimensions, although Schoen, Simon and Yau proved curvature estimates assuming an area bound in low dimensions; see [ScSiY]. The counter-examples to the Bernstein problem in dimensions seven and up show that such a bound can only hold in low dimensions. However, R. Schoen has conjectured that the Bernstein theorem and curvature estimate should be true also for stable hypersurfaces in \mathbf{R}^4 :

Conjecture 18. (*Schoen*) *If $\Sigma^3 \subset \mathbf{R}^4$ is a complete immersed 2-sided stable minimal hypersurface, then Σ is flat.*

Conjecture 19. (*Schoen*) *If $\Sigma^3 \subset B_{r_0} = B_{r_0}(x) \subset M^4$ is an immersed 2-sided stable minimal hypersurface where $|K_M| \leq k^2$, $r_0 < \rho_1(\pi/k, k)$, and $\partial\Sigma \subset \partial B_{r_0}$, then for some $C = C(k)$ and all $0 < \sigma \leq r_0$,*

$$\sup_{B_{r_0-\sigma}} |A|^2 \leq C \sigma^{-2}. \quad (21)$$

Any progress on these conjectures would be enormously important for the theory of minimal hypersurfaces in \mathbf{R}^4 .

²A multi-valued graph is a surface that is locally a graph over a subset of the plane, but the projection down to the plane is not one to one.

7 Classification of embedded minimal surfaces

One of the most fundamental questions about minimal surfaces is to classify or describe the space of all complete embedded minimal surfaces in \mathbf{R}^3 . We have already seen three results of this type:

1. Bernstein showed that a complete minimal graph must be a plane.
2. Catalan showed that a ruled minimal surface is either a plane or a helicoid.
3. A minimal surface of revolution must be a plane or a catenoid.

Each of these theorems makes a rather strong hypothesis on the class of surfaces. It would be more useful to have classifications under weaker hypotheses, such as just as the topological type of the surface.

The last decade has seen enormous progress on the classification of embedded minimal surfaces in \mathbf{R}^3 by their topology. The surfaces are generally divided into three cases, according to the topology:

- Disks.
- Planar domains - i.e., genus zero.
- Positive genus.

The classification of complete surfaces has relied heavily upon breakthroughs on the local descriptions of pieces of embedded minimal surfaces with finite genus.

7.1 The topology of minimal surfaces

The topology of a compact connected oriented surface without boundary is described by a single non-negative number: the genus. The sphere has genus zero, the torus has genus one, and the connected sum of k -tori has genus k .

The genus of an oriented surface with boundary is defined to be the genus of the compact surface that you get by gluing in a disk along each boundary component. Since an annulus with two disks glued in becomes a sphere, the annulus has genus zero. Thus, the topology of a connected oriented surface with boundary is described by two numbers: the genus and the number of boundary components.

The last topological notion that we will need is *properness*. An immersed submanifold $\Sigma \subset M$ is proper when the intersection of Σ with any compact set in M is compact. Clearly, every compact submanifold is automatically proper.

There are two important monotonicity properties for the topology of minimal surfaces in \mathbf{R}^3 ; one does not use minimality and one does.

Lemma 20. *If Σ has genus k and $\Sigma_0 \subset \Sigma$, then the genus of Σ_0 is at most k .*

Proof. This follows immediately from the definition of the genus and does not use minimality. \square

Lemma 21. *If $\Sigma \subset \mathbf{R}^3$ is a properly embedded minimal surface and $B_R(0) \cap \partial\Sigma = \emptyset$, then the inclusion of $B_R(0) \cap \Sigma$ into Σ is an injection on the first homology group.*

Proof. If not, then $B_R(0) \cap \Sigma$ contains a one-cycle γ that does not bound a surface in $B_R(0) \cap \Sigma$ but does bound a surface $\Gamma \subset \Sigma$. However, Γ is then a minimal surface that must leave $B_R(0)$ but with $\partial\Gamma \subset B_R(0)$, contradicting the convex hull property (Proposition 13). \square

This has the following immediate corollary for disks:

Corollary 22. *If Σ is a properly embedded minimal disk, then each component of $B_R(0) \cap \Sigma$ is a disk.*

7.2 Multi-valued graphs

We will need the notion of a multi-valued graph from [CM6]–[CM9]. At a first approximation, a multi-valued graph is locally a graph over a subset of the plane but the projection down is not one to one. Thus, it shares many properties with minimal graphs, including stability, but includes new possibilities such as the helicoid minus the vertical axis.

To be precise, let D_r be the disk in the plane centered at the origin and of radius r and let \mathcal{P} be the universal cover of the punctured plane $\mathbf{C} \setminus \{0\}$ with global polar coordinates (ρ, θ) so $\rho > 0$ and $\theta \in \mathbf{R}$. Given $0 \leq r \leq s$ and $\theta_1 \leq \theta_2$, define the “rectangle” $S_{r,s}^{\theta_1, \theta_2} \subset \mathcal{P}$ by

$$S_{r,s}^{\theta_1, \theta_2} = \{(\rho, \theta) \mid r \leq \rho \leq s, \theta_1 \leq \theta \leq \theta_2\}. \quad (22)$$

An N -valued graph of a function u on the annulus $D_s \setminus D_r$ is a single valued graph over

$$S_{r,s}^{-N\pi, N\pi} = \{(\rho, \theta) \mid r \leq \rho \leq s, |\theta| \leq N\pi\}. \quad (23)$$

($\Sigma_{r,s}^{\theta_1, \theta_2}$ will denote the subgraph of Σ over the smaller rectangle $S_{r,s}^{\theta_1, \theta_2}$). The multi-valued graphs that we will consider will never close up; in fact they will all be embedded. Note that embedded corresponds to that the separation never vanishes. Here the separation w is the difference in height between consecutive sheets and is therefore given by

$$w(\rho, \theta) = u(\rho, \theta + 2\pi) - u(\rho, \theta). \quad (24)$$

In the case where Σ is the helicoid [i.e., Σ can be parametrized by $(s \cos t, s \sin t, t)$ where $s, t \in \mathbf{R}$], then

$$\Sigma \setminus x_3\text{-axis} = \Sigma_1 \cup \Sigma_2, \quad (25)$$

where Σ_1, Σ_2 are ∞ -valued graphs. Σ_1 is the graph of the function $u_1(\rho, \theta) = \theta$ and Σ_2 is the graph of the function $u_2(\rho, \theta) = \theta + \pi$. In either case the separation $w = 2\pi$.

Note that for an embedded multi-valued graph, the sign of w determines whether the multi-valued graph spirals in a left-handed or right-handed manner, in other words, whether upwards motion corresponds to turning in a clockwise direction or in a counterclockwise direction.

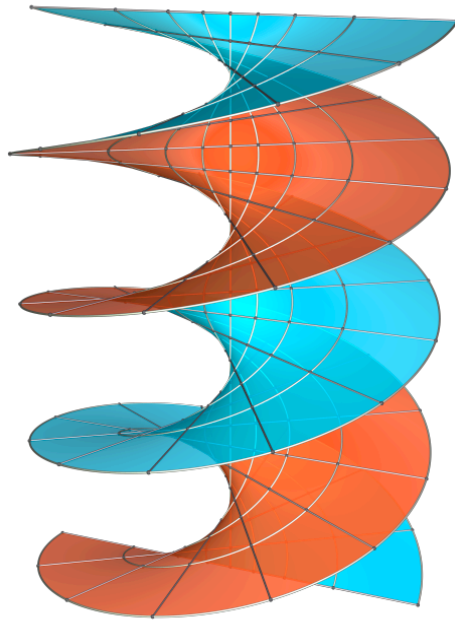


Figure 17: Multi-valued graphs. The helicoid is obtained by gluing together two ∞ -valued graphs along a line. Credit: Matthias Weber, www.indiana.edu/~minimal.

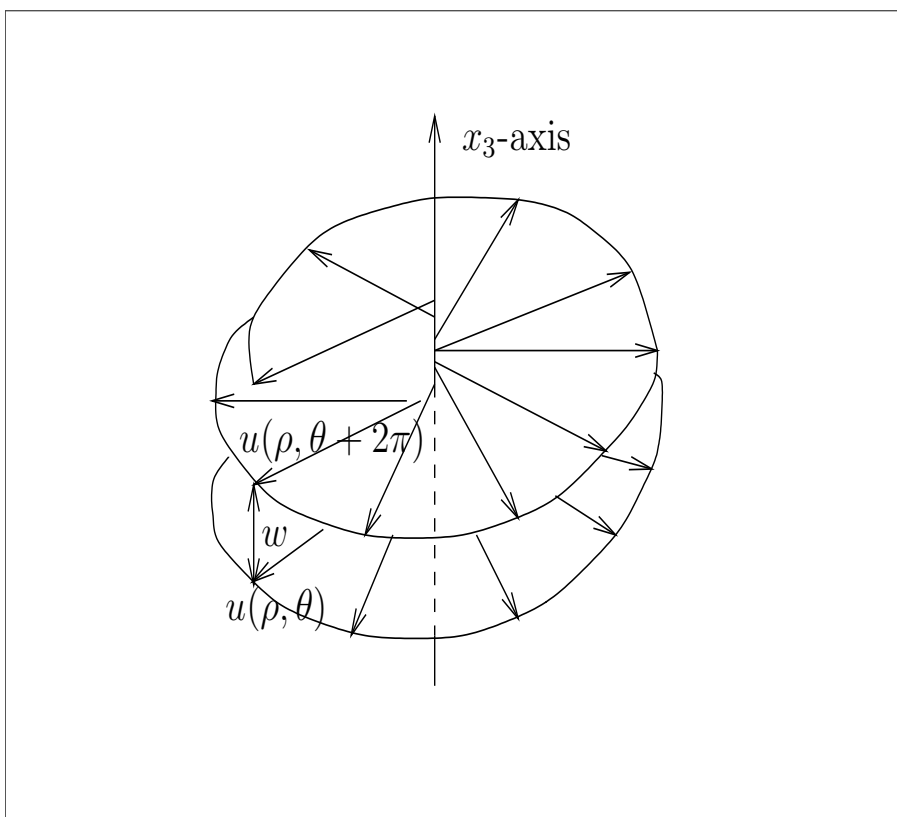


Figure 18: The separation w for a multi-valued minimal graph.

7.3 Disks are double spiral staircases or graphs

We will describe first the local classification of properly embedded minimal disks that follows from [CM6]–[CM9]. This turns out to be the key step for understanding embedded minimal surfaces with finite genus since any of these can be decomposed into pieces that are either disks or pairs of pants.

There are two classical models for embedded minimal disks. The first is a minimal graph over a simply-connected domain in \mathbf{R}^2 (such as the plane itself), while the second is a double spiral staircase like the helicoid. A double spiral staircase consists of two staircases that spiral around one another so that two people can pass each other without meeting.

In [CM6]–[CM9] we showed that these are the only possibilities and, in fact, every embedded minimal disk is either a minimal graph or can be approximated by a piece of a rescaled helicoid. It is graph when the curvature is small and is part of a helicoid when the curvature is above a certain threshold.

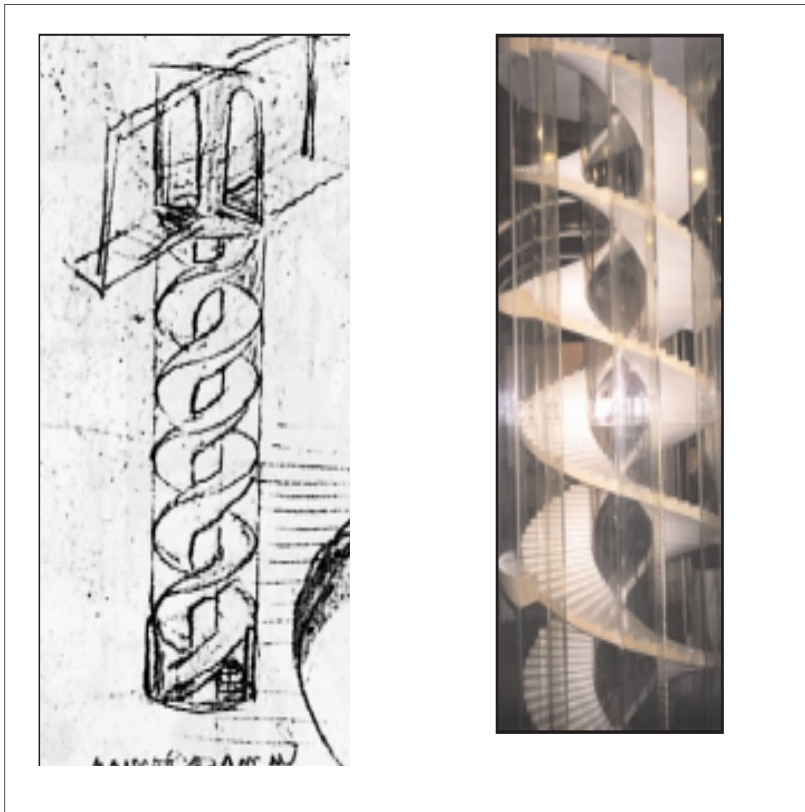


Figure 19: Left: Drawing by Leonardo Da Vinci of a double spiral staircase from around 1490. Right: Model of Da Vinci's double spiral staircase in Château de Chambord. Both figures reprinted from [CM20].

The main point in the proof is to show the double spiral staircase structure when the curvature is large. The proof of this is long, but can be split into three main steps.

Three main steps.

A. Fix an integer N (the “large” of the curvature in what follows will depend on N). If an embedded minimal disk Σ is not a graph (or equivalently if the curvature is large at some point), then it contains an N -valued minimal graph which initially is shown to exist on the scale of $1/\max|A|$. That is, the N -valued graph is initially shown to be defined on an annulus with both inner and outer radius inversely proportional to $\max|A|$.

B. Such a potentially small N -valued graph sitting inside Σ can then be seen to extend as an N -valued graph inside Σ almost all the way to the boundary. That is, the small N -valued graph can be extended to an N -valued graph defined on an annulus where the outer radius of the annulus is proportional to R . Here R is the radius of the ball in \mathbf{R}^3 that the boundary of Σ is contained in.

C. The N -valued graph not only extends horizontally (i.e., tangent to the initial sheets) but also vertically (i.e., transversally to the sheets). That is, once there are N sheets there are many more and, in fact, the disk Σ consists of two multi-valued graphs glued together along an axis.

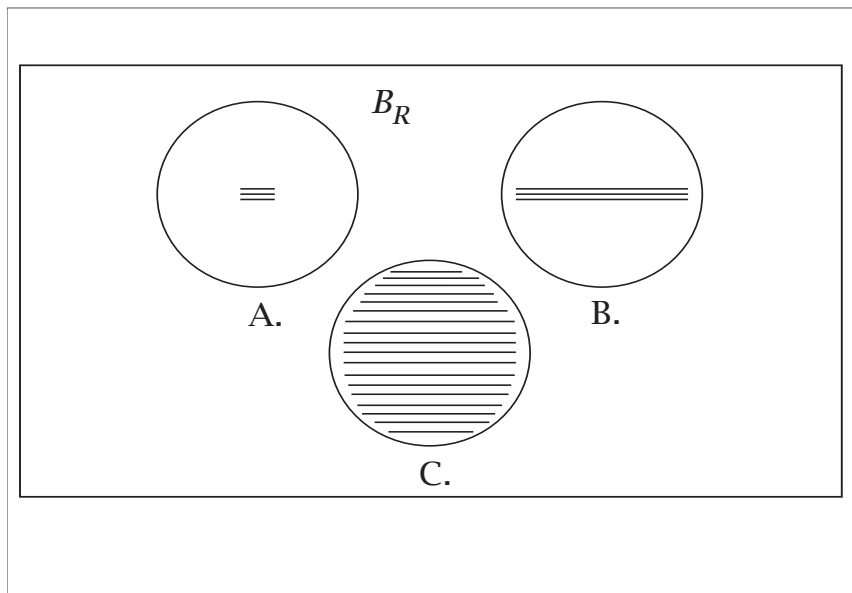


Figure 20: Three main steps: A. Finding a small N -valued graph in Σ . B. Extending it in Σ to a large N -valued graph. C. Extend the number of sheets.

This general structure result for embedded minimal disks, and the methods used in its proof, give a compactness theorem for sequences of embedded minimal disks. This theorem is modelled on rescalings of the helicoid and the precise

statement is as follows (we state the version for extrinsic balls; it was extended to intrinsic balls in [CM12]):

Theorem 23. (Theorem 0.1 in [CM9].) *Let $\Sigma_i \subset B_{R_i} = B_{R_i}(0) \subset \mathbf{R}^3$ be a sequence of embedded minimal disks with $\partial\Sigma_i \subset \partial B_{R_i}$ where $R_i \rightarrow \infty$. If*

$$\sup_{B_1 \cap \Sigma_i} |A|^2 \rightarrow \infty, \quad (26)$$

then there exists a subsequence, Σ_j , and a Lipschitz curve $\mathcal{S} : \mathbf{R} \rightarrow \mathbf{R}^3$ such that after a rotation of \mathbf{R}^3 :

1. $x_3(\mathcal{S}(t)) = t$. (That is, \mathcal{S} is a graph over the x_3 -axis.)
2. Each Σ_j consists of exactly two multi-valued graphs away from \mathcal{S} (which spiral together).
3. For each $1 > \alpha > 0$, $\Sigma_j \setminus \mathcal{S}$ converges in the C^α -topology to the foliation, $\mathcal{F} = \{x_3 = t\}_t$, of \mathbf{R}^3 .
4. $\sup_{B_r(\mathcal{S}(t)) \cap \Sigma_j} |A|^2 \rightarrow \infty$ for all $r > 0$, $t \in \mathbf{R}$. (The curvatures blow up along \mathcal{S} .)

This theorem is sometimes referred to as *the lamination theorem*. Meeks showed in [Me2] that the Lipschitz curve \mathcal{S} is in fact a straight line perpendicular to the foliation.

The assumption that the radii R_i go to infinity is used in several ways in the proof. This guarantees that the leaves are planes (this uses the Bernstein theorem), but it also is used to show that the singularities are removable. We will see in the next subsection that this is not always the case in the “local case” where the R_i remain bounded.

7.4 The local case

In contrast to the global case of the previous subsection, there are local examples of sequence of minimal surfaces that do not converge to a foliation. The first such example was constructed in [CM17], where we constructed a sequence of embedded minimal disks in a unit ball in \mathbf{R}^3 so that:

- Each contains the x_3 -axis.
- Each is given by two multi-valued graphs over $\{x_3 = 0\} \setminus \{0\}$.
- The graphs spiral faster and faster near $\{x_3 = 0\}$.

The precise statement is:

Theorem 24. (Colding-Minicozzi, [CM17]) *There is a sequence of compact embedded minimal disks $0 \in \Sigma_i \subset B_1 \subset \mathbf{R}^3$ with $\partial\Sigma_i \subset \partial B_1$ and containing the vertical segment $\{(0, 0, t) \mid |t| < 1\} \subset \Sigma_i$ so:*

- (1) $\lim_{i \rightarrow \infty} |A_{\Sigma_i}|^2(0) = \infty$.
- (2) $\sup_i \sup_{\Sigma_i \setminus B_\delta} |A_{\Sigma_i}|^2 < \infty$ for all $\delta > 0$.
- (3) $\Sigma_i \setminus \{x_3\text{-axis}\} = \Sigma_{1,i} \cup \Sigma_{2,i}$ for multi-valued graphs $\Sigma_{1,i}$ and $\Sigma_{2,i}$.
- (4) $\Sigma_i \setminus \{x_3 = 0\}$ converges to two embedded minimal disks $\Sigma^\pm \subset \{\pm x_3 > 0\}$ with $\bar{\Sigma}^\pm \setminus \Sigma^\pm = B_1 \cap \{x_3 = 0\}$. Moreover, $\Sigma^\pm \setminus \{x_3\text{-axis}\} = \Sigma_1^\pm \cup \Sigma_2^\pm$ for multi-valued graphs Σ_1^\pm and Σ_2^\pm each of which spirals into $\{x_3 = 0\}$; see fig. 21.

It follows from (4) that $\Sigma_i \setminus \{0\}$ converges to a lamination of $B_1 \setminus \{0\}$ (with leaves Σ^- , Σ^+ , and $B_1 \cap \{x_3 = 0\} \setminus \{0\}$) which does not extend to a lamination of B_1 . Namely, 0 is not a removable singularity.

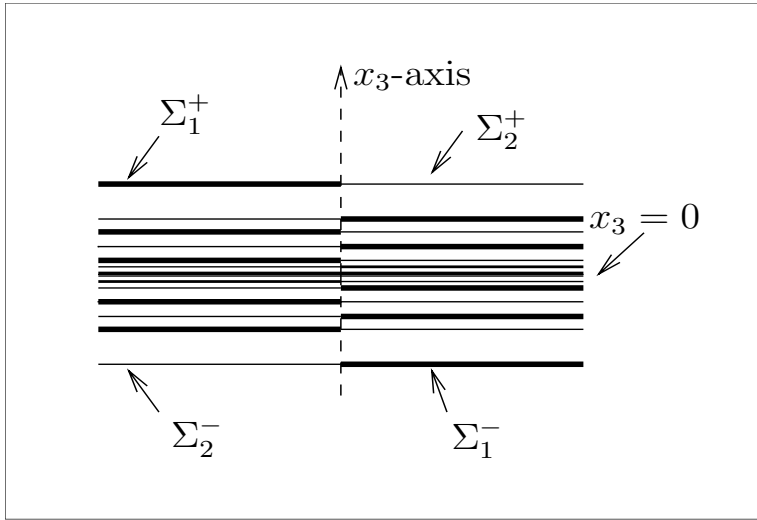


Figure 21: A schematic picture of the examples in Theorem 24. Removing the x_3 -axis disconnects the surface into two multi-valued graphs; one of these is in bold.

There are now a number of other interesting local examples of singular limit laminations:

- Meeks-Weber, [MeWe]: The Meeks-Weber bent helicoids are sequences of minimal surfaces defined in a tub about a curve that converge to a minimal foliation of the tube except along the curve itself and this curve is the singular set.
- Dean, [De]: Dean generalized the construction of [CM17] to get isolated singular points.
- Khan, [Kh]: Khan used the Weierstrass representation to construct sequences of spiraling multi-valued graphs where curvature blows up on half an interval.

- Hoffman-White, [HoWh2]: They proved the definitive existence result for subsets of an axis by getting an arbitrary closed subset as the singular set. Their proof is variational, seizing on the fact that half of the helicoid is area-minimizing (and then using reflection to construct the other half).
- Kleene, [Kl]: Gave different proof of Hoffman-White using the Weierstrass representation in the spirit of [CM17], [De] and [Kh].
- Calle-Lee, [CaL]: Constructed local helicoids in Riemannian manifolds.

One of the most interesting questions is when does a minimal lamination have removable singularities? This is most interesting when for minimal limit laminations that arise from sequences of embedded minimal surfaces. It is clear from these examples that this is a global question. This question really has two separate cases depending on the topology of the leaves near the singularity. When the leaves are simply connected, the only possibility is the spiraling and multi-valued graph structure proven in [CM6]–[CM9]; see [CM18] for a flux argument to get removability in the global case. A different type of singularity occurs when the injectivity radius of the leaves goes to zero at a singularity; examples of this were constructed by Colding and De Lellis in [CD]. The paper [CM10] has a similar flux argument for the global case where the leaves are not simply-connected.

7.5 The one-sided curvature estimate

One of the key tools used to understand embedded minimal surfaces is the one-sided curvature estimate proven in [CM9] using the structure theory developed in [CM6]–[CM9].

The one-sided curvature estimate roughly states that an embedded minimal disk that lies on one-side of a plane, but comes close to the plane, has bounded curvature. Alternatively, it says that if the curvature is large at the center of a ball, then the minimal disk propagates out in all directions so that it cannot be contained on one side of any plane that passes near the center of the ball.

Theorem 25. (Colding-Minicozzi, [CM9]) *There exists $\epsilon_0 > 0$ so that the following holds. Let $y \in \mathbf{R}^3$, $r_0 > 0$ and*

$$\Sigma^2 \subset B_{2r_0}(y) \cap \{x_3 > x_3(y)\} \subset \mathbf{R}^3 \quad (27)$$

be a compact embedded minimal disk with $\partial\Sigma \subset \partial B_{2r_0}(y)$. For any connected component Σ' of $B_{r_0}(y) \cap \Sigma$ with $B_{\epsilon_0 r_0}(y) \cap \Sigma' \neq \emptyset$,

$$\sup_{\Sigma'} |A_{\Sigma'}|^2 \leq r_0^{-2}. \quad (28)$$

The example of a rescaled catenoid shows that simply-connected and embedded are both essential hypotheses for the one-sided curvature estimate. More precisely, the height of the catenoid grows logarithmically in the distance to the axis of rotation. In particular, the intersection of the catenoid with B_{r_0} lies in a slab of thickness $\approx \log r_0$ and the ratio of

$$\frac{\log r_0}{r_0} \rightarrow 0 \text{ as } r_0 \rightarrow \infty. \quad (29)$$

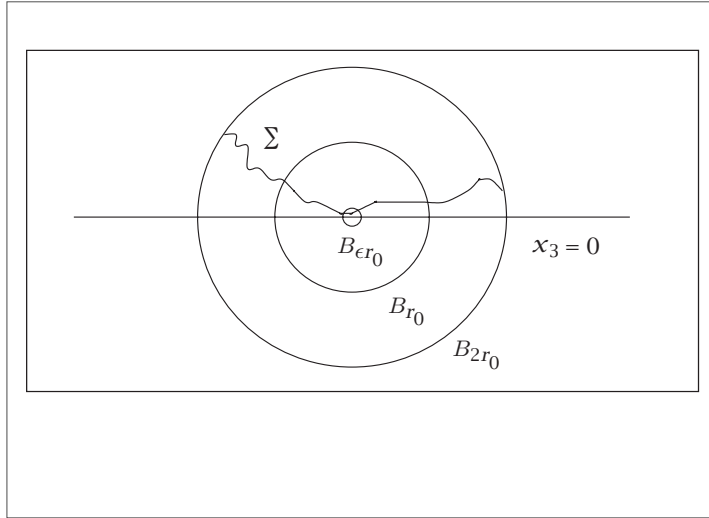


Figure 22: The one-sided curvature estimate.

Thus, after dilating the catenoid by $\frac{1}{j}$, we get a sequence of minimal surfaces in the unit ball that converges as sets to $\{x_3 = 0\}$ as $j \rightarrow \infty$. However, the catenoid is not flat, so these rescaled catenoids have $|A| \rightarrow \infty$ and (28) does not apply for j large.

7.6 Genus zero have pair of pants decomposition

Thus far, we have concentrated on the case of embedded minimal disks. We turn next to the general case of embedded minimal planar domains (i.e., where the surfaces have genus zero but may not be simply connected). The new possibilities are illustrated by Riemann's family of examples where small necks connect large graphical regions that are asymptotic to planes. Cutting along these small necks, one can decompose the Riemann examples into "pairs of pants" that are topologically disks with two sub-disks removed (think of the outer boundary as the waist and the two inner boundaries corresponding to the legs).

One of the main results from [CM10] is that a general embedded minimal planar domain has a similar pair of pants decomposition:

Theorem 26. *Any nonsimply connected embedded minimal planar domain with a small neck can be cut along a collection of short curves. After the cutting, we are left with graphical pieces that are defined over a disk with either one or two subdisks removed (a topological disk with two subdisks removed is called a pair of pants). Moreover, if for some point the curvature is large, then all of the necks are very small.*

The following compactness result is a consequence:

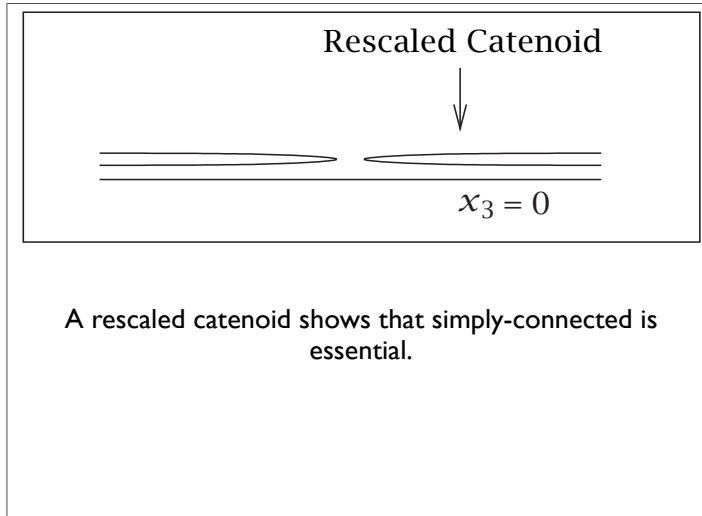
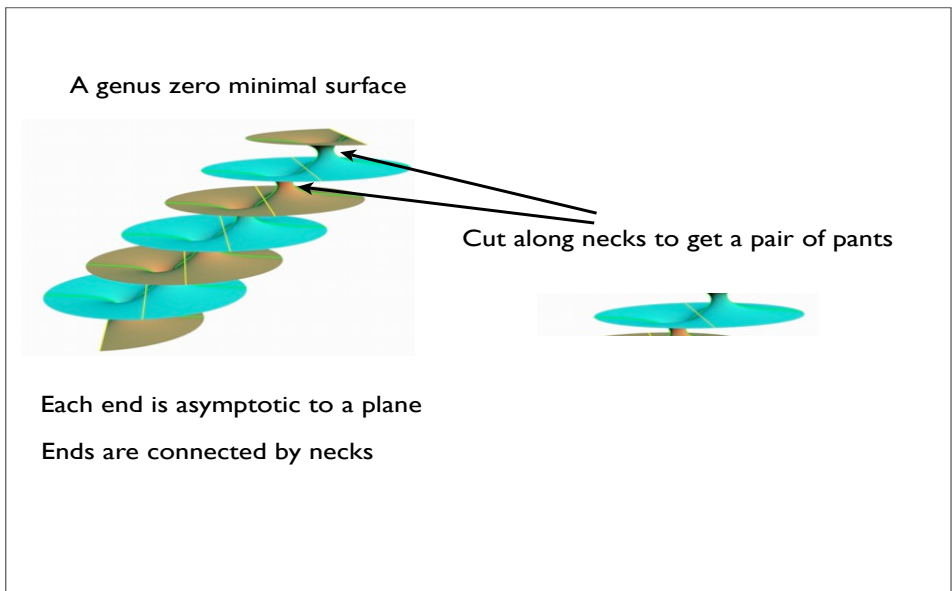


Figure 23: Rescaled catenoids.

Figure 24: The pair of pants decomposition. Credit: Matthias Weber, www.indiana.edu/~minimal.

Corollary 27. (Colding-Minicozzi, [CM10]) *A sequence of embedded minimal planar domains that are not ULSC, but with curvatures blowing up, has a subsequence that converges to a collection of flat parallel planes.*

In the next section, we will turn to finer structure and compactness theorems for sequences of planar domains.

7.7 Compactness theorems for planar domains

In order to describe the results for sequence of planar domains, it will be useful to divide things into two cases depending on whether or not the topology is concentrating a points. To distinguish between these cases, we will say that a sequence of surfaces $\Sigma_i^2 \subset \mathbf{R}^3$ is *uniformly locally simply connected* (or ULSC) if for each compact subset K of \mathbf{R}^3 , there exists a constant $r_0 > 0$ (depending on K) so that for every $x \in K$, all $r \leq r_0$, and every surface Σ_i

$$\text{each connected component of } B_r(x) \cap \Sigma_i \text{ is a disk.} \quad (30)$$

For instance, a sequence of rescaled catenoids where the necks shrink to zero is not ULSC, whereas a sequence of rescaled helicoids is.

Another way of locally distinguishing sequences where the topology does not concentrate from sequences where it does comes from analyzing the singular set. The singular set \mathcal{S} is defined to be the set of points where the curvature is blowing up. That is, a point y in \mathbf{R}^3 is in \mathcal{S} for a sequence Σ_i if

$$\sup_{B_r(y) \cap \Sigma_i} |A|^2 \rightarrow \infty \text{ as } i \rightarrow \infty \text{ for all } r > 0. \quad (31)$$

We will show that for embedded minimal surfaces \mathcal{S} consists of two types of points. The first type is roughly modelled on rescaled helicoids and the second on rescaled catenoids:

- A point y in \mathbf{R}^3 is in \mathcal{S}_{ulsc} if the curvature for the sequence Σ_i blows up at y and the sequence is ULSC in a neighborhood of y .
- A point y in \mathbf{R}^3 is in \mathcal{S}_{neck} if the sequence is not ULSC in any neighborhood of y . In this case, a sequence of closed non-contractible curves $\gamma_i \subset \Sigma_i$ converges to y .

The sets \mathcal{S}_{neck} and \mathcal{S}_{ulsc} are obviously disjoint and the curvature blows up at both, so $\mathcal{S}_{neck} \cup \mathcal{S}_{ulsc} \subset \mathcal{S}$. An easy argument will later show that, after passing to a subsequence, we can assume that

$$\mathcal{S} = \mathcal{S}_{neck} \cup \mathcal{S}_{ulsc}. \quad (32)$$

Note that $\mathcal{S}_{neck} = \emptyset$ is equivalent to that the sequence is ULSC as is the case for sequences of rescaled helicoids. On the other hand, $\mathcal{S}_{ulsc} = \emptyset$ for sequences of rescaled catenoids.

We will show that every sequence Σ_i has a subsequence that is either ULSC or for which \mathcal{S}_{ulsc} is empty. This is the next “no mixing” theorem. We will see later that these two different cases give two very different structures.

Theorem 28. (Colding-Minicozzi, [CM10]) *If $\Sigma_i \subset B_{R_i} = B_{R_i}(0) \subset \mathbf{R}^3$ is a sequence of compact embedded minimal planar domains with $\partial\Sigma_i \subset \partial B_{R_i}$ where $R_i \rightarrow \infty$, then there is a subsequence with either $\mathcal{S}_{ulsc} = \emptyset$ or $\mathcal{S}_{neck} = \emptyset$.*

In view of Theorem 28 and the earlier results for disks, it is natural to first analyze sequences that are ULSC, so where $\mathcal{S}_{neck} = \emptyset$, and second analyze sequences where \mathcal{S}_{ulsc} is empty. We will do this next.

Common for both the ULSC case and the case where \mathcal{S}_{ulsc} is empty is that the limits are always laminations by flat parallel planes and the singular sets are always closed subsets contained in the union of the planes. This is the content of the next theorem:

Theorem 29. (Colding-Minicozzi, [CM10]) *Let $\Sigma_i \subset B_{R_i} = B_{R_i}(0) \subset \mathbf{R}^3$ be a sequence of compact embedded minimal planar domains with $\partial\Sigma_i \subset \partial B_{R_i}$ where $R_i \rightarrow \infty$. If*

$$\sup_{B_1 \cap \Sigma_i} |A|^2 \rightarrow \infty, \quad (33)$$

then there exists a subsequence Σ_j , a lamination $\mathcal{L} = \{x_3 = t\}_{\{t \in \mathcal{I}\}}$ of \mathbf{R}^3 by parallel planes (where $\mathcal{I} \subset \mathbf{R}$ is a closed set), and a closed nonempty set \mathcal{S} in the union of the leaves of \mathcal{L} such that after a rotation of \mathbf{R}^3 :

- (A) *For each $1 > \alpha > 0$, $\Sigma_j \setminus \mathcal{S}$ converges in the C^α -topology to the lamination $\mathcal{L} \setminus \mathcal{S}$.*
- (B) *$\sup_{B_r(x) \cap \Sigma_j} |A|^2 \rightarrow \infty$ as $j \rightarrow \infty$ for all $r > 0$ and $x \in \mathcal{S}$. (The curvatures blow up along \mathcal{S} .)*

Loosely speaking, our next result shows that when the sequence is ULSC (but not simply connected), a subsequence converges to a foliation by parallel planes away from two lines \mathcal{S}_1 and \mathcal{S}_2 . The lines \mathcal{S}_1 and \mathcal{S}_2 are disjoint and orthogonal to the leaves of the foliation and the two lines are precisely the points where the curvature is blowing up. This is similar to the case of disks, except that we get two singular curves for non-disks as opposed to just one singular curve for disks.

Theorem 30. (Colding-Minicozzi, [CM10]) *Let a sequence Σ_i , limit lamination \mathcal{L} , and singular set \mathcal{S} be as in Theorem 29. Suppose that each $B_R(0) \cap \Sigma_i$ is not simply-connected. If every Σ_i is ULSC and*

$$\sup_{B_1 \cap \Sigma_i} |A|^2 \rightarrow \infty, \quad (34)$$

then the limit lamination \mathcal{L} is the foliation $\mathcal{F} = \{x_3 = t\}_t$ and the singular set \mathcal{S} is the union of two disjoint lines \mathcal{S}_1 and \mathcal{S}_2 such that:

- (C_{ulsc}) *Away from $\mathcal{S}_1 \cup \mathcal{S}_2$, each Σ_j consists of exactly two multi-valued graphs spiraling together. Near \mathcal{S}_1 and \mathcal{S}_2 , the pair of multi-valued graphs form double spiral staircases with opposite orientations at \mathcal{S}_1 and \mathcal{S}_2 . Thus, circling only \mathcal{S}_1 or only \mathcal{S}_2 results in going either up or down, while a path circling both \mathcal{S}_1 and \mathcal{S}_2 closes up.*

(D_{ulsc}) \mathcal{S}_1 and \mathcal{S}_2 are orthogonal to the leaves of the foliation.

Theorem 31. (Colding-Minicozzi, [CM10]) *Let a sequence Σ_i , limit lamination \mathcal{L} , and singular set \mathcal{S} be as in Theorem 29. If $\mathcal{S}_{ulsc} = \emptyset$ and*

$$\sup_{B_1 \cap \Sigma_i} |A|^2 \rightarrow \infty, \quad (35)$$

then $\mathcal{S} = \mathcal{S}_{neck}$ by (32) and

(C_{neck}) *Each point y in \mathcal{S} comes with a sequence of graphs in Σ_j that converge to the plane $\{x_3 = x_3(y)\}$. The convergence is in the C^∞ topology away from the point y and possibly also one other point in $\{x_3 = x_3(y)\} \cap \mathcal{S}$. If the convergence is away from one point, then these graphs are defined over annuli; if the convergence is away from two points, then the graphs are defined over disks with two subdisks removed.*

7.8 Uniqueness of complete examples: Catenoid

The catenoid is the only (non-flat) minimal surface of revolution, but there are a number of other ways to uniquely characterize it. We will discuss this next. In this subsection, Σ will always be **complete**, **minimal**, and **embedded** in \mathbf{R}^3 .

The first modern results assumed that Σ has finite total curvature³:

Theorem 32. (Schoen, [Sc2]) *The catenoid is the unique Σ with finite total curvature and two ends.*

It follows from Schoen's result that an embedded finite total curvature minimal surface with two ends cannot have positive genus.

Theorem 33. (Lopez and Ros, [LRo]) *The catenoid is the unique (non-flat) Σ with finite total curvature and genus zero.*

The main point of the Lopez-Ros theorem is to show that a (finite total curvature) genus zero minimal surface with more than two ends cannot be embedded.

A major breakthrough came in 1997 with Collin's proof of the generalized Nitsche conjecture:

Theorem 34. (Collin, [Co]) *If Σ is proper, has finite topology and at least two ends, then it has finite total curvature.*

[CM11] gives an alternative proof of Collin's theorem using the one-sided curvature estimate. The assumption that Σ has at least two ends rules out the possibility of the helicoid (which has infinite total curvature)

Finally, in 2008, Colding-Minicozzi, [CM12], showed that embeddedness and finite topology together imply properness, thus removing the assumption of properness. The final result is:

³A minimal surface Σ has finite total curvature if $\int_{\Sigma} |A|^2 < \infty$.

Theorem 35. (Schoen, Lopez-Ros, Collin, Colding-Minicozzi) *The catenoid is only complete embedded minimal surface with finite topology and either:*

- *Exactly two ends, or*
- *Genus zero and more than one end.*

There are local versions of these global uniqueness results for the catenoid. The starting point is a local version of Collin's result that follows from the argument of [CM11], using the one-sided curvature estimate, although it is not recorded there. This was done in [CM16], where the following local version was proven:

Theorem 36. (Colding-Minicozzi, [CM16]) *There exist $\epsilon > 0$ and $C_1, C_2, C_3 > 1$ so that: If $\Sigma \subset B_R \subset \mathbf{R}^3$ is an embedded minimal annulus with $\partial\Sigma \subset \partial B_R$ and $\pi_1(B_{\epsilon R} \cap \Sigma) \neq 0$, then there is a simple closed geodesic $\gamma \subset \Sigma$ of length ℓ so that:*

- *The curve γ splits the connected component of $B_{R/C_1} \cap \Sigma$ containing it into annuli Σ^+ and Σ^- , each with $\int |A|^2 \leq 5\pi$.*
- *Each of $\Sigma^\pm \setminus \mathcal{T}_{C_2\ell}(\gamma)$ is a graph with gradient ≤ 1 .*
- *$\ell \log(R/\ell) \leq C_3 h$ where the separation h is given by*

$$h \equiv \min \{ |x^+ - x^-| \mid x^\pm \in \partial B_{R/C_1} \cap \Sigma^\pm \} .$$

Here $\mathcal{T}_s(S)$ denotes the (intrinsic in Σ) tubular neighborhood of radius s about the set $S \subset \Sigma$.

7.9 Uniqueness of complete examples: Helicoid

In this subsection, Σ will always be **complete, minimal, and embedded** in \mathbf{R}^3 .

Using the lamination theorem and one-sided curvature estimate from [CM6]–[CM9], Meeks-Rosenberg proved the uniqueness of the helicoid in 2005:

Theorem 37. (Meeks-Rosenberg, [MeR2]) *The helicoid is the unique (non-flat) proper, simply-connected Σ .*

By [CM12], the assumption of properness can be removed in Theorem 37.

Again using [CM6]–[CM9], Meeks-Rosenberg and Bernstein-Breiner studied the ends of finite genus embedded minimal surfaces, showing that these are asymptotic to helicoids. The Bernstein-Breiner theorem gives:

Theorem 38. (Bernstein-Breiner, [BB2]) *Any (non-flat) finite genus Σ with one end is asymptotic to a helicoid.*

In particular, any finite genus embedded minimal surface with one end must be conformal to a punctured Riemann surface and one gets rather good control on the Weierstrass data (it has an essential singularity at the puncture, but of the same type that the helicoid does). It would be very interesting to get a finer description of the moduli space of such examples. One natural result in this direction is a recent theorem of Bernstein and Breiner (that proves a conjecture of Bobenko, [Bo]):

Theorem 39. (Bernstein-Breiner, [BB3]) *Let Σ be an embedded genus one helicoid in \mathbf{R}^3 . Then there is a line ℓ so that rotation by 180 degrees about ℓ is an orientation preserving isometry of Σ .*

7.10 Uniqueness of complete examples: Riemann examples

Using [CM6]–[CM10] and Colding-De Lellis-Minicozzi, [CDM], Meeks-Perez-Ros recently showed that the Riemann examples are the unique Σ 's with genus zero and infinitely many ends.

Theorem 40. (Meeks-Perez-Ros, [MePRs4]) *The Riemann examples are the unique complete properly embedded minimal planar domains with infinitely many ends.*

This theorem completes the classification of the genus zero properly embedded minimal surfaces. Remarkably, it turned out that the classical examples discovered in the 1700's and 1800's were the only ones. A number of central questions remain, including the structure of the moduli space of finite genus properly embedded minimal surfaces and the systematic construction of examples.

7.11 Calabi-Yau conjectures

Recall that an immersed submanifold in \mathbf{R}^n is proper if the pre-image of any compact subset of \mathbf{R}^n is compact in the surface. This property has played an important role in the theory of minimal submanifolds and many of the classical theorems in the subject assume that the submanifold is proper. It is easy to see that any compact submanifold is automatically proper. On the other hand, there is no reason to expect a general immersion to be proper. For example, the non-compact curve parametrized in polar coordinates by

$$\begin{aligned}\rho(t) &= \pi + \arctan(t), \\ \theta(t) &= t\end{aligned}$$

spirals infinitely between the circles of radius $\pi/2$ and $3\pi/2$. However, it was long thought that a minimal immersion (or embedding) should be better behaved. This principle was captured by the Calabi-Yau conjectures. Their original form was given in 1965 in [Ce] where E. Calabi made the following two conjectures about minimal surfaces (see also S.S. Chern, page 212 of [Cs] and S.T. Yau's 1982 problem list, [Ya3]):

Conjecture 41. *“Prove that a complete minimal hypersurface in \mathbf{R}^n must be unbounded.”*

Calabi continued: “It is known that there are no compact minimal submanifolds of \mathbf{R}^n (or of any simply connected complete Riemannian manifold with sectional curvature ≤ 0). A more ambitious conjecture is”:

Conjecture 42. *“A complete [non-flat] minimal hypersurface in \mathbf{R}^n has an unbounded projection in every $(n - 2)$ -dimensional flat subspace.”*

The immersed versions of these conjectures were shown to be false by examples of Jorge and Xavier, [JXa2], and N. Nadirashvili, [Na]. The latter constructed a complete immersion of a minimal disk into the unit ball in \mathbf{R}^3 , showing that Conjecture 41 also failed for immersed surfaces; cf. [MaMo1], [LMaMo1], [LMaMo2].

It is clear from the definition of proper that a proper minimal surface in \mathbf{R}^3 must be unbounded, so the examples of Nadirashvili are not proper.

The strong halfspace theorem of D. Hoffman and W. Meeks shows that properness also prevented a minimal surface from being contained in a slab, or even a half-space:

Theorem 43. (*Hoffman-Meeks, [HoMe]*) *A complete connected properly immersed minimal surface contained in $\{x_3 > 0\} \subset \mathbf{R}^3$ must be a horizontal plane $\{x_3 = \text{Constant}\}$.*

In [CM12], it was shown that the Calabi-Yau Conjectures were true for embedded surfaces. We will describe this more precisely below.

The main result of [CM12] is an effective version of properness for disks, giving a chord-arc bound. Obviously, intrinsic distances are larger than extrinsic distances, so the significance of a chord-arc bound is the reverse inequality, i.e., a bound on intrinsic distances from above by extrinsic distances. This is accomplished in the next theorem:

Theorem 44. (*Colding-Minicozzi, [CM12]*) *There exists a constant $C > 0$ so that if $\Sigma \subset \mathbf{R}^3$ is an embedded minimal disk, $B_{2R}^\Sigma = B_{2R}^\Sigma(0)$ is an intrinsic ball in $\Sigma \setminus \partial\Sigma$ of radius $2R$, and if $\sup_{B_{r_0}^\Sigma} |A|^2 > r_0^{-2}$ where $R > r_0$, then for $x \in B_R^\Sigma$*

$$C \operatorname{dist}_\Sigma(x, 0) < |x| + r_0. \quad (36)$$

The assumption of a lower curvature bound, $\sup_{B_{r_0}^\Sigma} |A|^2 > r_0^{-2}$, in the theorem is a necessary normalization for a chord-arc bound. This can easily be seen by rescaling and translating the helicoid.

Properness of a complete embedded minimal disk is an immediate consequence of Theorem 44. Namely, by (36), as intrinsic distances go to infinity, so do extrinsic distances. Precisely, if Σ is flat, and hence a plane, then obviously Σ is proper and if it is non-flat, then $\sup_{B_{r_0}^\Sigma} |A|^2 > r_0^{-2}$ for some $r_0 > 0$ and hence Σ is proper by (36).

A consequence of Theorem 44 together with the one-sided curvature estimate is the following version of that estimate for intrinsic balls:

Corollary 45. (*Colding-Minicozzi, [CM12]*) *There exists $\epsilon > 0$, so that if*

$$\Sigma \subset \{x_3 > 0\} \subset \mathbf{R}^3 \quad (37)$$

is an embedded minimal disk, $B_{2R}^\Sigma(x) \subset \Sigma \setminus \partial\Sigma$, and $|x| < \epsilon R$, then

$$\sup_{B_R^\Sigma(x)} |A_\Sigma|^2 \leq R^{-2}. \quad (38)$$

As a corollary of this intrinsic one-sided curvature estimate we get that the second, and “more ambitious”, of Calabi’s conjectures is also true for embedded minimal disks.

In fact, [CM12] proved both of Calabi’s conjectures and properness also for embedded surfaces with finite topology:

Theorem 46. (Colding-Minicozzi, [CM12]) *The plane is the only complete embedded minimal surface with finite topology in \mathbf{R}^3 in a halfspace.*

Theorem 47. (Colding-Minicozzi, [CM12]) *A complete embedded minimal surface with finite topology in \mathbf{R}^3 must be proper.*

There have been several properness results for Riemannian three-manifolds. W. Meeks and H. Rosenberg, [MeR3], generalized this to get a local version in Riemannian three-manifolds; they also extended it to embedded minimal surfaces with finite genus and positive injectivity radius in \mathbf{R}^3 . In [Cb], B. Coskunuzer proved properness for area minimizing disks in hyperbolic three-space, assuming that there is at least one C^1 point in the boundary at infinity. Finally, Daniel, Meeks and Rosenberg proved a version for Lie Groups in [DMR].

There has been extensive work on both properness and the halfspace property assuming various curvature bounds. Jorge and Xavier, [JXa1] and [JXa2], showed that there cannot exist a complete immersed minimal surface with bounded curvature in $\cap_i \{x_i > 0\}$; later Xavier proved that the plane is the only such surface in a halfspace, [Xa]. Recently, G.P. Bessa, Jorge and G. Oliveira-Filho, [BJO], and H. Rosenberg, [Ro], have shown that if complete embedded minimal surface has bounded curvature, then it must be proper. This properness was extended to embedded minimal surfaces with locally bounded curvature and finite topology by Meeks and Rosenberg in [MeR2]; finite topology was subsequently replaced by finite genus in [MePRs1] by Meeks, J. Perez and A. Ros.

Inspired by Nadirashvili’s examples, F. Martin and S. Morales constructed in [MaMo2] a complete bounded minimal immersion which is proper in the (open) unit ball. That is, the preimages of compact subsets of the (open) unit ball are compact in the surface and the image of the surface accumulates on the boundary of the unit ball. They extended this in [MaMo3] to show that any convex, possibly noncompact or nonsmooth, region of \mathbf{R}^3 admits a proper complete minimal immersion of the unit disk. There are a number of interesting related results, including [AFM], [MaMeNa], and [ANa].

8 Mean curvature flow

We will now turn to the gradient flow for volume, i.e., mean curvature flow (or MCF). This is the higher dimensional analog of the curve shortening flow. In this section, we will give a rapid overview of the subject.

A one-parameter family of hypersurfaces $\Sigma_t \subset \mathbf{R}^{n+1}$ flows by mean curvature if

$$\partial_t x = -H \mathbf{n},$$

where \mathbf{n} is the unit normal and H is the mean curvature. Since the first variation formula gives that

$$\frac{d}{dt} \text{Vol}(\Sigma_t) = \int_{\Sigma_t} \langle \partial_t x, H \mathbf{n} \rangle,$$

we see that mean curvature flow is the (negative) gradient flow for volume and

$$\frac{d}{dt} \text{Vol}(\Sigma_t) = - \int_{\Sigma_t} H^2.$$

Minimal surfaces (where $H = 0$) are fixed points for this flow. The next simplest example is given by concentric round n -dimensional spheres of radius $\sqrt{-2nt}$ for $t < 0$.

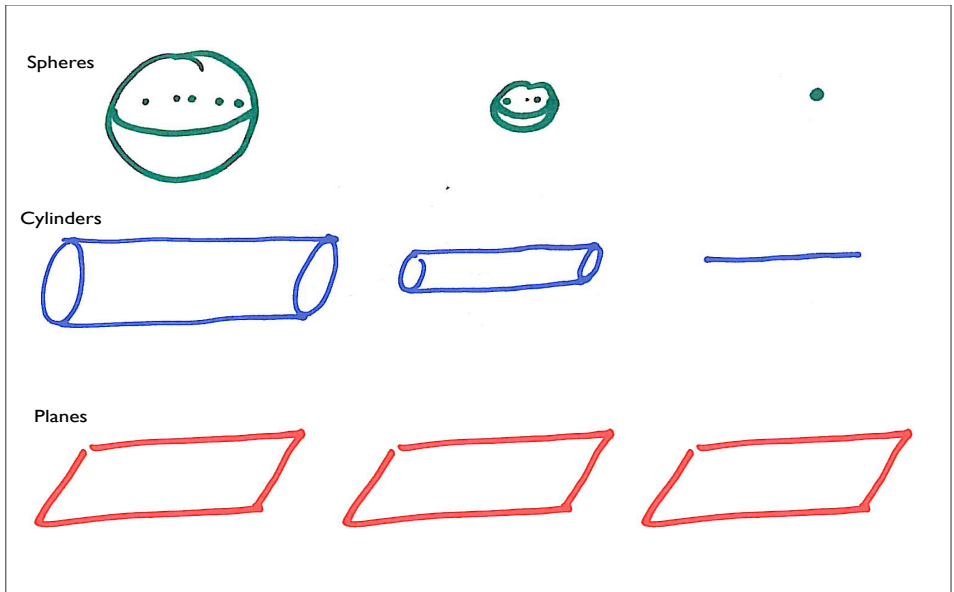


Figure 25: Cylinders, spheres and planes are self-similar solutions of the mean curvature flow. The shape is preserved, but the scale changes with time.

8.1 MCF of graphs

We saw earlier that the mean curvature of the graph of a function $u : \mathbf{R}^n \rightarrow \mathbf{R}$ is given by

$$H = -\text{div}_{\mathbf{R}^n} \left(\frac{\nabla_{\mathbf{R}^n} u}{\sqrt{1 + |\nabla_{\mathbf{R}^n} u|^2}} \right).$$

Thus, the graph of $u(x, t)$ flows by MCF if

$$\frac{\partial u}{\partial t} = \left(1 + |\nabla_{\mathbf{R}^n} u|^2\right)^{\frac{1}{2}} \operatorname{div}_{\mathbf{R}^n} \left(\frac{\nabla_{\mathbf{R}^n} u}{\sqrt{1 + |\nabla_{\mathbf{R}^n} u|^2}} \right).$$

The factor $\left(1 + |\nabla_{\mathbf{R}^n} u|^2\right)^{\frac{1}{2}}$ on the right compensates for the fact that the x_{n+1} direction is not normal to the graph.

We already saw that Calabi's grim reaper $u(x, t) = t - \log \sin x$ gives an example of graphs flowing by mean curvature; see [AW] and [CSS] for similar examples and stability results.

8.2 Self-similar shrinkers

Let $\Sigma_t \subset \mathbf{R}^{n+1}$ be a one-parameter family of hypersurfaces flowing by MCF for $t < 0$. Σ_t is said to be a self-similar shrinker if

$$\Sigma_t = \sqrt{-t} \Sigma_{-1}$$

for all $t < 0$. We saw that spheres of radius $\sqrt{-2nt}$ give such a solution. Unlike the case of curves, numerical evidence suggests that a complete classification of embedded self-shrinkers is impossible. In spite of all the numerical evidence, there are very few rigorous examples of self-shrinkers.

In 1992, Angenent, [A], constructed a self-similar shrinking donut in \mathbf{R}^3 . The shrinking donut was given by rotating a simple closed curve around an axis. See Kleene and Möller, [KlMo], for a classification of self-shrinkers of rotation (including ones with boundary).

8.3 The maximum principle

The parabolic maximum principle plays an important role in mean curvature flow. For instance, it is used to prove the following key facts:

1. If two closed hypersurfaces are disjoint, then they remain disjoint under MCF.
2. A closed embedded hypersurface remains embedded under MCF.
3. If a closed hypersurface is convex, then it remains convex under MCF.
4. Likewise, mean convexity (i.e., $H > 0$) is preserved under MCF.

In 1989, Grayson, [G2], showed that his result for curves does not extend to surfaces. In particular, he showed that a dumbbell with a sufficiently long and narrow bar will develop a pinching singularity before extinction. A later proof was given by Angenent, [A], using the shrinking donut and the avoidance property (1). Figures 27 to 30 show 8 snapshots in time of the evolution of a dumbbell; the figures were created by computer simulation by U. Mayer.

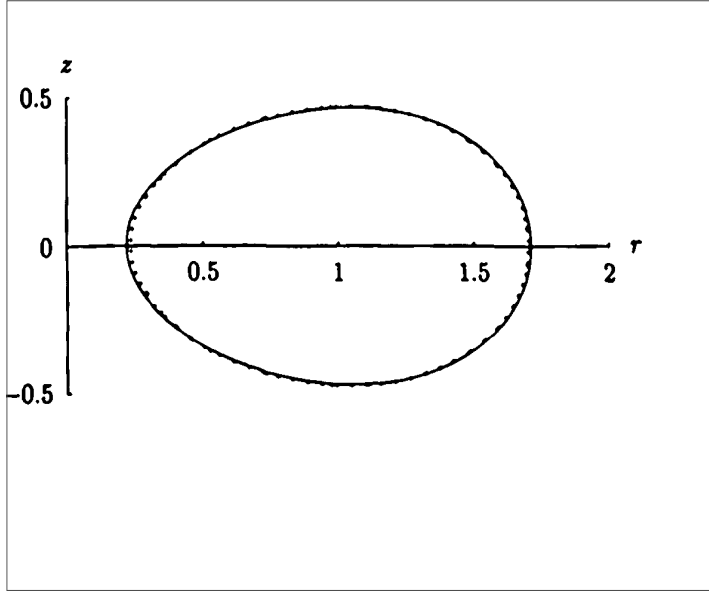


Figure 26: Angenent's shrinking donut from numerical simulations of D. Chopp, [Ch]. The vertical z -axis is the axis of rotation and the horizontal r -axis is a line of reflection symmetry.

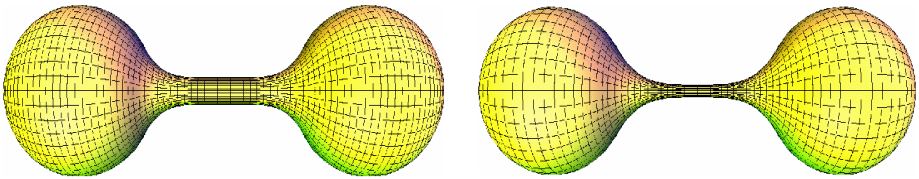


Figure 27: Grayson's dumbbell; initial surface and step 1.

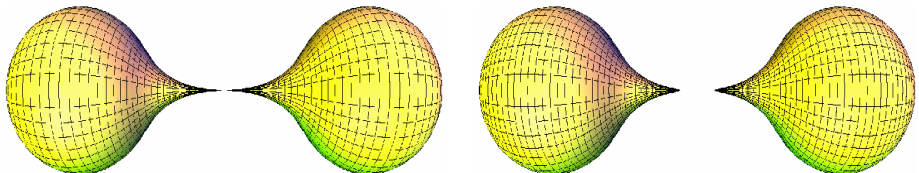


Figure 28: The dumbbell; steps 2 and 3.

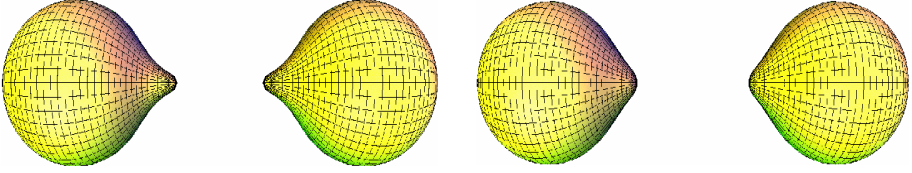


Figure 29: The dumbbell; steps 4 and 5.

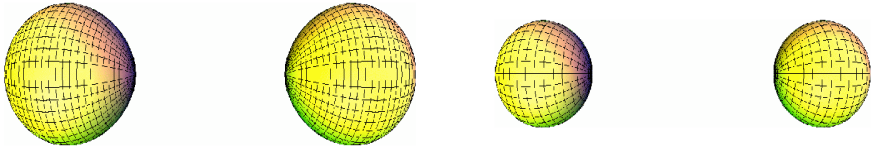


Figure 30: The dumbbell; steps 6 and 7.

8.4 The self-shrinker equation

A MCF M_t is a self-similar shrinker if $M_t = \sqrt{-t}M_{-1}$ for $t < 0$. This is equivalent to that $\Sigma = M_{-1}$ satisfies the equation⁴

$$H = \frac{\langle x, \mathbf{n} \rangle}{2}.$$

That is: $M_t = \sqrt{-t}M_{-1} \iff M_{-1}$ satisfies $H = \frac{\langle x, \mathbf{n} \rangle}{2}$.

The self-shrinker equation arises variationally in two closely related ways: as minimal surfaces for a conformally changed metric and as critical points for a weighted area functional. We return to the second later, but state the first now:

Lemma 48. Σ is a self-shrinker $\iff \Sigma$ is a minimal surface in the metric

$$g_{ij} = e^{-\frac{|x|^2}{2n}} \delta_{ij}.$$

The proof follows immediately from the first variation. Unfortunately, this metric is not complete (the distance to infinity is finite) and the curvature blows up exponentially.

8.5 Huisken's theorem about MCF of convex hypersurfaces

In 1984, Huisken, [H1], showed that convexity is preserved under MCF and showed that the surfaces become round:

Theorem 49. (Huisken, [H1]) Under MCF, every closed convex hypersurface in \mathbf{R}^{n+1} remains convex and eventually becomes extinct in a "round point".

⁴This equation differs by a factor of two from Huisken's definition of a self-shrinker; this is because Huisken works with the time $-1/2$ slice.

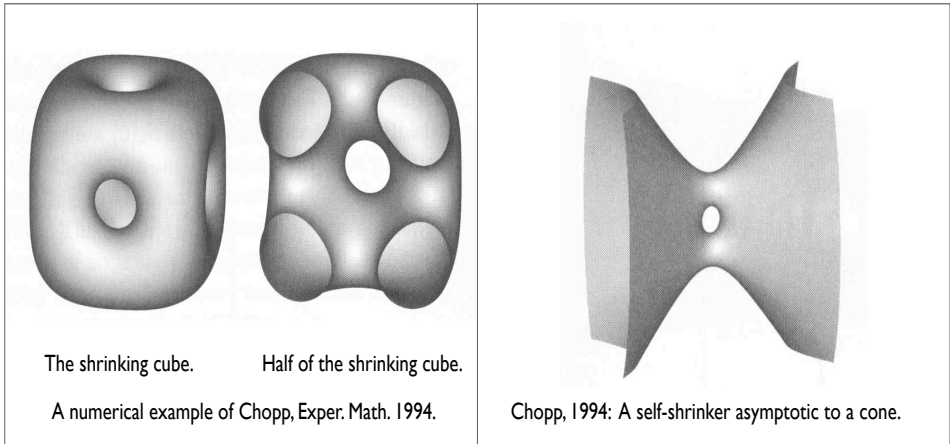


Figure 31: A numerical example of a closed shrinker from Chopp, [Ch].

Figure 32: A non-compact numerical example from Chopp, [Ch].

This is exactly analogous to the result of Gage-Hamilton for convex curves, but it's interesting to note that Huisken's proof works only for $n > 1$. Namely, he shows that the hypersurfaces become closer and closer to being umbilic and that the limiting shapes are umbilic. A hypersurface is umbilic if all of the eigenvalues of the second fundamental form are the same; this characterizes the sphere when there are at least two eigenvalues, but is meaningless for curves.

We mention a few related results. First, Schulze showed a generalization of this for flows by other powers of mean curvature in [Sf1] and [Sf2]. Second, Sesum showed that the rescaled mean curvature flow converges exponentially to a round sphere in [Se].

Convexity means that every eigenvalue of A has the right sign. There are weaker conditions that are also preserved under mean curvature flow and where significant results have been obtained. The first of these is mean convexity, where the hypersurfaces have positive mean curvature. **Mean convex** flows have been analyzed by Huisken-Sinestrari, [HS1] and [HS2], and White, [W2] and [W3]. A related class of hypersurfaces are the **2-convex** ones, where the sum of any pair of principal curvatures is positive (it is not hard to see that this implies mean convexity); this case has been studied by Huisken-Sinestrari, [HS3]. In addition, Smoczyk, [Sm1], showed that **Star-shaped** hypersurfaces remain star-shaped under MCF. Finally, Ecker-Huisken, [EH1] and [EH2], showed that being graphical is also preserved under MCF and proved estimates for graphical mean curvature flow. In each of these cases, the maximum principle is used to show that the condition is preserved under MCF.

9 Width and mean curvature flow

We saw previously that every closed hypersurface must become extinct under MCF in a finite amount of time. It is interesting then to estimate this extinction time. One obvious estimate is in terms of the diameter since the hypersurface must become extinct before a ball that encloses it. However, there are cases where this estimate is far from sharp. In this section, we will prove another extinction time estimate in terms of the geometric invariant called the width that was previously introduced.

9.1 Sweepouts and one-dimensional width

Let M be a smooth closed convex surface in \mathbf{R}^3 .⁵ Convexity implies that M is diffeomorphic to \mathbf{S}^2 and, thus, we can fix a map $\sigma : \mathbf{S}^1 \times [0, 1] \rightarrow M$ that maps $\mathbf{S}^1 \times \{0\}$ and $\mathbf{S}^1 \times \{1\}$ to points and that is topologically a degree one map from \mathbf{S}^2 to \mathbf{S}^2 . Let Ω_σ denote the homotopy class of such maps.

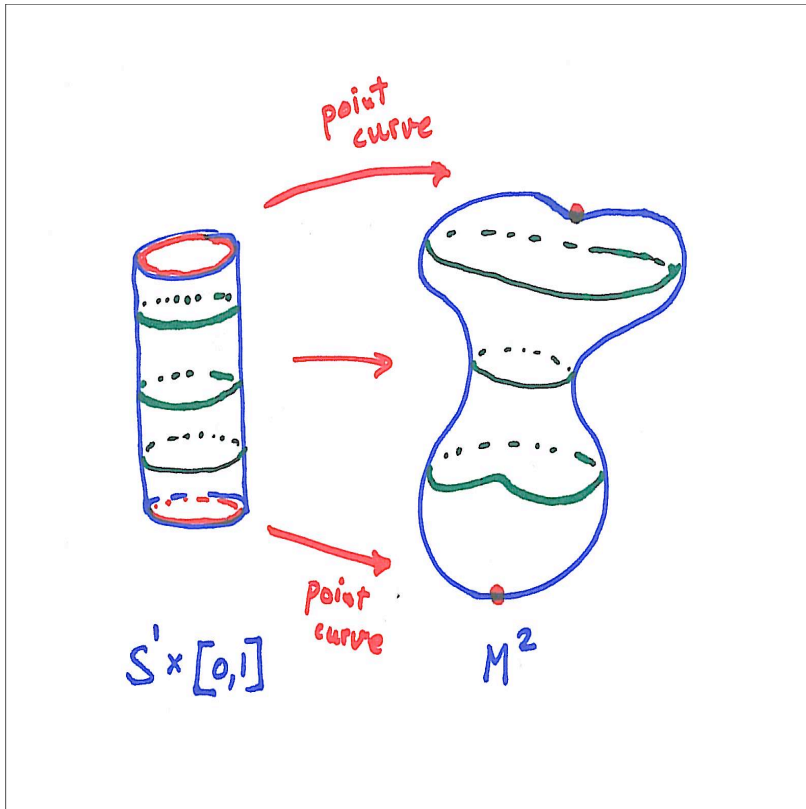


Figure 33: A sweepout.

⁵This works for convex hypersurfaces in \mathbf{R}^{n+1} too with the obvious modifications.

Given this homotopy class, the width $W = W(\sigma)$ was defined in (7) to be

$$W = \inf_{\hat{\sigma} \in \Omega_\sigma} \max_{s \in [0,1]} E(\hat{\sigma}(\cdot, s)),$$

where the energy is given by

$$E(\hat{\sigma}(\cdot, s)) = \frac{1}{2} \int_{\mathbf{S}^1} |\partial_x \hat{\sigma}(x, s)|^2 dx.$$

It is not hard to see that the width is continuous in the metric, though the curve realizing it may not be.

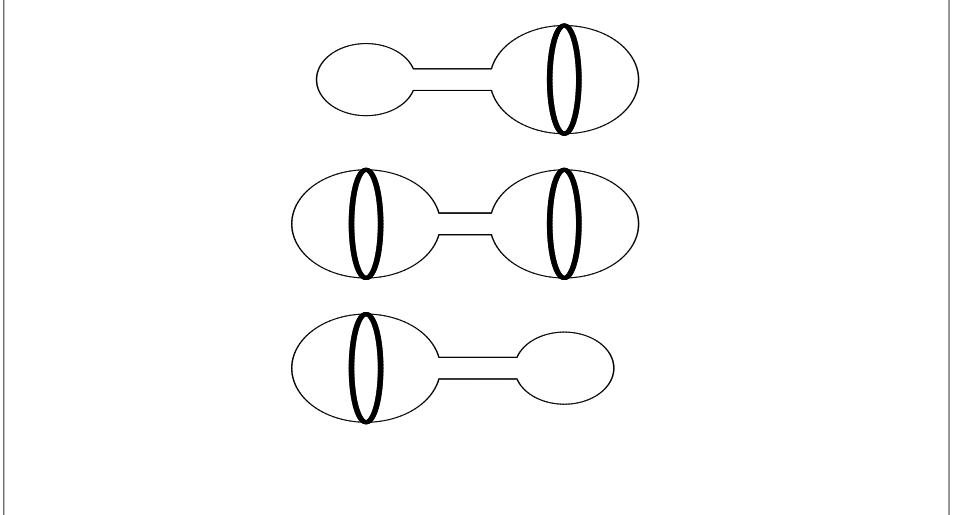


Figure 34: Three snapshots of a one-parameter family of “dumbbell” metrics. The geodesic realizing the width jumps from one bell to the other. The jump occurs in the middle picture where the geodesic is not unique.

9.2 Estimates for rate of change of width under the mean curvature flow

In [CM2], we proved the following estimate for the rate of change of the width under MCF:

Theorem 50. (Colding-Minicozzi, [CM2]) *If M_t is a MCF of closed convex hypersurfaces and $W(t)$ is the width of M_t , then*

$$\frac{d}{dt} W \leq -2\pi \tag{39}$$

in the sense of limsup of forward difference quotients.

Note that $W(t)$ is continuous but may not be differentiable in t , so (39) may not hold in the classical sense. Still, the fact that it holds in the sense of limsup of forward difference quotients is enough to integrate and get that

$$W(t) \leq W(0) - 2\pi t. \quad (40)$$

Since the width is obviously positive until M_t becomes extinct, we see that M_t becomes extinct by time $\frac{W(0)}{2\pi}$.

Finally, observe that capping off a long thin cylinder gives convex surfaces with a fixed bound on the width (coming from the radius of the cylinder) but with arbitrarily large diameter. For these surfaces, the estimate on the extinction time coming from the width is much better than what one would get from the diameter.

10 Singularities for MCF

We will now leave convex hypersurfaces and go to the general case. As Grayson's dumbbell showed, there is no higher dimensional analog of Grayson's theorem for curves. The key for analyzing singularities is a blow up (or rescaling) analysis similar to the tangent cone analysis for minimal surfaces. As for minimal surfaces, the starting point is a monotonicity formula that gives uniform control over the rescalings.

10.1 Huisken's monotonicity

We will need to recall Huisken's monotonicity formula (see [H3], [E1], [E2]). To do this, first define the non-negative function Φ on $\mathbf{R}^{n+1} \times (-\infty, 0)$ by

$$\Phi(x, t) = [-4\pi t]^{-\frac{n}{2}} e^{\frac{|x|^2}{4t}}, \quad (41)$$

and then set $\Phi_{(x_0, t_0)}(x, t) = \Phi(x - x_0, t - t_0)$. In 1990, G. Huisken proved the following monotonicity formula for mean curvature flow, [H3]:

Theorem 51. (*Huisken, [H3]*) *If M_t is a solution to the MCF and u is a C^2 function, then*

$$\frac{d}{dt} \int_{M_t} u \Phi_{(x_0, t_0)} = - \int_{M_t} \left| H\mathbf{n} - \frac{(x - x_0)^\perp}{2(t_0 - t)} \right|^2 u \Phi_{(x_0, t_0)} + \int_{M_t} [u_t - \Delta u] \Phi. \quad (42)$$

When u is identically one, we get the monotonicity formula

$$\frac{d}{dt} \int_{M_t} \Phi_{(x_0, t_0)} = - \int_{M_t} \left| H\mathbf{n} - \frac{(x - x_0)^\perp}{2(t_0 - t)} \right|^2 \Phi_{(x_0, t_0)}. \quad (43)$$

Huisken's density is the limit of $\int_{M_t} \Phi_{x_0, t_0}$ as $t \rightarrow t_0$. That is,

$$\Theta_{x_0, t_0} = \lim_{t \rightarrow t_0} \int_{M_t} \Phi_{x_0, t_0}; \quad (44)$$

this limit exists by the monotonicity (43) and the density is non-negative as the integrand Φ_{x_0, t_0} is non-negative.

It is also interesting to note that Huisken's Gaussian volume is constant in time if and only if M_t is a self-similar shrinker with

$$M_t = \sqrt{-t} (M_{-1}) .$$

One drawback to Huisken's formula is that it requires one to integrate over all of space. In 2001, K. Ecker discovered a local monotonicity formula where the integral is over bounded sets. This formula is modeled on Watson's mean-value formula for the linear heat equation; see [E2] for details.

10.2 Tangent flows

If M_t is a MCF, then so is the parabolic scaling for any constant $\lambda > 0$

$$\tilde{M}_t = \lambda M_{\lambda^{-2}t} .$$

When λ is large, this magnifies a small neighborhood of the origin in space-time.

If we now take a sequence $\lambda_i \rightarrow \infty$ and let $M_t^i = \lambda_i M_{\lambda_i^{-2}t}$, then Huisken's monotonicity gives uniform Gaussian area bounds on the rescaled sequence. Combining this with Brakke's weak compactness theorem for mean curvature flow, [B], it follows that a subsequence of the M_t^i converges to a limiting flow M_t^∞ (cf., for instance, page 675–676 of [W2] and chapter 7 of [I2]). Moreover, Huisken's monotonicity implies that the Gaussian area (centered at the origin) is now constant in time, so we conclude that M_t^∞ is a self-similar shrinker. This M_t^∞ is called a *tangent flow* at the origin. The same construction can be done at any point of space-time.

We will return to this point of view later when we describe results from [CM1] classifying the generic tangent flows.

10.3 Gaussian integrals and the F functionals

For $t_0 > 0$ and $x_0 \in \mathbf{R}^{n+1}$, define F_{x_0, t_0} by

$$\begin{aligned} F_{x_0, t_0}(\Sigma) &= (4\pi t_0)^{-n/2} \int_{\Sigma} e^{-\frac{|x-x_0|^2}{4t_0}} d\mu \\ &= \int_{\Sigma} \Phi_{x_0, t_0}(\cdot, 0) . \end{aligned}$$

We will think of x_0 as being the point in space that we focus on and t_0 as being the scale. By convention, we set $F = F_{0,1}$.

We will next compute the first variation of the F functionals, but we will allow variations in all three parameters: the hypersurface Σ_0 , the center x_0 , and the scale t_0 . Namely, fix a hypersurface $\Sigma_0 \subset \mathbf{R}^{n+1}$ with unit normal \mathbf{n} , a function f , vectors $x_0, y \in \mathbf{R}^{n+1}$ and constants $t_0, h \in \mathbf{R}$ with $t_0 > 0$. Define variations (i.e.,

one-parameter families) by

$$\begin{aligned}\Sigma_s &= \{x + s f(x) \mathbf{n}(x) \mid x \in \Sigma_0\}, \\ x_s &= x_0 + s y, \\ t_s &= t_0 + s h.\end{aligned}$$

The first variation is given by:

Lemma 52. (Colding-Minicozzi, [CM1]) *If Σ_s , x_s and t_s are variations as above, then $\frac{\partial}{\partial s} (F_{x_s, t_s}(\Sigma_s))$ is*

$$(4\pi t_0)^{-\frac{n}{2}} \int_{\Sigma} \left[f \left(H - \frac{\langle x - x_0, \mathbf{n} \rangle}{2t_0} \right) + h \left(\frac{|x - x_0|^2}{4t_0^2} - \frac{n}{2t_0} \right) + \frac{\langle x - x_0, y \rangle}{2t_0} \right] e^{-\frac{|x - x_0|^2}{4t_0}} d\mu.$$

Proof. From the first variation formula (for area), we know that

$$(d\mu)' = f H d\mu. \quad (45)$$

The s derivative of the weight $e^{-|x - x_s|^2/(4t_s)}$ will have three separate terms coming from the variation of the surface, the variation of x_s , and the variation of t_s . Using, respectively, that $\nabla|x - x_s|^2 = 2(x - x_s)$,

$$\partial_{t_s} \log \left[(4\pi t_s)^{-n/2} e^{-\frac{|x - x_s|^2}{4t_s}} \right] = \frac{-n}{2t_s} + \frac{|x - x_s|^2}{4t_s^2} \quad (46)$$

and $\partial_{x_s}|x - x_s|^2 = 2(x_s - x)$, we get that the derivative of

$$\log \left[(4\pi t_s)^{-\frac{n}{2}} e^{-|x - x_s|^2/(4t_s)} \right]$$

at $s = 0$ is given by

$$-\frac{f}{2t_0} \langle x - x_0, \mathbf{n} \rangle + h \left(\frac{|x - x_0|^2}{4t_0^2} - \frac{n}{2t_0} \right) + \frac{1}{2t_0} \langle x - x_0, y \rangle. \quad (47)$$

Combining this with (45) gives the lemma. \square

We will say that Σ is a critical point for F_{x_0, t_0} if it is simultaneously critical with respect to variations in all three parameters, i.e., variations in Σ and all variations in x_0 and t_0 . Strictly speaking, it is the triplet (Σ, x_0, t_0) that is a critical point of F , but we will refer to Σ as a critical point of F_{x_0, t_0} . The next proposition shows that Σ is a critical point for F_{x_0, t_0} if and only if it is the time $-t_0$ slice of a self-shrinking solution of the mean curvature flow that becomes extinct at the point x_0 and time 0.

Proposition 53. (Colding-Minicozzi, [CM1]) *Σ is a critical point for F_{x_0, t_0} if and only if $H = \frac{\langle x - x_0, \mathbf{n} \rangle}{2t_0}$.*

By Lemma 52, Σ is critical if and only if

$$\int_{\Sigma_0} \left[f \left(H - \frac{\langle x - x_0, \mathbf{n} \rangle}{2t_0} \right) + h \left(\frac{|x - x_0|^2}{4t_0^2} - \frac{n}{2t_0} \right) + \frac{\langle x - x_0, y \rangle}{2t_0} \right] e^{-\frac{|x - x_0|^2}{4t_0}} = 0$$

for any choice of f , y and h .

It is clear why this holds for f , but why h and y ? The answer is that h and y correspond to scalings and translations, respectively, and these can equivalently be achieved by appropriate choices of f .

A self-shrinker Σ satisfies $H = \frac{\langle x, \mathbf{n} \rangle}{2}$, so it is a critical point of the $F = F_{0,1}$ functional. We will use these functionals to understand dynamical stability of self-shrinkers. The first step is to compute the Hessian, or second variation, of this functional. Before doing this, it will be useful to introduce some of the operators that will arise.

10.4 Weighted inner products and the drift Laplacian

Let f and g be functions. It is natural to look at the weighted L^2 inner product

$$\int_{\Sigma} f g e^{-\frac{|x|^2}{4}}.$$

Similarly, we have the weighted inner product for gradients:

$$\int_{\Sigma} \langle \nabla^T f, \nabla^T g \rangle e^{-\frac{|x|^2}{4}}.$$

Since

$$\operatorname{div}_{\Sigma} \left(e^{-\frac{|x|^2}{4}} \nabla^T f \right) = \left(\Delta_{\Sigma} f - \frac{1}{2} \langle x, \nabla^T f \rangle \right) e^{-\frac{|x|^2}{4}},$$

the divergence theorem applied to $\left(g e^{-\frac{|x|^2}{4}} \nabla^T f \right)$ gives

$$\int_{\Sigma} \langle \nabla^T f, \nabla^T g \rangle e^{-\frac{|x|^2}{4}} = - \int_{\Sigma} g \left(\Delta_{\Sigma} f - \frac{1}{2} \langle x, \nabla^T f \rangle \right) e^{-\frac{|x|^2}{4}}.$$

We call this operator the “drift Laplacian” \mathcal{L}

$$\mathcal{L} f = \Delta_{\Sigma} f - \frac{1}{2} \langle x, \nabla^T f \rangle.$$

It follows that \mathcal{L} is symmetric in the weighted space.

The \mathcal{L} operator plays a similar role for self-shrinkers that the Laplacian did for minimal surfaces. To see this, recall that given $f : \mathbf{R}^{n+1} \rightarrow \mathbf{R}$, the Laplacian on Σ applied to f is

$$\Delta_{\Sigma} f = \sum_{i=1}^n \operatorname{Hess}_f(e_i, e_i) - \langle \nabla f, \mathbf{n} \rangle H,$$

where e_i is a frame for Σ and Hess_f is the \mathbf{R}^{n+1} Hessian of f . Therefore, when Σ is a self-shrinker, it follows that

$$\mathcal{L}x_i = -\frac{1}{2}x_i, \quad (48)$$

$$\mathcal{L}|x|^2 = 2n - |x|^2. \quad (49)$$

The second formula is closely related to the fact that self-shrinkers are critical points for variations in all three parameters of the $F_{0,1}$ functional. Namely, we saw earlier that on any self-shrinker Σ we must have

$$\int_{\Sigma} \left(\frac{|x|^2}{4} - \frac{n}{2} \right) e^{-\frac{|x|^2}{4}} = 0$$

This can also be seen by using \mathcal{L} operator. To do this, use the symmetry of \mathcal{L} to get for any u and v (that do not grow too quickly)

$$\int_{\Sigma} (u\mathcal{L}v) e^{-\frac{|x|^2}{4}} = - \int_{\Sigma} \langle \nabla^T u, \nabla^T v \rangle e^{-\frac{|x|^2}{4}}.$$

Applying this with $u = 1$ and $v = |x|^2$ and using (49) gives

$$\int_{\Sigma} (2n - |x|^2) e^{-\frac{|x|^2}{4}} = 0.$$

We will need another second order operator L which differs from \mathcal{L} by a zero-th order term:

$$L = \mathcal{L} + |A|^2 + \frac{1}{2},$$

where the drift Laplacian \mathcal{L} is given by

$$\mathcal{L}f = \Delta_{\Sigma}f - \frac{1}{2} \langle x, \nabla^T f \rangle.$$

Clearly, L is also symmetric with respect to the weighted inner product. The operator L plays the role of the second variation operator $\Delta + |A|^2 + \text{Ric}(\mathbf{n}, \mathbf{n})$ for minimal surfaces.

10.5 Second variation

Let $\Sigma_0 \subset \mathbf{R}^{n+1}$ be a self-shrinker with unit normal \mathbf{n} , a function f , a vector $y \in \mathbf{R}^{n+1}$ and a constant $h \in \mathbf{R}$. We will assume that Σ_0 is complete, $\partial\Sigma_0 = \emptyset$, and Σ_0 has polynomial volume growth (so that all of our Gaussian integrals converge). As before, define variations

$$\begin{aligned} \Sigma_s &= \{x + s f(x) \mathbf{n}(x) \mid x \in \Sigma_0\}, \\ x_s &= s y, \\ t_s &= 1 + s h. \end{aligned}$$

Theorem 54. (Colding-Minicozzi, [CM1]) *If we set $F'' = \partial_{ss}|_{s=0} (F_{x_s, t_s}(\Sigma_s))$, then*

$$F'' = (4\pi)^{-n/2} \int_{\Sigma} \left(-f Lf + 2f h H - h^2 H^2 + f \langle y, \mathbf{n} \rangle - \frac{\langle y, \mathbf{n} \rangle^2}{2} \right) e^{-\frac{|x|^2}{4}} d\mu. \quad (50)$$

First observation: All (compact) critical points are unstable in the usual sense. Namely, if we set $h = 0$, $y = 0$ and $f \equiv 1$ so that

$$L1 = \mathcal{L}1 + |A|^2 + \frac{1}{2} = |A|^2 + \frac{1}{2},$$

then we see that

$$\frac{\partial^2}{\partial s^2} \Big|_{s=0} (F_{0,1}(\Sigma_s)) = (4\pi)^{-\frac{n}{2}} \int_{\Sigma_0} \left(-|A|^2 - \frac{1}{2} \right) < 0.$$

This instability explains why there are very few examples of embedded self-shrinkers that have been proven to exist. Namely, they are difficult to construct variationally since they tend to be highly unstable critical points of $F_{0,1}$.

In fact, we get the same instability for non-compact self-shrinkers, at least when the volume growth is under control:

Theorem 55. (Colding-Minicozzi, [CM1]) *If $\Sigma \subset \mathbf{R}^{n+1}$ is a smooth complete self-shrinker without boundary and with polynomial volume growth, then there exists a function u with compact support so that*

$$- \int (u L u) e^{-\frac{|x|^2}{4}} < 0. \quad (51)$$

10.6 The L operator applied to H and translations

The link between the mean curvature H of a self-shrinker Σ and the second variation is that H is an eigenfunction for L with eigenvalue -1 ; moreover, if y is a constant vector, then $\langle y, \mathbf{n} \rangle$ is also an eigenfunction for L .

Theorem 56. (Colding-Minicozzi, [CM1]) *The mean curvature H and the normal part $\langle v, \mathbf{n} \rangle$ of a constant vector field v are eigenfunctions of L with*

$$LH = H \text{ and } L\langle v, \mathbf{n} \rangle = \frac{1}{2} \langle v, \mathbf{n} \rangle. \quad (52)$$

This will be important later, but it is worth noting that this explains an odd fact in the second variation formula. Namely, since L is a symmetric operator (in the weighted L^2 space) and H and $\langle v, \mathbf{n} \rangle$ are eigenfunctions with different eigenvalues, it follows that H and $\langle v, \mathbf{n} \rangle$ are orthogonal. This explains why there was no $H \langle y, \mathbf{n} \rangle$ term in the second variation, Theorem 54.

Remark 57. *Interestingly, there is an analogous situation for Ricci flow. In this case, Cao, Hamilton and Ilmanen, [CaHI], computed the second variation formula for Perelman's shrinker entropy and discovered an analog of the L operator. Moreover, Cao and Zhu showed in [CaZ] that the Ricci tensor is an eigenvector for this operator.*

11 Smooth compactness theorem for self-shrinkers

In [CM3], we proved the following smooth compactness theorem for self-shrinkers in \mathbf{R}^3 :

Theorem 58. (*Colding-Minicozzi, [CM3]*) *Given an integer $g \geq 0$ and a constant $V > 0$, the space of smooth complete embedded self-shrinkers $\Sigma \subset \mathbf{R}^3$ with*

- *genus at most g ,*
- *$\partial\Sigma = \emptyset$,*
- *Area $(B_R(x_0) \cap \Sigma) \leq V R^2$ for all $x_0 \in \mathbf{R}^3$ and all $R > 0$*

is compact.

Namely, any sequence of these has a subsequence that converges in the topology of C^m convergence on compact subsets for any $m \geq 2$.

The surfaces in this theorem are assumed to be homeomorphic to closed surfaces with finitely many disjoint disks removed. The genus of the surface is defined to be the genus of the corresponding closed surface. For example, an annulus is a sphere with two disks removed and, thus, has genus zero.

The main motivation for this result is that self-shrinkers model singularities in mean curvature flow. Thus, the above theorem can be thought of as a compactness result for the space of all singularities.

This should be compared with the Choi-Schoen compactness theorem for minimal surfaces in a manifold with positive Ricci curvature, [CiSc]. However, the conformal metric is not complete and even the scalar curvature changes sign.

11.1 The proof of smooth compactness

There are five main points in the proof of Theorem 58:

1. The bound on the genus plus local area bounds imply local bounds on $\int |A|^2$ (this follows from the local Gauss-Bonnet estimate in theorem 3 of [I1]).
2. Using (1) and the Choi-Schoen curvature estimate, [CiSc], we get a subsequence that converges smoothly, possibly with multiplicity, away from isolated “singular points” where the curvature concentrates.
3. By Allard’s theorem, [Al], the existence of singular points implies that the convergence is with multiplicity greater than one.
4. If the limit has multiplicity greater than one, then the limit is stable as a minimal surface in the conformally changed metric (by rescaling to get a Jacobi field as in [CM13]).
5. Combining (4) and Theorem 55 shows that there cannot be any singular points.

We will say a bit more about step (4) and why multiplicity implies stability. The basic point is that as 2 sheets come together, they are both graphs over the limit and the difference w_i between these 2 graphs does not vanish (by embeddedness). Thus, w_i does not change sign and (almost) satisfies the linearized equation $Lw_i = 0$. The w_i 's go to 0, but the Harnack inequality gives convergence for (a subsequence of)

$$u_i = \frac{w_i}{w_i(p)}.$$

It is not hard to show that the limiting function u is a positive solution of $Lu = 0$ with $u(p) = 1$. Of course, u is initially defined only away from the isolated singular points, but it is possible to show that it extends across these potential singularities. Finally, as we saw for minimal surfaces, this implies positivity of the operator L .

12 The entropy

The F_{x_0, t_0} functional was defined for $t_0 > 0$ and $x_0 \in \mathbf{R}^{n+1}$ by

$$F_{x_0, t_0}(\Sigma) = (4\pi t_0)^{-n/2} \int_{\Sigma} e^{-\frac{|x-x_0|^2}{4t_0}} d\mu.$$

If M_t flows by mean curvature and $t > s$, then Huisken's monotonicity formula gives

$$F_{x_0, t_0}(M_t) \leq F_{x_0, t_0+(t-s)}(M_s). \quad (53)$$

Thus, we see that a fixed F_{x_0, t_0} functional is not monotone under the flow, but the supremum over all of these functionals is monotone. We call this invariant the entropy and denote it by

$$\lambda(\Sigma) = \sup_{x_0, t_0} F_{x_0, t_0}(\Sigma). \quad (54)$$

The entropy has four key properties:

1. λ is invariant under dilations, rotations, and translations.
2. $\lambda(M_t)$ is non-increasing under MCF.
3. If Σ is a self-shrinker, then $\lambda(\Sigma) = F_{0,1}(\Sigma) = \Theta_{0,0}$.
4. Entropy is preserved under products with a line, i.e., $\lambda(\Sigma \times \mathbf{R}) = \lambda(\Sigma)$.

12.1 A few entropies

Stone, [St], computed the densities $\Theta_{0,0}$, and thus also λ , for self-shrinking spheres, planes and cylinders:

- $\lambda(\mathbf{R}^2) = 1$.
- $\lambda(\mathbf{S}_2^2) = \frac{4}{e} \approx 1.4715$.
- $\lambda(\mathbf{S}_{\sqrt{2}}^1) = \sqrt{\frac{2\pi}{e}} \approx 1.5203$.

Moreover, he also showed that $\lambda(\mathbf{S}^n)$ is decreasing in n .

12.2 How entropy will be used

The main point about λ is that it can be used to rule out certain singularities because of the monotonicity of entropy under MCF and its invariance under dilations:

Corollary 59. *If Σ is a self-shrinker given by a tangent flow for M_t with $t > 0$, then*

$$F_{0,1}(\Sigma) = \lambda(\Sigma) \leq \lambda(M_0).$$

12.3 Classification of entropy stable singularities

To illustrate our results, we will first specialize to the case where $n = 2$, that is to mean curvature flow of surfaces in \mathbf{R}^3 .

Theorem 60. *(Colding-Minicozzi, [CM1]) Suppose that $\Sigma \subset \mathbf{R}^3$ is a smooth complete embedded self-shrinker without boundary and with polynomial volume growth.*

- *If Σ is not a sphere, a plane, or a cylinder, then there is a graph $\tilde{\Sigma}$ over Σ of a compactly supported function with arbitrarily small C^m norm (for any fixed m) so that $\lambda(\tilde{\Sigma}) < \lambda(\Sigma)$.*

In particular, Σ cannot arise as a tangent flow to the MCF starting from $\tilde{\Sigma}$.

Thus, spheres, planes and cylinders are the only generic self-shrinkers. This should be contrasted with Huisken's result for convex flows, where we see that any small perturbation remains convex and, thus, still becomes extinct at a round point.

Essentially the same result holds in all dimensions, with one small difference: the perturbation does not have compact support if the shrinker is a product of a lines with an unstable shrinker in one dimension less; see [CM1].

12.4 F-stability

We saw that every self-shrinker is unstable as a critical point of $F_{0,1}$ and, in fact, it is already unstable just from the variations corresponding to translations and dilations. Roughly speaking, we will say that a self-shrinker is F -stable if these are the only sources of instability (this is essentially orbital stability for a corresponding dynamical system). Namely, a self-shrinker Σ is F -stable if for every variation Σ_s there exist variations x_s and t_s so that

$$\frac{d^2}{ds^2} \Big|_{s=0} F_{x_s, t_s}(\Sigma_s) \geq 0.$$

It is not hard to see that \mathbf{S}^n and \mathbf{R}^n are F -stable:

Lemma 61. *(Colding-Minicozzi, [CM1]) The n -sphere of radius $\sqrt{2n}$ in \mathbf{R}^{n+1} is F -stable.*

Proof. Note that $x^T = 0$, A is $1/\sqrt{2n}$ times the metric, and $L = \Delta + 1$. Therefore, by Theorem 54, the lemma will follow from showing that given an arbitrary normal variation $f\mathbf{n}$, there exist $h \in \mathbf{R}$ and $y \in \mathbf{R}^{n+1}$ so that

$$\int_{\mathbf{S}^n} \left[-f(\Delta f + f) + \sqrt{2n}fh - \frac{n}{2}h^2 + f\langle y, \mathbf{n} \rangle - \frac{\langle y, \mathbf{n} \rangle^2}{2} \right] \geq 0. \quad (55)$$

Recall that the eigenvalues of the Laplacian⁶ on the n -sphere of radius one are given by $k^2 + (n-1)k$ for $k = 0, 1, \dots$ with 0 corresponding to the constant function and the first non-zero eigenvalue n corresponding to the restrictions of the linear functions in \mathbf{R}^{n+1} . It follows that the eigenvalues of Δ on the sphere of radius $\sqrt{2n}$ are given by

$$\mu_k = \frac{k^2 + (n-1)k}{2n}, \quad (56)$$

with $\mu_0 = 0$ corresponding to the constant functions and $\mu_1 = \frac{1}{2}$ corresponding to the linear functions. Let E be the space of $W^{1,2}$ functions that are orthogonal to constants and linear functions; equivalently, E is the span of all the eigenfunctions for μ_k for all $k \geq 2$. Therefore, we can choose $a \in \mathbf{R}$ and $z \in \mathbf{R}^{n+1}$ so that

$$f_0 \equiv f - a - \langle z, \mathbf{n} \rangle \in E. \quad (57)$$

Using the orthogonality of the different eigenspaces, we get that

$$\begin{aligned} \int_{\mathbf{S}^n} -f(\Delta f + f) &\geq (\mu_2 - 1) \int_{\mathbf{S}^n} f_0^2 + (\mu_1 - 1) \int_{\mathbf{S}^n} \langle z, \mathbf{n} \rangle^2 + (\mu_0 - 1) \int_{\mathbf{S}^n} a^2 \\ &= \frac{1}{n} \int_{\mathbf{S}^n} f_0^2 - \frac{1}{2} \int_{\mathbf{S}^n} \langle z, \mathbf{n} \rangle^2 - \int_{\mathbf{S}^n} a^2. \end{aligned} \quad (58)$$

Again using the orthogonality of different eigenspaces, we get

$$\int_{\mathbf{S}^n} \left[\sqrt{2n}fh + f\langle y, \mathbf{n} \rangle \right] = \int_{\mathbf{S}^n} \left[\sqrt{2n}ah + \langle z, \mathbf{n} \rangle \langle y, \mathbf{n} \rangle \right]. \quad (59)$$

Combining (58) and (59), we get that the left hand side of (55) is greater than or equal to

$$\begin{aligned} \int_{\mathbf{S}^n} \left[\frac{f_0^2}{n} - \frac{1}{2} \langle z, \mathbf{n} \rangle^2 - a^2 + \sqrt{2n}ah - \frac{n}{2}h^2 + \langle z, \mathbf{n} \rangle \langle y, \mathbf{n} \rangle - \frac{\langle y, \mathbf{n} \rangle^2}{2} \right] \\ = \int_{\mathbf{S}^n} \left[\frac{f_0^2}{n} - \frac{1}{2} (\langle z, \mathbf{n} \rangle - \langle y, \mathbf{n} \rangle)^2 - \left(a - \frac{\sqrt{nh}}{\sqrt{2}} \right)^2 \right]. \end{aligned} \quad (60)$$

This can be made non-negative by choosing $y = z$ and $h = \frac{\sqrt{2}a}{\sqrt{n}}$. □

⁶See, e.g., (14) on page 35 of Chavel, [Ca].

12.5 The splitting theorem

The importance of F -stability comes from the following “splitting theorem” from [CM1]:

If Σ_0 is a self-shrinker that does not split off a line and Σ_0 is F -unstable, then there is a compactly supported variation Σ_s with

$$\lambda(\Sigma_s) < \lambda(\Sigma_0) \quad \forall s \neq 0.$$

The precise statement of the splitting theorem is :

Theorem 62. (Colding-Minicozzi, [CM1]) *Suppose that $\Sigma \subset \mathbf{R}^{n+1}$ is a smooth complete embedded self-shrinker with $\partial\Sigma = \emptyset$, with polynomial volume growth, and Σ does not split off a line isometrically.*

If Σ is F -unstable, then there is a compactly supported variation Σ_s with $\Sigma_0 = \Sigma$ so that $\lambda(\Sigma_s) < \lambda(\Sigma)$ for all $s \neq 0$.

The idea of the splitting theorem is roughly:

- Use that Σ does not split to show that $F_{0,1}$ is a strict maximum for F_{x_0,t_0} .
- Deform Σ_0 in the F -unstable direction Σ_s .
- Consider the function $G(s, x_0, t_0)$ given by

$$G(s, x_0, t_0) = F_{x_0,t_0}(\Sigma_s).$$

and show that this has a strict maximum at $x_0 = 0$, $t_0 = 1$ and $s = 0$.

The precise statement of the first step is:

Lemma 63. (Colding-Minicozzi, [CM1]) *Suppose that Σ is a smooth complete embedded self-shrinker with $\partial\Sigma = \emptyset$, polynomial volume growth, and Σ does not split off a line isometrically. Given $\epsilon > 0$, there exists $\delta > 0$ so*

$$\sup \{F_{x_0,t_0}(\Sigma) \mid |x_0| + |\log t_0| > \epsilon\} < \lambda - \delta. \quad (61)$$

Proof. (sketch of Theorem 62). Assume that Σ is not F -stable and, thus, there is a one-parameter normal variation Σ_s for $s \in [-2\epsilon, 2\epsilon]$ with $\Sigma_0 = \Sigma$ so that:

- (V1) For each s , the variation vector field is given by a function f_{Σ_s} times the normal \mathbf{n}_{Σ_s} where every f_{Σ_s} is supported in a fixed compact subset of \mathbf{R}^{n+1} .
- (V2) For any variations x_s and t_s with $x_0 = 0$ and $t_0 = 1$, we get that

$$\partial_{ss} \Big|_{s=0} F_{x_s,t_s}(\Sigma_s) < 0. \quad (62)$$

We will use this to prove that Σ is also entropy-unstable.

Setting up the proof: Define a function $G : \mathbf{R}^{n+1} \times \mathbf{R}^+ \times [-2\epsilon, 2\epsilon] \rightarrow \mathbf{R}^+$ by

$$G(x_0, t_0, s) = F_{x_0,t_0}(\Sigma_s). \quad (63)$$

We will show that there exists some $\epsilon_1 > 0$ so that if $s \neq 0$ and $|s| \leq \epsilon_1$, then

$$\lambda(\Sigma_s) \equiv \sup_{x_0, t_0} G(x_0, t_0, s) < G(0, 1, 0) = \lambda(\Sigma), \quad (64)$$

and this will give the theorem with $\tilde{\Sigma}$ equal to Σ_s for any $s \neq 0$ in $(-\epsilon_1, \epsilon_1)$; by taking $s > 0$ small enough, we can arrange that $\tilde{\Sigma}$ is as close as we like to $\Sigma_0 = \Sigma$.

The remainder of the proof is devoted to establishing (64). The key points will be:

1. G has a strict local maximum at $(0, 1, 0)$.
2. The restriction of G to Σ_0 , i.e., $G(x_0, t_0, 0)$, has a strict global maximum at $(0, 1)$.
3. $|\partial_s G|$ is uniformly bounded on compact sets.
4. $G(x_0, t_0, s)$ is strictly less than $G(0, 1, 0)$ whenever $|x_0|$ is sufficiently large.
5. $G(x_0, t_0, s)$ is strictly less than $G(0, 1, 0)$ whenever $|\log t_0|$ is sufficiently large.

The proof of (64) assuming (1)–(5): We will divide into three separate regions depending on the size of $|x_0|^2 + (\log t_0)^2$.

First, it follows from steps (4) and (5) that there is some $R > 0$ so that (64) holds for every s whenever

$$x_0^2 + (\log t_0)^2 > R^2. \quad (65)$$

Second, as long as s is small, step (1) implies that (64) holds when $x_0^2 + (\log t_0)^2$ is sufficiently small.

Finally, in the intermediate region where $x_0^2 + (\log t_0)^2$ is bounded from above and bounded uniformly away from zero, step (2) says that G is strictly less than $\lambda(\Sigma)$ at $s = 0$ and step (3) says that the s derivative of G is uniformly bounded. Hence, there exists some $\epsilon_3 > 0$ so that $G(x_0, t_0, s)$ is strictly less than $\lambda(\Sigma)$ whenever (x_0, t_0) is in the intermediate region as long as $|s| \leq \epsilon_3$.

This completes the proof of (64) assuming (1)–(5). See [CM1] for the proofs of (1)–(5). \square

12.6 Classification of F-stable self-shrinkers

Theorem 64. (*Colding-Minicozzi, [CM1]*) *If Σ is a smooth⁷ complete embedded self-shrinker in \mathbf{R}^{n+1} without boundary and with polynomial volume growth that is F-stable with respect to compactly supported variations, then it is either the round sphere or a hyperplane.*

Combined with the splitting theorem, this gives the classification of generic self-shrinkers.

The main steps in the proof of Theorem 64 are:

⁷The theorem holds when $n \leq 6$ and Σ is an oriented integral varifold that is smooth off of a singular set with locally finite $(n - 2)$ -dimensional Hausdorff measure.

- Show that F -stability implies mean convexity (i.e., $H \geq 0$).
- Classify the mean convex self-shrinkers (see Theorem 65 below).

The classification of mean convex self-shrinkers began with [H3], where Huisken showed that the only smooth closed self-shrinkers with non-negative mean curvature in \mathbf{R}^{n+1} (for $n > 1$) are round spheres (i.e., \mathbf{S}^n). When $n = 1$, Abresch and Langer, [AbLa], had already shown that the circle is the only simple closed self-shrinking curve. In a second paper, [H4], Huisken dealt with the non-compact case. He showed in [H4] that the only smooth open embedded self-shrinkers in \mathbf{R}^{n+1} with $H \geq 0$, polynomial volume growth, and $|A|$ bounded are isometric products of a round sphere and a linear subspace (i.e. $\mathbf{S}^k \times \mathbf{R}^{n-k} \subset \mathbf{R}^{n+1}$). We will show that Huisken's classification holds even without the $|A|$ bound which will be crucial for our applications:

Theorem 65. (*[H3], [H4] and [CM1]*) $\mathbf{S}^k \times \mathbf{R}^{n-k}$ are the only smooth complete embedded self-shrinkers without boundary, with polynomial volume growth, and $H \geq 0$ in \mathbf{R}^{n+1} .

The \mathbf{S}^k factor in Theorem 65 is round and has radius $\sqrt{2k}$; we allow the possibilities of a hyperplane (i.e., $k = 0$) or a sphere ($n - k = 0$).

12.7 Proof in the compact case

Since L is symmetric in the weighted space, its spectral theory is similar to the Laplacian:

1. There are eigenvalues $\mu_1 < \mu_2 \leq \dots$ with $\mu_i \rightarrow \infty$ and eigenfunctions u_i with

$$L u_i = -\mu_i u_i.$$

2. The lowest eigenfunction u_1 does not change sign.
3. If $\mu_i \neq \mu_j$, then u_i and u_j are orthogonal, i.e.,

$$\int_{\Sigma} u_i u_j e^{-\frac{|x|^2}{4}} = 0.$$

Let Σ be a closed self-shrinker and suppose that H changes sign. We will show that Σ is F -unstable. We know that $LH = H$. Since H changes sign, it is NOT the lowest eigenfunction. It follows that $\mu_1 < -1$. Let u_1 be the corresponding (lowest) eigenfunction and define the variation

$$\Sigma_s = \{x + s u_1(x) \mathbf{n}(x) \mid x \in \Sigma\}.$$

Given variations $x_s = sy$ and $t_s = 1 + sh$, the second variation is $(4\pi)^{-\frac{n}{2}}$ times

$$\int \left[\mu_1 u_1^2 + 2u_1 h H - h^2 H^2 + u_1 \langle y, \mathbf{n} \rangle - \frac{\langle y, \mathbf{n} \rangle^2}{2} \right] e^{-\frac{|x|^2}{4}}.$$

But u_1 is orthogonal to the other eigenfunctions H and $\langle y, \mathbf{n} \rangle$, so

$$= \int \left[\mu_1 u_1^2 - h^2 H^2 - \frac{\langle y, \mathbf{n} \rangle^2}{2} \right] e^{-\frac{|x|^2}{4}}.$$

This is obviously negative no matter what h and y are.

13 An application

Fix D , V and g and let $\mathcal{M}_{D,V,g}$ be all self-shrinkers in \mathbf{R}^3 with:

- Diameter at most D .
- Entropy at most V .
- Genus at most g .

Then: C-M compactness theorem implies that $\mathcal{M}_{D,V,g}$ is smoothly compact.

Combined with our entropy stability: There exists $\epsilon > 0$ so that if $\Sigma \in \mathcal{M}_{D,V,g}$ is not \mathbf{S}^2 , then there is a graph $\tilde{\Sigma}$ over Σ with

$$\lambda(\tilde{\Sigma}) \leq \lambda(\Sigma) - \epsilon.$$

13.1 Piece-wise MCF

We next define an ad hoc notion of generic MCF that requires the least amount of technical set-up, yet should suffice for many applications.

A piece-wise MCF is a finite collection of MCF's M_t^i on time intervals $[t_i, t_{i+1}]$ so that each $M_{t_{i+1}}^{i+1}$ is the graph over $M_{t_{i+1}}^i$ of a function u_{i+1} ,

$$\begin{aligned} \text{Area} \left(M_{t_{i+1}}^{i+1} \right) &= \text{Area} \left(M_{t_{i+1}}^i \right), \\ \lambda \left(M_{t_{i+1}}^{i+1} \right) &\leq \lambda \left(M_{t_{i+1}}^i \right). \end{aligned}$$

With this definition, area is non-increasing in t even across the jumps.

13.2 Generic compact singularities

In this subsection, we will assume that the multiplicity one conjecture of Ilmanen holds. Under this assumption, we have the following generalization of the Grayson-Huisken theorems:

Theorem 66. (Colding-Minicozzi, [CM1]) For any closed embedded surface $\Sigma \subset \mathbf{R}^3$, there exists a piece-wise MCF M_t starting at Σ and defined up to time t_0 where the surfaces become singular. Moreover, M_t can be chosen so that if

$$\liminf_{t \rightarrow t_0} \frac{\text{diam} M_t}{\sqrt{t_0 - t}} < \infty,$$

then M_t becomes extinct in a round point.

14 Non-compact self-shrinkers

14.1 The spectrum of L when Σ is non-compact

If Σ is non-compact, there may not be a lowest eigenvalue for $L = \mathcal{L} + |A|^2 + \frac{1}{2}$. However, we can still define the bottom of the spectrum (which we still call μ_1) by

$$\mu_1 = \inf_f \frac{-\int_{\Sigma} (f L f) e^{-\frac{|x|^2}{4}}}{\int_{\Sigma} f^2 e^{-\frac{|x|^2}{4}}},$$

where the infimum is taken over smooth functions f with compact support.

Warning: Since Σ is non-compact, we must allow the possibility that $\mu_1 = -\infty$.

We have the following characterization of μ_1 generalizing the compact case (as usual Σ is a complete self-shrinker without boundary and with polynomial volume growth):

Proposition 67. (Colding-Minicozzi, [CM1]) If $\mu_1 \neq -\infty$, then:

- There is a positive function u on Σ with $L u = -\mu_1 u$.
- If v is in the weighted $W^{1,2}$ space and $L v = -\mu_1 v$, then $v = C u$ for $C \in \mathbf{R}$.
- $|A| |x|$ is in the weighted L^2 space.

(This proposition combines lemmas 9.15 and 9.25 in [CM1].)

14.2 μ_1 when H changes sign

We have already seen that the mean curvature H is an eigenfunction of L with eigenvalue -1 . The next theorem shows that if H changes, then the bottom of the spectrum μ_1 is strictly less than -1 .

Theorem 68. (Colding-Minicozzi, [CM1]) If the mean curvature H changes sign, then $\mu_1 < -1$.

The idea of the proof follows:

1. We can assume that $\mu_1 \neq -\infty$. Thus, Proposition 67 gives that $|A| |x|$ is in the weighted L^2 space.

2. Differentiating the self-shrinker equation $H = \frac{1}{2} \langle x, \mathbf{n} \rangle$ gives

$$2 \nabla_{e_1} H = -A_{ij} \langle x, e_j \rangle.$$

It follows from this and (1) that H , ∇H , and $|A|H$ are in the weighted L^2 space.

3. The bounds in (3) are enough to justify using H as a test function in the definition of μ_1 and get that $\mu_1 \leq -1$.
4. It remains to rule out that $\mu_1 = -1$. But this would imply that H does not change sign by the uniqueness part of Proposition 67.

14.3 The F -unstable variation when $\mu_1 < -1$

We have shown that if H changes sign, then Σ has $\mu_1 < -1$. When Σ was closed, it followed immediately from this and the orthogonality of eigenfunctions with different eigenvalues (for a symmetric operator) that Σ was F -unstable. However, this orthogonality uses an integration by parts which is not justified when Σ is open. Instead, we show that the lowest eigenfunction on a sufficiently large ball is *almost* orthogonal to H and the translations. This turns out to be enough to prove F -instability:

Lemma 69. (*Colding-Minicozzi, [CM1]*) *If $\mu_1 < -1$, then there exists \bar{R} so that if $R \geq \bar{R}$ and u is a Dirichlet eigenfunction for $\mu_1(B_R)$, then for any $h \in \mathbf{R}$ and any $y \in \mathbf{R}^{n+1}$ we have*

$$\left[-u L u + 2u h H + u \langle y, \mathbf{n} \rangle - h^2 H^2 - \frac{\langle y, \mathbf{n} \rangle^2}{2} \right]_{B_R} < 0. \quad (66)$$

Here, in (66), we used $[\cdot]_{B_R}$ to denote the Gaussian weighted integral over the ball B_R .

To illustrate how the almost orthogonality comes in, we will explain a simple case of Lemma 69 when $\mu_1 < -\frac{3}{2}$ (this still leaves the possibility that μ_1 is between $-\frac{3}{2}$ and -1).

Sketch of (66) when $\mu_1 < -\frac{3}{2}$: Using the Cauchy-Schwartz inequality $ab \leq \frac{1}{2}(a^2 + b^2)$ on the cross-term $u \langle y, \mathbf{n} \rangle$, the left hand side of (66) is bounded from above by

$$\left[\left(\frac{1}{2} + \mu_1(B_R) \right) u^2 + 2u h H - h^2 H^2 \right]_{B_R}. \quad (67)$$

We will show that this is negative when R is large. Since $\mu_1 < -\frac{3}{2}$, we can choose \bar{R} so that $\mu_1(B_{\bar{R}}) < -\frac{3}{2}$. Given any $R \geq \bar{R}$, then (67) is strictly less than

$$\left[-u^2 + 2u h H - h^2 H^2 \right]_{B_R} = - \left[(u - hH)^2 \right]_{B_R}, \quad (68)$$

which gives (66) in this case.

14.4 Classification of mean convex self-shrinkers

Throughout this subsection, Σ is a complete, non-compact self-shrinker with polynomial volume growth, $\partial\Sigma = \emptyset$ and $H > 0$. We will sketch the proof of the classification theorem, i.e., Theorem 65, which gives that Σ is a cylinder.

The classification relies heavily upon the following ‘‘Simons’ identity’’ for the second fundamental form A of a self-shrinker Σ :

$$L A = A,$$

where we have extended L to act on tensors in the natural way. Taking the trace of this recovers that $L H = H$ since traces and covariant derivatives commute (the metric is parallel).

Roughly speaking, the identity $L A = A$ says that the whole matrix A is a lowest eigenfunction for L . Moreover, the matrix strong maximum principle shows that the kernel of A consists of parallel vector fields that split off a factor of \mathbf{R}^k . The remaining principle curvatures must then all be multiples of each other (by the uniqueness of the lowest eigenfunctions for L). We will show that the remaining non-zero principle curvature are in fact the same, i.e., Σ is the product of an affine space and a totally umbilic submanifold.

The main steps in the proof Theorem 65 are:

1. Using $L A = A$, it follows that

$$L |A| = |A| + \frac{|\nabla A|^2 - |\nabla |A||^2}{|A|} \geq |A|.$$

2. Using $L A = A$ and the ‘‘stability inequality’’ coming from $H > 0$, we show that

$$\int (|A|^2 + |A|^4 + |\nabla |A||^2 + |\nabla A|^2) e^{-\frac{|x|^2}{4}} < \infty.$$

(This should remind you of the Schoen-Simon-Yau, [ScSiY], curvature estimates for stable minimal hypersurfaces.)

3. Using (2) to show that various integrals converge and justify various integrations by parts, (1) and $L H = H$ imply that $H = C |A|$ for $C > 0$.
4. The combination of $|\nabla A|^2 = |\nabla |A||^2$ and $H = C |A|$ - and some work - give the classification. This last step is essentially the same argument as in [H3].

References

- [AbLa] U. Abresch and J. Langer, The normalized curve shortening flow and homothetic solutions. *J. Differential Geom.* 23 (1986), no. 2, 175–196.
- [AFM] A. Alarcon, L. Ferrer, and F. Martin, *Density theorems for complete minimal surfaces in \mathbb{R}^3* , *Geom. Funct. Anal.* 18 (2008), no. 1, 1–49.

- [ANa] A. Alarcon and N. Nadirashvili, *Limit sets for complete minimal immersions*, Math. Z. 258 (2008), no. 1, 107–113.
- [Al] W.K Allard, On the first variation of a varifold. Ann. of Math. (2) 95 (1972), 417–491.
- [AAG] S. Altschuler, S. Angenent, and Y. Giga, Mean curvature flow through singularities for surfaces of rotation. J. Geom. Anal. 5 (1995), no. 3, 293–358.
- [AW] S. Altschuler and L. Wu, Translating surfaces of the non-parametric mean curvature flow with prescribed contact angle, Calc. Var. Partial Differential Equations 2(1), 101–111 (1994)
- [An] B. Andrews, Classification of limiting shapes for isotropic curve flows. J. Amer. Math. Soc. 16 (2003), no. 2, 443–459.
- [AnB] B. Andrews and P. Bryan Curvature bound for curve shortening flow via distance comparison and a direct proof of Grayson’s theorem, Crelle, to appear.
- [A] S. Angenent, Shrinking doughnuts, In: Nonlinear diffusion equations and their equilibrium states, Birkhäuser, Boston-Basel-Berlin, 3, 21-38, 1992.
- [AChI] S. B. Angenent, D. L. Chopp, and T. Ilmanen. A computed example of nonuniqueness of mean curvature flow in \mathbf{R}^3 . Comm. Partial Differential Equations, 20 (1995), no. 11-12, 1937–1958.
- [BB1] J. Bernstein and C. Breiner, *Distortions of the helicoid*, Geom. Dedicata 137 (2008), 143–147.
- [BB2] J. Bernstein and C. Breiner, *Conformal Structure of Minimal Surfaces with Finite Topology*, Crelle, to appear.
- [BB3] J. Bernstein and C. Breiner, *Symmetry of Embedded Genus-One Helicoids*, To appear, Duke Math. J.
- [Be] S. Bernstein, *Über ein geometrisches Theorem und seine Anwendung auf die partiellen Differentialgleichungen vom ellipschen* Typos. Math. Zeit. 26 (1927) 551–558 (translation of the original version in Comm. Soc. Math. Kharkov 2-ème sér. 15 (1915–17) 38–45).
- [BJO] G.P. Bessa, L. Jorge and G. Oliveira-Filho, *Half-space theorems for minimal surfaces with bounded curvature*, J. Diff. Geom. 57 (2001) 493–508.
- [B1] G.D. Birkhoff, Dynamical systems with two degrees of freedom. *TAMS* 18 (1917), no. 2, 199–300.
- [B2] G.D. Birkhoff, Dynamical systems, AMS Colloq. Publ. vol 9, Providence, RI, 1927.
- [B] K. Brakke, The motion of a surface by its mean curvature. Mathematical Notes, 20. Princeton University Press, Princeton, N.J., 1978.

- [Bo] A. Bobenko, Helicoids with handles and Baker-Akhiezer spinors. *Math. Z.* 229 (1998), no. 1, 9–29.
- [Ce] E. Calabi, Problems in differential geometry, Ed. S. Kobayashi and J. Eells, Jr., *Proceedings of the United States-Japan Seminar in Differential Geometry, Kyoto, Japan, 1965*. Nippon Hyoronsha Co., Ltd., Tokyo (1966) 170.
- [CaKK] M. Calle, S. Kleene and J. Kramer, Width and flow of hypersurfaces by curvature functions, *Trans. Amer. Math. Soc.* 363 (2011), 1125–1135.
- [CaL] M. Calle and D. Lee, *Non-proper helicoid-like limits of closed minimal surfaces in 3-manifolds*, *Math. Z.* 261 (2009), no. 4, 725–736.
- [CaHI] H-D. Cao, R.S. Hamilton, and T. Ilmanen, Gaussian densities and stability for some Ricci solitons, preprint 2004.
- [CaZ] H-D. Cao and M. Zhu, On second variation of Perelman’s Ricci shrinker entropy, preprint 2010.
- [Ca] I. Chavel, Eigenvalues in Riemannian Geometry. Pure and Applied Mathematics, 115. Academic Press, Inc., Orlando, FL, 1984.
- [CGG] Y. Chen, Y. Giga, and S. Goto, Uniqueness and existence of viscosity solutions of generalized mean curvature flow equations. *J. Differential Geom.* 33 (1991), no. 3, 749–786.
- [Cs] S.S. Chern, The geometry of G -structures, *Bull. Amer. Math. Soc.* 72 (1966) 167–219.
- [CiSc] H.I. Choi and R. Schoen, *The space of minimal embeddings of a surface into a three-dimensional manifold of positive Ricci curvature*, *Invent. Math.* 81 (1985) 387–394.
- [Ch] D. Chopp, Computation of self-similar solutions for mean curvature flow. *Experiment. Math.* 3 (1994), no. 1, 1–15.
- [CSS] J. Clutterbuck, O. Schnürer, and F. Schulze, Stability of translating solutions to mean curvature flow. *Calc. Var. Partial Differential Equations* 29 (2007), no. 3, 281–293.
- [CD] T.H. Colding and C. De Lellis, Singular limit laminations, Morse index, and positive scalar curvature. *Topology* 44 (2005), no. 1, 2545.
- [CDM] T.H. Colding, C. De Lellis, and W.P. Minicozzi II, *Three circles theorems for Schrödinger operators on cylindrical ends and geometric applications*, *Comm. Pure Appl. Math.* 61 (2008), no. 11, 1540–1602.
- [CM1] T.H. Colding and W.P. Minicozzi II, *Generic mean curvature flow I; generic singularities*, preprint, <http://lanl.arxiv.org/abs/0908.3788>.
- [CM2] T.H. Colding and W.P. Minicozzi II, *Width and mean curvature flow*, *Geom. Topol.* 12 (2008), no. 5, 2517–2535.

- [CM3] T.H. Colding and W.P. Minicozzi II, *Smooth compactness of self-shrinkers*, Comm. Math. Helv., to appear, <http://arxiv.org/pdf/0907.2594>.
- [CM4] T.H. Colding and W.P. Minicozzi II, *Minimal surfaces*. Courant Lecture Notes in Mathematics, 4. NYU, Courant Institute of Math. Sciences, NY, 1999.
- [CM5] T. H. Colding and W.P. Minicozzi II, *Shapes of embedded minimal surfaces*. Proc. Natl. Acad. Sci. USA 103 (2006), no. 30, 11106–11111
- [CM6] T. H. Colding and W.P. Minicozzi II, *The space of embedded minimal surfaces of fixed genus in a 3-manifold. I. Estimates off the axis for disks*. Ann. of Math. (2) 160 (2004), no. 1, 27–68.
- [CM7] T. H. Colding and W.P. Minicozzi II, *The space of embedded minimal surfaces of fixed genus in a 3-manifold. II. Multi-valued graphs in disks*. Ann. of Math. (2) 160 (2004), no. 1, 69–92.
- [CM8] T. H. Colding and W.P. Minicozzi II, *The space of embedded minimal surfaces of fixed genus in a 3-manifold. III. Planar domains*. Ann. of Math. (2) 160 (2004), no. 2, 523–572.
- [CM9] T. H. Colding and W.P. Minicozzi II, *The space of embedded minimal surfaces of fixed genus in a 3-manifold. IV. Locally simply connected*. Ann. of Math. (2) 160 (2004), no. 2, 573–615.
- [CM10] T. H. Colding and W.P. Minicozzi II, *The space of embedded minimal surfaces of fixed genus in a 3-manifold. V. Fixed genus*, preprint.
- [CM11] T.H. Colding and W.P. Minicozzi II, *Complete properly embedded minimal surfaces in \mathbf{R}^3* , Duke Math. J. 107 (2001) 421–426.
- [CM12] T.H. Colding and W.P. Minicozzi II, *The Calabi-Yau conjectures for embedded surfaces*, Ann. of Math. (2) 167 (2008), no. 1, 211–243.
- [CM13] T.H. Colding and W.P. Minicozzi II, *Embedded minimal surfaces without area bounds in 3-manifolds*. Geometry and topology: Aarhus (1998), 107–120, Contemp. Math., 258, Amer. Math. Soc., Providence, RI, 2000.
- [CM14] T.H. Colding and W.P. Minicozzi II, *A course in minimal surfaces*, Graduate Studies in Math., Amer. Math. Soc., Providence, RI, 2011.
- [CM15] T.H. Colding and W.P. Minicozzi II, *Estimates for parametric elliptic integrands*, International Mathematics Research Notices, no. 6 (2002) 291–297.
- [CM16] T.H. Colding and W.P. Minicozzi II, *On the structure of embedded minimal annuli*, International Mathematics Research Notices, no. 29 (2002) 1539–1552.

- [CM17] T.H. Colding and W.P. Minicozzi II, Embedded minimal disks: Proper versus nonproper - global versus local, *Transactions of the AMS*, 356 (2004) 283-289.
- [CM18] T.H. Colding and W.P. Minicozzi II, Multi-valued minimal graphs and properness of disks, *International Mathematics Research Notices*, no. 21 (2002) 1111-1127.
- [CM19] T.H. Colding and W.P. Minicozzi II, *Width and finite extinction time of Ricci flow*, *Geom. Topol.* 12 (2008), no. 5, 2537–2586.
- [CM20] T.H. Colding and W.P. Minicozzi II, Disks that are double spiral staircases, *Notices Amer. Math. Soc.* 50 (2003), no. 3, 327–339.
- [Co] P. Collin, *Topologie et courbure des surfaces minimales proprement plongees de \mathbf{R}^3* , *Ann. of Math.* (2) 145 (1997) 1–31.
- [CoRo] P. Collin and H. Rosenberg, Notes sur la démonstration de N. Nadirashvili des conjectures de Hadamard et Calabi-Yau. *Bull. Sci. Math.* 123 (1999), no. 7, 563–575.
- [Cb] B. Coskunuzer, *Least area planes in hyperbolic 3-space are properly embedded*, *Indiana Univ. Math. J.* 58 (2009), no. 1, 381–392.
- [Cc] C. Costa, *Example of a complete minimal immersion in R^3 of genus one and three embedded ends*, *Bol. Soc. Brasil. Mat.* 15 (1984), no. 1-2, 47–54.
- [Cr] C.B. Croke, *Area and the length of the shortest closed geodesic*, *J. Diff. Geom.*, 27 (1988), no. 1, 1–21.
- [DMR] B. Daniel, W. Meeks and H. Rosenberg, Half-space theorems and the embedded Calabi-Yau problem in Lie groups, preprint, 2010.
- [De] B. Dean, *Embedded minimal disks with prescribed curvature blowup*, *Proc. Amer. Math. Soc.* 134 (2006), no. 4, 1197–1204.
- [dCP] M. do Carmo and C. K. Peng, *Stable complete minimal surfaces in R^3 are planes*, *Bull. Amer. Math. Soc. (N.S.)* 1 (1979), no. 6, 903–906.
- [E1] K. Ecker, Local monotonicity formulas for some nonlinear diffusion equations. *Calc. Var. Partial Differential Equations* 23 (2005), no. 1, 67–81.
- [E2] K. Ecker, Regularity theory for mean curvature flow. *Progress in Nonlinear Differential Equations and their Applications*, 57. Birkhuser Boston, Inc., Boston, MA, 2004.
- [E3] K. Ecker, A Formula Relating Entropy Monotonicity to Harnack Inequalities. *Communications in Analysis and Geometry*, Volume 15, Number 5, 1025 - 1061, 2008.
- [E4] K. Ecker, Heat equations in geometry and topology. *Jahresber. Deutsch. Math.-Verein.* 110 (2008), no. 3, 117–141.

- [EH1] K. Ecker and G. Huisken, Mean curvature evolution of entire graphs, *Ann. of Math.* (2) 130 (1989), no. 3, 453–471.
- [EH2] K. Ecker and G. Huisken, Interior estimates for hypersurfaces moving by mean curvature. *Invent. Math.* 105 (1991), no. 3, 547–569.
- [EpG] C. Epstein and M. Gage, *The curve shortening flow. Wave motion: theory, modelling, and computation* (Berkeley, Calif., 1986), 15–59, *Math. Sci. Res. Inst. Publ.*, 7, Springer, New York, 1987.
- [EpW] C. Epstein and M. Weinstein, A stable manifold theorem for the curve shortening equation, *Comm. Pure Appl. Math.* 40 (1987), no. 1, 119–139.
- [Ev] L. C. Evans, *Partial differential equations*. Graduate Studies in Mathematics, 19. AMS, Providence, RI, 1998.
- [EvSp] L. C. Evans and J. Spruck, Motion of level sets by mean curvature. I. *J. Differential Geom.* 33 (1991), no. 3, 635–681.
- [FiSc] D. Fischer-Colbrie and R. Schoen, *The structure of complete stable minimal surfaces in 3-manifolds of nonnegative scalar curvature*, *Comm. Pure Appl. Math.* 33 (1980) 199–211.
- [Ga1] M. Gage, Curve shortening makes convex curves circular, *Invent. Math.* 76 (1984), no. 2, 357–364.
- [Ga2] M. Gage, An isoperimetric inequality with applications to curve shortening, *Duke Math. J.* 50 (1983), no. 4, 1225–1229.
- [GaH] M. Gage and R. S. Hamilton, The heat equation shrinking convex plane curves. *J. Differential Geom.* 23 (1986) 69–96.
- [G1] M. Grayson, The heat equation shrinks embedded plane curves to round points. *J. Differential Geom.* 26 (1987), no. 2, 285–314.
- [G2] M. Grayson, A short note on the evolution of a surface by its mean curvature. *Duke Math. J.* 58 (1989), no. 3, 555–558.
- [G3] M. Grayson, Shortening embedded curves. *Ann. of Math.* (2) 129 (1989), no. 1, 71–111.
- [Hh] H. Halldorsson, Self-similar solutions to the curve shortening flow, preprint 2010.
- [Ha1] R. S. Hamilton, Isoperimetric estimates for the curve shrinking flow in the plane. *Modern methods in complex analysis* (Princeton, NJ, 1992), 201–222, *Ann. of Math. Stud.*, 137, Princeton Univ. Press, Princeton, NJ, 1995.
- [Ha2] R. S. Hamilton, Harnack estimate for the mean curvature flow. *J. Differential Geom.* 41 (1995), no. 1, 215–226.

- [HP] L. Hauswirth and F. Pacard, Higher genus Riemann minimal surfaces. *Invent. Math.* 169 (2007), no. 3, 569–620.
- [HMR] L. Hauswirth, F. Morabito, and M. Rodríguez, An end-to-end construction for singly periodic minimal surfaces. *Pacific J. Math.* 241 (2009), no. 1, 1–61.
- [HoK] D. Hoffman and H. Karcher, *Complete embedded minimal surfaces with finite total curvature*, Geometry V (R. Osserman, ed.) *Encyclopaedia Math. Sci.* 90, Springer-Verlag, New York (1997) 5–93.
- [HoMe] D. Hoffman and W. Meeks III, The strong halfspace theorem for minimal surfaces, *Invent. Math.* 101 (1990) 373–377.
- [HoWW] D. Hoffman, M. Weber, and M. Wolf, *An embedded genus-one helicoid*, *Ann. of Math. (2)* 169 (2009), no. 2, 347–448.
- [HoWh1] D. Hoffman and B. White, *Genus-one helicoids from a variational point of view*, *Comment. Math. Helv.* 83 (2008), no. 4, 767–813.
- [HoWh2] D. Hoffman and B. White, *Sequences of embedded minimal disks whose curvatures blow up on a prescribed subset of a line*, arXiv:0905.0851v2.
- [HoWh3] D. Hoffman and B. White, The geometry of genus-one helicoids. *Comment. Math. Helv.* 84 (2009), no. 3, 547569.
- [H1] G. Huisken, Flow by the mean curvature of convex surfaces into spheres. *JDG* 20 (1984) no. 1, 237–266.
- [H2] G. Huisken, Local and global behaviour of hypersurfaces moving by mean curvature, *Proc. CMA, ANU*, vol. 26, 1991.
- [H3] G. Huisken, Asymptotic behavior for singularities of the mean curvature flow. *J. Differential Geom.* 31 (1990), no. 1, 285–299.
- [H4] G. Huisken, Local and global behaviour of hypersurfaces moving by mean curvature. *Differential geometry: partial differential equations on manifolds* (Los Angeles, CA, 1990), 175–191, *Proc. Sympos. Pure Math.*, 54, Part 1, Amer. Math. Soc., Providence, RI, 1993.
- [H5] G. Huisken, A distance comparison principle for evolving curves. *Asian J. Math.* 2 (1998), no. 1, 127–133.
- [HS1] G. Huisken and C. Sinestrari, Convexity estimates for mean curvature flow and singularities of mean convex surfaces, *Acta Math.* 183 (1999) no. 1, 45–70.
- [HS2] G. Huisken and C. Sinestrari, Mean curvature flow singularities for mean convex surfaces. *Calc. Var. Partial Differential Equations*, 8 (1999), 1–14.
- [HS3] G. Huisken and C. Sinestrari, Mean curvature flow with surgeries of two-convex hypersurfaces, *Invent. Math.* 175 (2009), no. 1, 137–221.

- [I1] T. Ilmanen, Singularities of Mean Curvature Flow of Surfaces, preprint, 1995, <http://www.math.ethz.ch/~papers/pub.html>.
- [I2] T. Ilmanen, Elliptic regularization and partial regularity for motion by mean curvature. *Mem. Amer. Math. Soc.* 108 (1994), no. 520.
- [I3] T. Ilmanen, *Lectures on Mean Curvature Flow and Related Equations* (Trieste Notes), 1995.
- [JXa1] L. Jorge and F. Xavier, On the existence of complete bounded minimal surfaces in \mathbf{R}^n , *Bol. Soc. Brasil. Mat.* 10 (1979), no. 2, 171–173.
- [JXa2] L. Jorge and F. Xavier, A complete minimal surface in \mathbf{R}^3 between two parallel planes, *Annals of Math.* (2) 112 (1980) 203–206.
- [Jo] J. Jost, *Two-dimensional geometric variational problems*, J. Wiley and Sons, Chichester, N.Y. (1991).
- [Ka] N. Kapouleas, *Complete embedded minimal surfaces of finite total curvature*, *J. Diff. Geom.*, 47 (1997) 95–169.
- [KWH] H. Karcher, F. Wei, and D. Hoffman, The genus one helicoid and the minimal surfaces that led to its discovery. *Global analysis in modern mathematics* (Orono, ME, 1991; Waltham, MA, 1992), 119170, Publish or Perish, Houston, TX, 1993.
- [Kh] S. Khan, *A Minimal Lamination of the Unit Ball with Singularities along a Line Segment*, *Illinois J. Math.*, Volume 53, Number 3 (2009), 833–855.
- [Kl] S. Kleene, *A Minimal Lamination with Cantor Set-Like Singularities*, arXiv:0910.0199.
- [KlMo] S. Kleene and N. M. Möller, *Self-shrinkers with a rotational symmetry*, preprint 2010.
- [L] H. B. Lawson, Jr., Local rigidity theorems for minimal hypersurfaces. *Ann. of Math.* (2) 89 1969 187–197.
- [LzWl] L. Lin and L. Wang, *Existence of good sweepouts on closed manifolds*, *Proc. Amer. Math. Soc.* 138 (2010), 4081–4088.
- [LMaMo1] F. Lopez, F. Martin, and S. Morales, *Adding handles to Nadirashvili's surfaces*, *J. Diff. Geom.* 60 (2002), no. 1, 155–175.
- [LMaMo2] F. Lopez, F. Martin, and S. Morales, *Complete nonorientable minimal surfaces in a ball of \mathbf{R}^3* , *Trans. Amer. Math. Soc.*, 358 (2006), no. 9, 3807–3820.
- [LRo] F. Lopez and A. Ros, *On embedded complete minimal surfaces of genus zero*. *J. Differential Geom.* 33 (1991), no. 1, 293–300.

- [MaMeNa] F. Martin, W. Meeks, and N. Nadirashvili, *Bounded domains which are universal for minimal surfaces*, Amer. J. Math. 129 (2007), no. 2, 455–461.
- [MaMo1] F. Martin and S. Morales, *A complete bounded minimal cylinder in \mathbf{R}^3* , Michigan Math. J. 47 (2000), no. 3, 499–514.
- [MaMo2] F. Martin and S. Morales, *On the asymptotic behavior of a complete bounded minimal surface in \mathbf{R}^3* , Trans. AMS, 356 (2004), no. 10, 3985–3994.
- [MaMo3] F. Martin and S. Morales, *Complete proper minimal surfaces in convex bodies*, Duke Math. J. 128 (2005), no. 3, 559–593.
- [Mz] L. Mazet, *Adding one handle to half-plane layers*. J. Differential Geom. 84 (2010), no. 2, 389407.
- [Me1] W. Meeks III, *The geometry, topology, and existence of periodic minimal surfaces*, Proc. Sympos. Pure Math., 54, Part 1, American Mathematical Society, Providence, 1993.
- [Me2] W. Meeks III, *The regularity of the singular set in the Colding and Minicozzi lamination theorem*, Duke Math. J. 123 (2004), no. 2, 329–334.
- [Me3] W. Meeks III, *The limit lamination metric for the Colding-Minicozzi minimal lamination*, Illinois J. Math. 49 (2005), no. 2, 645–658.
- [MePRs1] W. Meeks III, J. Perez, and A. Ros, *The geometry of minimal surfaces of finite genus I. Curvature estimates and quasiperiodicity*, J. Differential Geom. 66 (2004), no. 1, 1–45.
- [MePRs2] W. Meeks III, J. Perez, and A. Ros, *The geometry of minimal surfaces of finite genus II. Nonexistence of one limit end examples*, Invent. Math. 158 (2004), no. 2, 323–341.
- [MePRs3] W. Meeks III, J. Perez, and A. Ros, *The geometry of minimal surfaces of finite genus III; bounds on the topology and index of classical minimal surfaces*, preprint.
- [MePRs4] W. Meeks III, J. Perez, and A. Ros, *Properly embedded minimal planar domains*, preprint.
- [MeR1] W. Meeks III and H. Rosenberg, *The geometry and conformal structure of properly embedded minimal surfaces of finite topology in \mathbf{R}^3* , Invent. Math. 114, no. 3 (1993) 625–639.
- [MeR2] W. Meeks III and H. Rosenberg, *The uniqueness of the helicoid*, Ann. of Math. (2) 161 (2005), no. 2, 727–758.
- [MeR3] W. Meeks III and H. Rosenberg, *The minimal lamination closure theorem*, Duke Math. J. 133 (2006), no. 3, 467–497.
- [MeWe] W.H. Meeks and M. Weber, *Bending the helicoid*, Math. Ann. 339 (2007), no. 4, 783–798.

- [MiSi] J. H. Michael and L. M. Simon, Sobolev and mean-value inequalities on generalized submanifolds of \mathbf{R}^n . *Comm. Pure Appl. Math.* 26 (1973), 361–379.
- [Na] N. Nadirashvili, *Hadamard's and Calabi-Yau's conjectures on negatively curved and minimal surfaces*, *Invent. Math.* 126 (1996) 457–465.
- [N1] X. H. Nguyen, Construction of complete embedded self-similar surfaces under mean curvature flow. Part I, *Trans. Amer. Math. Soc.*, 361 (2009), no. 4, 1683–1701.
- [N2] X. H. Nguyen, Construction of complete embedded self-similar surfaces under mean curvature flow. Part II, *Adv. Differential Equations* 15 (2010), no. 5-6, 503530.
- [N3] X. H. Nguyen, Translating Tridents, *Comm. in PDE*, Vol. 34 (2009), no. 3, 257 - 280.
- [OSe] S. Osher and J. Sethian, Fronts propagating with curvature-dependent speed: algorithms based on Hamilton-Jacobi formulations. *J. Comput. Phys.* 79 (1988), no. 1, 12–49.
- [Os1] R. Osserman, *A survey of minimal surfaces*, Dover, 2nd. edition (1986).
- [Os2] R. Osserman, *Global properties of minimal surfaces in E^3 and E^n* , *Ann. of Math.* (2) 80 1964 340–364.
- [Os3] R. Osserman, *The convex hull property of immersed manifolds*, *J. Diff. Geom.*, 6 (1971/72) 267–270.
- [Pe1] G. Perelman, Finite extinction time for the solutions to the Ricci flow on certain three-manifolds, [math.DG/0307245](https://arxiv.org/abs/math.DG/0307245).
- [Ra1] T. Rado, *On Plateau's problem*, *Ann. of Math.* 31 (1930) 457–469.
- [Ra2] T. Rado, *On the problem of Plateau*, *Ergebnisse der Mathematic und ihrer Grenzgebiete*, vol. 2. Springer-Verlag, Berlin (1953).
- [Ri] B. Riemann, *Über die Fläche vom kleinsten Inhalt bei gegebener Begrenzung*, *Abh. Königl. d. Wiss. Göttingen, Mathem. Cl.*, 13, 3–52 (1867).
- [Ro] H. Rosenberg, *Some recent developments in the theory of properly embedded minimal surfaces in \mathbf{R}^3* , *Seminare Bourbaki 1991/92*, Asterisque No. 206 (1992) 463–535.
- [RoTo] H. Rosenberg and E. Toubiana, *A cylindrical type complete minimal surface in a slab of \mathbf{R}^3* , *Bull. Sci. Math. III* (1987) 241–245.
- [SaUh] J. Sacks and K. Uhlenbeck, *The existence of minimal immersions of 2-spheres*, *Ann. of Math.* (2) 113 (1981) no. 1, 1–24.

- [Sc1] R. Schoen, *Estimates for stable minimal surfaces in three-dimensional manifolds*, In Seminar on Minimal Submanifolds, Ann. of Math. Studies, vol. 103, 111–126, Princeton University Press, Princeton, N.J., 1983.
- [Sc2] R. Schoen, *Uniqueness, symmetry, and embeddedness of minimal surfaces*, J. Diff. Geom. 18 (1983), no. 4, 791–809.
- [ScSi1] R.M. Schoen and L.M. Simon, Regularity of stable minimal hypersurfaces. Comm. Pure Appl. Math. 34 (1981), no. 6, 741–797.
- [ScSi2] R. Schoen and L. Simon, *Regularity of simply connected surfaces with quasi-conformal Gauss map*, In Seminar on Minimal Submanifolds, Annals of Math. Studies, vol. 103, 127–145, Princeton University Press, Princeton, N.J., 1983.
- [ScSiY] R.M. Schoen, L.M. Simon, and S.T. Yau, Curvature estimates for minimal hypersurfaces. Acta Math. 134 (1975), no. 3-4, 275–288.
- [ScYa1] R. Schoen and S.T. Yau, *On the proof of the positive mass conjecture in general relativity*, Comm. Math. Phys. 65 (1979), no. 1, 45–76.
- [ScYa2] R. Schoen and S.T. Yau, Lectures on harmonic maps, Int. Press (1997).
- [Sf1] F. Schulze, Evolution of convex hypersurfaces by powers of the mean curvature. Math. Z. 251 (2005), no. 4, 721–733.
- [Sf2] F. Schulze, Convexity estimates for flows by powers of the mean curvature. Ann. Sc. Norm. Super. Pisa Cl. Sci. (5) 5 (2006), no. 2, 261–277.
- [Se] N. Sesum, Rate of convergence of the mean curvature flow. Comm. Pure Appl. Math. 61 (2008), no. 4, 464–485.
- [Si] L. M. Simon, Lectures on Geometric Measure Theory, Proceedings of the CMA, ANU No. 3, Canberra, 1983.
- [Sim] J. Simons, *Minimal varieties in Riemannian manifolds*, Ann. of Math. 88 (1968) 62–105.
- [Sm1] K. Smoczyk, Starshaped hypersurfaces and the mean curvature flow, Manuscripta Math. 95 (1998), no. 2, 225–236.
- [Sm2] K. Smoczyk, Self-shrinkers of the mean curvature flow in arbitrary codimension. Int. Math. Res. Not. 2005, no. 48, 2983–3004.
- [St] A. Stone, A density function and the structure of singularities of the mean curvature flow, Calc. Var. 2 (1994), 443–480.
- [Ti1] G. Tinaglia, Multi-valued graphs in embedded constant mean curvature disks, Trans. Amer. Math. Soc. 359 (2007), no. 1, 143–164.
- [Ti2] G. Tinaglia, Structure theorems for embedded disks with mean curvature bounded in L^p . Comm. Anal. Geom. 16 (2008), no. 4, 819836.

- [V] J.J.L. Velázquez, Curvature blow-up in perturbations of minimal cones evolving by mean curvature flow. *Ann. Scuola Norm. Sup. Pisa Cl. Sci. (4)* 21 (1994), no. 4, 595–628.
- [Tr1] M. Traizet, *Construction de surfaces minimales en recollant des surfaces de Scherk*, *Ann. Inst. Fourier (Grenoble)* 46 (1996), no. 5, 1385–1442.
- [Tr2] M. Traizet, *Adding handles to Riemann’s minimal surfaces*, *J. Inst. Math. Jussieu* 1 (2002) 145–174.
- [Wa] L. Wang, A Bernstein Type Theorem For Self-similar Shrinkers, preprint December 2009, submitted.
- [WeWo1] M. Weber and M. Wolf, *Minimal surfaces of least total curvature and moduli spaces of plane polygonal arcs*, *Geom. Funct. Anal.* 8 (1998), no. 6, 1129–1170.
- [WeWo2] M. Weber and M. Wolf, *Teichmüller theory and handle addition for minimal surfaces*, *Ann. of Math. (2)*, 156 (2002) 713–795.
- [W1] B. White, Evolution of curves and surfaces by mean curvature. *Proceedings of the International Congress of Mathematicians, Vol. I (Beijing, 2002)*, 525–538, Higher Ed. Press, Beijing, 2002.
- [W2] B. White, The size of the singular set in mean curvature flow of mean-convex sets. *J. Amer. Math. Soc.* 13 (2000), no. 3, 665–695
- [W3] B. White, The nature of singularities in mean curvature flow of mean-convex sets. *J. Amer. Math. Soc.* 16 (2003), no. 1, 123–138.
- [W4] B. White, Stratification of minimal surfaces, mean curvature flows, and harmonic maps. *J. Reine Angew. Math.* 488 (1997), 1–35.
- [W5] B. White, A local regularity theorem for mean curvature flow. *Ann. of Math. (2)* 161 (2005), no. 3, 1487–1519.
- [Wi] N. Wickramasekera, in preparation.
- [Xa] F. Xavier, *Convex hulls of complete minimal surfaces*, *Math. Ann.* 269 (1984) 179–182.
- [Ya1] S.T. Yau, *Nonlinear analysis in geometry*, *L’Eseignement Mathématique* (2) 33 (1987) 109–158.
- [Ya2] S.T. Yau, *Open problems in geometry*, *Proc. Sympos. Pure Math.*, 54, Part 1, American Mathematical Society, Providence, 1993.
- [Ya3] S.T. Yau, Problem section, *Seminar on Differential Geometry*, *Ann. of Math. Studies*, v. 102, Princeton University Press (1982) 669–706.
- [Ya4] S.T. Yau, Review of geometry and analysis, *Mathematics: frontiers and perspectives*, Amer. Math. Soc., Providence, RI, (2000) 353–401.